BALANCE MAINTENANCE FOR HUMAN-LIKE MODELS WITH WHOLE BODY MOTION
人型モデルのための全身動作を用いた バランス保持動作の生成

by

Shunsuke KUDOH
工藤 俊亮

A Doctral Thesis
博士論文

Submitted to
the Department of Computer Science
the Graduate School of Information Science and Technology
the University of Tokyo
on December 16, 2004
in Partial Fulfillment of the Requirements
for the Degree of Doctor of Information Science and Technology
in Computer Science

Thesis Supervisor: Kastushi IKEUCHI　池内 克史

ABSTRACT

Recently, interest in generating dynamically consistent motion of human-like characters has been increasing in various areas. In computer graphics, due to an increase in the demand for realistic three-dimensional animation, many researchers have developed techniques to generate consistent human motion easily. In robotics, in order to operate a humanoid robot, it is necessary to generate motions that have strict dynamic consistency. In this thesis, we study the mechanism that generates motion that looks like human motion using a simple model as much as possible based on observation and analysis of human motion.

Maintaining balance is one of the most fundamental topics in this field of research. In a human-like characters that supports its body by standing on two feet, the support area by the feet is small and the center of mass (CM) is in a high position; therefore, it is impossible to realize stable motion without an adequate method for maintaining balance. Hence, many studies about balance maintenance have been conducted in computer graphics, robotics, and so on.

In particular, balance maintenance against perturbation caused by external force is an indispensable problem, since variation of motion becomes too small if we cannot deal with the perturbation. In this thesis, we discuss motion for maintaining balance against perturbation, in particular sudden and large perturbation, and propose a method to generate such motion using a simple mechanism.

With regard to coping with sudden perturbation, it can be said that humans themselves have realized the most flexible and effective balance maintenance to sudden disturbance. Humans maintain their balance against sudden perturbation by large-scale whole-body motion, such as bending down, rotating their arms, squatting down, taking a step, and so on. However, in the research on balance control of human-like characters, most of the techniques of these human-like balance maintenance have not been investigated. In this thesis, we observe such human motion, extract essential parameters from it, construct a simple model of balance maintenance based on them, and maintain balance with an appropriate whole-body motion against various perturbation using a simple model.

First, we capture human motion using a motion-capturing system and force plates. We analyze it by paying attention to macro quantities, such as the position of the CM, and the zero moment point (ZMP), and abstract a simple structure with parameters controlling it. At the same time, parameters that have individual variety, such as the spring constant of the legs, are also extracted. Next, we make a model of balance maintenance based on the result. Finally, we generate the motion of maintaining balance with human-like whole-body motion by optimization calculation with the model and the parameters. In order to cope with

larger perturbation, we design two modes for the model; balance maintenance by keeping feet on the ground and balance maintenance by stepping.

Comparing the generated motion by the model with human motion, it is found that characteristics of human motion are well reproduced in the generated motion. In addition, we examine the magnitude of perturbation that can be handled without stepping, which decides the timing of switching the mode. As a result, a good correspondence appears between the generated motion and human motion. It shows the fact that the generated motion represents characteristics of human motion not only in an apparent aspect but also in a quantitative aspect.

In summary, the contributions of this thesis are as follows: (1) It is shown that characteristics of complex human whole-body motion against large perturbation can be represented using only a simple structure with parameters extracted from human motion and optimization calculation. (2) It is found that the threshold to choose the mode can be represented by the model. (3) Various motions that are similar to human motion can be generated using the model.

論文要旨

近年，力学的に正しい人型モデルの動作を生成することに対する需要が高まってきている。コンピュータ・グラフィクスの分野ではリアルな三次元アニメーションへの需要の高まりから，正しい人間の動作を簡単に生成する手法の開発への取り組みがなされている。ロボティクスの分野では，ヒューマノイド・ロボットを動作させるために，厳密に力学的整合性のとれた動きを生成することは必要不可欠なものとなっている。我々は，人間動作の観察・分析に基づいてできるだけ簡単なモデルで人らしく見える動きを生成できるメカニズムの研究を行う。

人型モデルの動作生成に関する研究の中で，バランスの保持に関する研究はもっとも重要なトピックの内の 1 つである。2 本足で体を支える人型モデルは，支持面の面積が小さく重心が高いためにバランスを崩しやすく，適切な制御手法なしでは安定的に動作することは不可能だからである。そのためロボティクスやコンピュータ・グラフィクスの分野などを中心に，バランスのとれた動きを生成する手法に関する研究が数多くなされてきた。

中でも外力の作用などの外乱に対してのバランス保持は，人型モデルの動作生成にとって避けることのできない課題といえる。なぜなら，外部環境とのインタラクションを上手く取り扱うことができないとしたら，生成可能な動作の幅が著しく狭められることになるからである。本論文では，比較的簡単な制御メカニズムと簡単なモデルでもって，人型モデルの外乱に対するバランス保持動作，それも突発的で大きな外乱に対するバランス保持動作が生成できることを示す。

突発的な外乱に対して最も柔軟かつ有効なバランス保持を実現しているのは，他ならぬ人間自身であると言える。実際，人間は突発的な外乱に対して，腰を大きく屈める，腕をぐるぐる回す，足を踏み出すなどの大きな全身動作を自発的に用いて，きわめて質の高いバランス保持動作を実現している。ところが人型モデルのバランス保持に関する研究において，これらの「人間らしい」バランス制御の手法はほとんど取り上げられてこなかった。ここでは，上に挙げたような人間のバランス保持動作を観察，基本的なパラメータを抽出し，これを用いて比較的単純なモデルを構築することで，様々な大きさの外乱に対して適切な全身動作を用いてバランスを保持する動作を生成する。

まず外乱が加えられたときの人間のバランス保持動作を，モーションキャプチャやフォースプレートを用いて複数の被験者に対して計測した。その結果を重心，ゼロモーメント・ポイント（ZMP）などのマクロな物理量に注目して解析・抽象化し，それに基づいてバランス保持モデルを構築した。また，踏み出した脚をばねに見立てた時のばね定数など個人差のあるパラメタも同時に抽出した。これらのモデルとパラメタを用いて最適化計算を行うことにより，人間が行うような全身動作によるバランス保持動作が生成される。この際，脚を踏み出さないで踏ん張るモードと，より大きな外乱に対処するため脚を踏み出すモードの 2 つのモードを用意した。

このようにして生成された動作を人間の動作と比較した結果，人間のバランス保

持動作に見られる特徴がよく再現されていることが分かった。また手法の定量的な評価として，足を踏み出すことなくバランスを保持できる外乱の大きさに関して，提案手法と実際の人間に外乱を加えた結果とで定量的な比較を行った。その結果，本手法が単に人間の動きの特徴を再現しているだけでなく，定量的な側面からも人間のバランス保持動作を再現していることが示された。特に，どの程度までの外乱なら脚を踏み出さないモードをとるかという閾値に関して，制御モデルと人間の行動に一致が見られた。

以上これを要するに，人間の動作を観察して得られた比較的単純な構造とそれを制御する基本的なパラメタと最適化計算のみによって，人間が行う複雑な全身動作を伴うバランス保持についてその特徴を再現できるということを示すことができ，2 つのバランス保持のモードを分けるパラメタもこのモデルで表現できることが分かり，これを用いて各種の人間らしい人型モデルの動きが生成できたという点に本論文の寄与があると考えられる。

Acknowledgements

First of all, I would like to thank my adviser, Prof. Katsushi Ikeuchi, for his strong support and encouragement. He generously took me on as his student in the middle of my master's studies and allowed me to continue my doctoral research under his guidance.

I would like to thank my ex-adviser, Prof. Yoshihisa Shinagawa, for his guidance during my master's studies. He introduced me to research on human motion. I would like to thank Prof. Tatsuyuki Ohtsuki for his valuable advice on various topics in biomechanics. I would like to thank Prof. Minoru Ueda, who is at Aizu University, for allowing us to use a motion-capturing system at that university. Without this excellent system, this work would not be accomplished.

I would like to thank Dr. Taku Komura. He instructed me in computer graphics and dynamics during my master's studies. Although he has gone to Hong Kong far from Japan, his advice through an international call was a significant help to me.

I would also like to thank members of our laboratory, especially in the *odori* group. Atsushi Nakazawa, Jun Takamatsu, Shin'ichiro Nakaoka, Takaaki Shiratori, and Miti Ruchanurucks deserve special thanks for discussing my field of study with me, for giving me valuable advice, and for making me relax with enjoyable conversation.

I would like to thank Dr. Joan Knapp for proofreading this thesis. Although I could not arrange enough time to proofread, she kindly improved my writing and gave me appropriate suggestions.

I would also like to thank many people outside the laboratory. In particular, I am grateful to Maestro Hiroshi Tada for his profound teaching about life and for his warmhearted encouragement. I am also grateful to my friends, Satoshi Kagiwada, Hiroyuki Toyota, and Nobuyuki Uchikoga, for their contributions to the excitement of my student days. I am most grateful to Tomomi Masuda, whose lovely smile has made my daily life delightful.

Finally, I would like to thank my family for their support and encouragement.

Contents

1 Introduction **13**

1.1 Background 13

1.2 Thesis Organization 15

2 Previous Work **17**

2.1 Overview 17

2.2 Computer Graphics 17

2.3 Robotics 23

2.4 Biomechanics 28

3 Overview of the Model of Balance Maintenance **31**

3.1 Overview 31

3.2 Outline of the Model 32

3.3 Human Body Model 34

3.4 Zero Moment Point 34

3.5 Balance Maintenance in Stable State (PD Control) 38

4 Obtaining Human Motion **41**

4.1 Overview 41

4.2 Motion-Capturing System 41

4.3 Extracting Physical Parameters 42

4.3.1 Local Coordinates 42

4.3.2 Center of Mass 45

4.3.3 Zero Moment Point 46

4.4 Experiments 47

5 Balance Maintenance by Keeping Feet on the Ground **51**

5.1 Overview 51

5.2 Preliminary 52

5.2.1 Quadratic Programming Method 52

5.2.2 Linearization of Physical Parameters 52

5.3 Observing Human Motion 56
5.4 Model of Balance Maintenance 60
5.5 Experiments 67

6 Balance Maintenance by Stepping 73
6.1 Overview 73
6.2 Observing Human Motion 74
6.2.1 Inverted Pendulum Model 74
6.2.2 Extracting Parameters 76
6.3 Model of Balance Maintenance 77
6.3.1 Determining Trajectory of the CM 77
6.3.2 Generating Lower Body Motion 80
6.3.3 Generating Whole-Body Motion 82
6.4 Experiments 84

7 Discussion 89
7.1 Overview 89
7.2 Comparison of the Generated Motion and Human Motion 90
7.2.1 Appearance 90
7.2.2 Dynamic Property 91
7.3 Influence of Parameters on the Result 97

8 Conclusion 103
8.1 Summary 103
8.2 Future Work 105

A Determining Local Coordinates 107
A.1 Determining Points 107
A.2 Determining Coordinates 108

B Markers of Motion-Capturing System 115

C Force Plate 119

D Weight Matrix and Range of Motion for Joints 121

List of Figures

3.1 Overview of the system 33
3.2 Human body model 35
3.3 Closed loop in the legs 35
3.4 ZMP vs. Projection of the CM 36
3.5 Zero moment point 38
3.6 Supporting area by the feet 39
3.7 Stable area 39

4.1 Scene of capturing motion 43
4.2 Captured motion 43
4.3 Body elements 44
4.4 Local coordinates of the body elements 44
4.5 Two ways to calculate the acceleration of the CM 47

5.1 Procedure for determining the coefficients and the constant of $\ddot{\boldsymbol{\theta}}$ . . 55
5.2 Relationship among the position(m), the velocity(m/s), and the acceleration(m/s^2) of the CM in the sagittal plane 58
5.3 Relationship between the position and the acceleration of the CM . 58
5.4 Relationship between the velocity(m/s) and the acceleration(m/s^2) of the CM 58
5.5 Model of the motion of the CM for maintaining balance by keeping the feet on the ground 59
5.6 Torque vs. acceleration 61
5.7 Flowchart of balance maintenance by keeping feet on the ground . 63
5.8 Supporting area by the feet 65
5.9 Force applied from the backward direction 69
5.10 Force applied from the forward direction 70
5.11 Force applied from the side direction 71
5.12 Sinusoidal force applied back and forward 72

6.1 Inverted pendulum model 75
6.2 Inverted pendulum model in this method 75

6.3 Relationship between the length of the leg spring and the ground reaction . . . 78
6.4 Link structures for solving inverse kinematics . . . 81
6.5 Relationship among $\boldsymbol{P}$, $\boldsymbol{\Omega}$, $\boldsymbol{p}_i$, and $\boldsymbol{z}_i$ . . . 82
6.6 Procedure for solving inverse kinematics . . . 83
6.7 Balance maintenance by stepping . . . 86
6.8 Combination of the two methods of balance maintenance . . . 87
6.9 Balance Maintenance during Walking . . . 88

7.1 Human motion vs. generated motion (Balance maintenance by keeping feet on the ground) . . . 92
7.2 Human motion vs. generated motion (Balance maintenance by stepping) . . . 93
7.3 Human motion vs. generated motion (Combination of two modes) 94
7.4 Human motion vs. generated motion (Balance maintenance during walking) . . . 95
7.5 Applied force . . . 96
7.6 Comparison of impulse that can be handled without stepping . . . 98
7.7 Motion for various A_θ . . . 99
7.8 Trajectory of the CM for various A_θ . . . 100

A.1 Points on the body . . . 109
A.2 Point $\langle 31 \rangle$ . . . 111
A.3 Local coordinates of the body elements . . . 111

B.1 Marker labels of the motion-capturing system . . . 116

C.1 Force plate . . . 120

List of Tables

4.1 Standard mass distribution of a body 45
4.2 Properties of subjects 48

5.1 Average and standard deviation of the slope of the regression line . 57

6.1 Average and standard deviation of the spring constant k_a 79
6.2 Average and standard deviation of the stepping duration 79
6.3 Average and standard deviation of the value α_c/θ_c 79
6.4 Average and standard deviation of the value k_b 79

7.1 Impulse applied to the subject 97

A.1 Description of the points 110

B.1 Position of the markers 117

D.1 Value of A_θ and Range of motion for the joints 122

Chapter1

Introduction

1.1 Background

Recently, human and human-like motion has received a great deal of attention in many areas. In computer graphics, for example, because it is crucial to represent human motion realistically in high-quality animation, researchers have developed efficient techniques of generating human motion. As another example, in the development of industrial products, a precise model of the human body and generation of its motion are important in order to design products that are easy to use by a human, as well as to predict injury during accidents. And in robotics, a humanoid robot by Honda caused excitement because of its smooth walking.

When we consider realistic human motion, dynamic consistency of the motion is essential, and maintaining balance is fundamental to dynamic consistency. In a human-like model that supports its body by standing on two feet, the support area of the feet is small and the center of mass (CM) is in a high position; therefore, it is impossible to realize stable motion without an adequate method of balance maintenance. In particular, a method to cope with a sudden large perturbation is indispensable for stable motion. Hence, many studies of balance maintenance have been conducted in computer graphics, robotics, and so on.

In coping with large perturbations, humans themselves use flexible and effective ways to maintain balance. Humans employ large-scale whole-body motions for the purpose, such as bending down, rotating their arms, squatting down, taking a step, and so on. However, in research on balance maintenance of human-like models, such human techniques for maintaining balance maintenance have not been adequately studied.

In this study, we focus on large-scale whole-body motion against external perturbation and propose a method to generate it. Our interest is in studying a mechanism of human motion and representing it using a simple model as much as possible. Making high-quality computer graphics or controlling a humanoid robot is not our goal for the present. When making the model of the whole-body motion, we adopt the following policies:

- The model is based on the observation of human motion.
- The model is as simple a model as possible.

In order to observe human motion, we use a motion-capturing system with force plates. However, we do not use the captured motion directly to generate motion. Instead, we extract characteristics of human motion from the captured motion and construct a model of balance maintenance with whole-body motion. We design the model as simply as possible: The basic structure of it is like an inverted pendulum model, it is controlled by paying attention to global parameters, such as the CM, and the zero moment point (ZMP), and motion is generated by optimization calculation. The model does not have any reference motion or advance knowledge of the whole-body motion. It is the most important characteristic of our method that it can represent the human skill of maintaining balance with whole-body motion using a simple mechanism without any advance knowledge.

The reasons why we make a model as simple as possible are as follows: One reason is that it allows us to pay attention to only essential dynamic parameters. The difficulty of treating a human-like character is its high degrees of freedom, so it is not desirable to control all aspects of this freedom directly. The second reason is that it allows us to plan a strategy to recover balance without regard to posture. That is to say, we can generate effective whole-body motion for maintaining balance even if the posture itself momentarily gets farther away from a stable posture. The third reason is that it allows us to decouple the motion of maintaining balance from other motion. Since only essential behavior is extracted, and the model is constructed based on it, it can easily be re-coupled with another motion. For example, the motion of maintaining balance during walking can easily be generated our model.

We captured human motion of maintaining balance for four subjects. All of them are students. The reason why we choose only students is that they are considered ideal subjects to maintain balance with whole-body motion. In order to extract the fundamental essence of human motion, we observed the motion of only ideal persons who have similar properties and extracted common

characteristics.

In this thesis, first, we observe human motion and extract its essence. Next, we construct a model of balance maintenance based on the observation and generate motion using the model. Finally, we compare the generated motion with human motion. The contribution of this thesis is to make a model of complex human whole-body motion against large perturbation with a simple structure, and to confirm that characteristics of human motion are well reproduced in the generated motion by the model.

1.2 Thesis Organization

The remainder of this thesis is organized as follows: In Chapter 2, we survey previous work on motion of a human or a human-like character. In particular, since many researchers have been engaged in the study of obtaining, analyzing, and generating human motion in computer graphics, robotics, and biomechanics, we survey previous work focusing on these fields.

In Chapter 3, the overview of the proposed model is described. We present the outline of the whole system, define the human character and its notation, and introduce some important concepts, such as a closed loop and a ZMP. In this system, the human character is controlled by proportional-derivative (PD) control while it is in a stable state. We describe it in this section.

In Chapter 4, the way to obtain human motion is described. In this study, we obtain human motion using a motion-capturing system and force plates, and extract characteristic parameters from it. They play an essential role in modeling the motion of maintaining balance with whole-body motion. First, the motion-capturing system and the force plates that we used are explained. Next, the procedure to extract the parameters from the captured motion is described. Finally, what kind of motion is actually captured is described. The model constructed from the captured motion is described in the following chapters.

In Chapter 5 and Chapter 6, the model of balance maintenance with whole-body motion is described. It has two modes: keeping feet on the ground and taking a step. We describe each mode in an individual chapter. First, we observe the captured human motion precisely and extract essential behavior from it. Next, we construct the model of balance maintenance based on the result. Finally, we generate the motion of maintaining balance using the model.

In Chapter 7, the generated motion is compared with human motion. We compare it in an apparent aspect and in a quantitative aspect. From the compar-

ison, we confirm that the proposed model well represents human motion for maintaining balance with whole-body motion. In addition, we examine the influence of the parameters on the result, and we discuss the factor in the correspondence between the generated motion by our method and human motion.

In Chapter 8, we conclude our study.

Chapter2

Previous Work

2.1 Overview

Studies about motion of a human or a human-like character have taken place in various areas. In particular, many researchers have been engaged in the study of obtaining, analyzing, and generating human motion in computer graphics, robotics, and biomechanics. In computer graphics, due to an increase in the demand for realistic three-dimensional animation, researchers have developed techniques to generate consistent human motion easily. In robotics, in order to operate a humanoid robot, it is necessary to generate motions that have strict dynamic consistency. In biomechanics, researchers examine human motion from the viewpoint of dynamics. They measure human motion precisely under various conditions and make a model of it. In this section, we survey the previous work in each field.

2.2 Computer Graphics

In the computer graphics area, demand for realistic three-dimensional animation is increasing. In response to this demand, many methods to create animation effectively are proposed and have been developed. With regard to creating animation of human motion, it is important to generate human motion that *appears* to be natural, and to generate human motion as automatically as possible so that the workload of animators is minimized. A human character is usually modeled to have very high degrees of freedom, often 30 to 60 degrees of freedom, so if an animator were to generate animation by hand for such models, the workload

would be quite heavy, and high levels of skill would be required. Therefore, a method that generates natural animation of human motion from rough key frames is required.

In order to realize such a method, two approaches may be taken:

- Generate realizable motion by considering dynamic conditions.
- Generate human-like motion by using human motion captured by a motion-capturing system.

Generating Realizable Motion from Dynamic Conditions

The first approach reduces the freedom of the human character by eliminating motions that cannot actually exist based on considerations of dynamic consistency. In this approach, the issues are what criteria are adopted to examine dynamic consistency, and how strictly the consistency is pursued. In addition, another criterion is required to generate human-like motion because some dynamically consistent motion is not the same as human-like motion. Some researchers use captured human motion as the initial motion in order to realize human-like motion.

When assembling dynamic criteria, a human model with mass and inertia is an obvious starting point. This is a basic approach to considering dynamics, and many researchers have proposed such human models. Hodgins et al. developed a human model containing information about mass and inertia, and generated dynamically reasonable motion by applying torque to its joints based on PD control [32]. In this method, although only limited motions are modeled beforehand, such as running, bicycling, and vaulting, users can freely specify parameters for the motion, such as speed, direction, and so on. Extending this model, they developed a method of translating human motion into motion of another human, for example from an adult to a child, by parameterizing motion about differing mass and inertia [31].

Another approach is a model that considers not only mass and inertia but also musculoskeletal structure. Komura et al. designed a human model based on the musculoskeletal configuration of humans, performed optimization calculation on the level of available muscle power, and generated more realistic motion of a human figure [50, 51]. Such an approach can create a human figure model in a way that is similar to human movement. However, a musculoskeletal model is very costly to make and requires heavy computation because of its many degrees of freedom.

In this way, although a human model considering dynamic information can simulate a human body accurately, it is hard to deal with because of its many degrees of freedom. In order to overcome this difficulty, approaches using a simple human model have been proposed. A human body can be modeled considering only essential physical quantities, and motion is generated based on the behavior of the physical quantities. Popvić et al. proposed a human model with the following three simplifications: elbows and spine are abstracted away, upper body is reduced to the CM, and movement is abstracted to symmetric movement. Space-time optimization and dynamic calculation are performed on the simple model. As a result, the more fundamental properties of human motion are more readily handled because only essential degrees of freedom are contained in the simplified model [83]. Liu et al. made a similar simple human model including a mathematical model of body contact with the ground that could realistically generate complex motions such as running, jumping, rotating, etc., based on the model's dynamic constraints on linear and angular momentum [61]. Safanova et al. proposed a method to generate motion in low-dimensional space. The approximately 60 degrees of freedom in captured human motion can be reduced to less than ten by Principal Component Analysis (PCA). In this reduced space, physical laws such as the conservation of angular momentum, are honored. [87].

In addition to using a dynamic human model, some methods consider dynamic conditions between the model and its environment in order to treat the model in more dynamically correct way. Because most human motion is performed under the condition of contact with the ground, the ground reaction force is one of the most important external conditions. In particular, a ZMP is often used as one criterion when the interaction between the model and the ground is considered. Tak et al. proposed a dynamic filter in which a dynamically inconsistent motion created by an animator is converted to a dynamically consistent one by modifying the trajectory of the ZMP [91]. Fang et al. proposed a method to model more general cases of interaction with the environment. In this method, cases such as jumping and hanging on a bar are modeled by resolving external forces and moments, and generating dynamically consistent motion [16].

Extending approaches that consider reactions with the external environment make it possible to easily handle aggressive external perturbations. This is a great advantage of such models when considering dynamic conditions. Ko et al. generated a walking motion where the character handles a heavy load from captured motions of normal walking using inverse dynamics [49]. Oshita et al. generated the motion of maintaining balance when carrying a heavy load on the back, or receiving an impulse to the body. They controlled angular acceleration of joints in

carefully designed steps [78]. Zordan et al. designed a human model that receives joint torque as the input, and proposed a method to generate motion satisfying a space-time constraint and reacting to external perturbation, such as being boxed by someone [110].

Generating Human-like Motion based on Captured Motion Data

On the other hand, human motions can be captured and human-like motion is then generated based on captured motions. In this approach, the original motion is automatically dynamically consistent because it is human motion, but synthesized motion based on these models is not always dynamically consistent. However, because the important thing for computer graphics is that the generated motion *appears* to be natural, it is not so important whether it is dynamically consistent or not.

The most common way to edit motion is "spacetime constraints," a method to generate motion under the constraint that a specified point of the body is in a specified position at a specified time. This method was originally proposed by Witkin et al. The original spacetime method was designed for a general articulated object, not only for a human figure, and calculates required external forces and joint torques so that the object exists in the specified position at the specified time [96]. After that, Liu et al. developed an efficient way to solve spacetime constraints using hierarchical calculation [62], and Rose et al. applied it to generating motion of a human figure [86]. In the method, spacetime constraints are solved so that the torque at the joints becomes minimal, and thus dynamic calculation is required to solve spacetime constraints. However, Gleicher proposed a new type of spacetime constraints, in which all dynamic calculations are omitted and motion is generated using captured human motion for the reference and constraints about the position and the time [21]. The omission of dynamic calculation enables spacetime constraints to be solved easily. Indeed the resultant motion is not necessarily dynamically consistent, but because the captured human motion is used for reference, it is sufficiently realistic to be used for computer graphics, in which appearance is more important than dynamic consistency. Since then, many researchers in computer graphics have used spacetime constraints. Lee et al. improved the Gleicher method to a more efficient one using hierarchical calculation [59]. Yamane et al. developed a real-time system called a "pin-and-drag interface" to edit motion that satisfies spacetime constraints based on inherently efficient inverse kinematics calculations. [104, 107].

In spacetime constraints, motion is modified indirectly through constraints

about body parts. On the other hand, there are methods to directly modify motion by controlling the parameters of motion. Bruderlin et al. proposed "motion signal processing" in which human motion was decomposed in the frequency domain and the trajectory was modified for every frequency component [8]. Witkin et al. proposed "motion warping", in which motion was warped not only in space but also in time [97].

For another way to generate human motion, methods of blending human motions are often used, but there is the problem that they usually generate unrealistic results unless the input motions are similar and are chosen carefully by a user. Kovar et al. developed an improved blending method that can allow a variety of input motions compared to previous methods. In Kovar's method, matching of input motion is first found by a "dynamic time warping" technique, and then high quality blended motion is generated based on a matching process [52].

The above methods are mainly methods that modify a motion sequence captured by a motion-capturing system. On the other hand, methods to generate motion from a limited number of keyframes are proposed. These methods interpolate frames between the keyframes so that the result will look like natural human motion. The interpolation often uses a database made from a large set of human motions as well as empirical knowledge gained by observing human motion. Pullen et al. proposed a technique of interpolation based on "motion signal processing" and "dynamic time warping" [84]. Yamane et al. proposed a method based on path planning [101]. This method is used to generate natural-looking, whole-body motions for a wide range of manipulation tasks, while respecting environmental and posture constraints. Knowledge obtained from captured human motion and constraint-based inverse kinematics is used here. Neff et al. proposed a method to generate human motion based on knowledge from observation of human motion [73].

Statistical models and learning models are also used to generate motion. Brand et al. proposed a "style machine " that is based on the Hidden Markov Model (HMM) [7]. It can generate new motion sequences in a broad range of styles by adjusting a small number of stylistic knobs (parameters). Faloutsos et al. proposed a motion controller based on a support vector machine (SVM) learning method that could generate various kinds of motion such as walking, running, falling down, and so on [14]. Li et al. proposed a method of motion editing based on a linear dynamic system (LDS) [60]. In this model, captured motion is divided into small segments, and continuous motion is generated by concatenating the segments based on the LDS model. Grochow et al. proposed a method of

inverse kinematics based on the Scaled Gaussian Process Latent Variable Model (SGPLVM) [24]. Likelihood of a posture is calculated from captured motion, and reasonable posture is determined by it. As the study by Li et al. shows, many researchers have developed a method to generate motion by concatenating small segments. Typical methods are "motion graphs" by Kovar et al. [53], real-time methods by Lee et al. [58] and Arikan et al. [2], a method considering rhythms by Kim et al. [48], and a method using annotations by humans (for example, run, walk, jump, etc.) by Arikan et al. [3]

From what have been surveyed above, we can see that very few attempts have been made in computer graphics to generate active motion for handling external large perturbations. The reason for this may be that researchers are interested in a method to modify motion after a creator decides its outline, instead of a method to generate an active reaction automatically. In studies mentioned above, only Oshita et al. [78] and Zordan et al. [110] consider active reaction.

Oshita et al. generated the motion of a human figure responding to a heavy weight and an external impulse in real-time. They simplified a human body to three parts, and then adopted carefully designed control techniques to these parts. The simplification is for reducing the computational cost. In our study, we also simplify a human body. However, our objective is not reducing computational cost, but extracting an essential mechanism of human balance maintenance. They designed control techniques for the simplified model. These are well designed, but too heuristic. We use optimization calculation to generate motion, and confirm that it is sufficient to represent the characteristics of human motion.

Zordan et al. generated reactive motion using PD control. In this method, when a external perturbation is applied to a character, it sways the body along the perturbation and then returns the body to its initial position. This is one strategy to handle external perturbation. However, a human has more complex ways of maintaining balance, such as rotating the arms, bending down, and taking a step, and these motion cannot be generated by Zordan's method.

The objective of studies in computer graphics is developing a method to generate the motion of a human figure that looks like actual human motion as automatically as possible. It is similar to our objective to construct a model of balance maintenance that can represent human balance maintenance using a structure as simple as possible. Therefore, our method shares a similar framework with many methods in computer graphics. This framework, which begins with the outline of motion determined by a simplified human body and then uses optimizing calculation to achieve full-body motion, is adopted by many methods used in computer graphics.

However, our objective is not only generating human-like motion, but also extracting essential mechanisms of human motion by observing this motion and making a model of human motion based on the observation. In computer graphics, a creator decides that a certain condition simulates human motion. The motion becomes similar to human motion by the creator's appropriate tuning of keyframes. In our study, such a condition is extracted from the observation of human motion and is included in the model.

2.3 Robotics

Research into humanoid robots generates great interest in both the scientific community and popular culture. Needless to say, the most important feature of a humanoid robot is that it has a human-like figure. Ideally, a humanoid robot could perform a cooperative task with a human [109] or work in a dangerous area such as a construction site instead of a human [26, 27]. A humanoid robot is also desirable for entertainment. Current production models include the Honda P2, P3 and ASHIMO, all of which have had a great impact on the robotics field, [28, 29, 30] as well as the Sony QRIO, a small robot that can walk, dance, jump, and run, [36, 35, 57, 34].

However, generation of stable motion for a humanoid robot is quite difficult because of its high degrees of freedom and its unstable structure. The CM of a humanoid robot is located at a high position, and the area presented by the convex hull of the feet is small. Although gait motion is one of the most fundamental motions for humans, stable biped locomotion for robots is still a challenging problem and many studies about it have been conducted.

The problem is not only that the computational cost increases with the number of degrees of freedom, but also that we have to treat a closed-loop structure caused by the contact between the body and its environment during dynamic calculations. When treating a closed-loop structure, the degree of freedom at every joint is restricted, and, moreover, the torque at joints is not determined uniquely by inverse dynamics. Nikravesh et al. investigated dynamics of the articulated object containing a closed loop, and proposed a systematic method to deal with multi-body systems containing closed kinematic loops [75, 76, 74]. It is also a problem that the kinematics of the model often changes during motion depending on the method of contact with the environment. Yamane et al. proposed an algorithm for computing the forward dynamics of such structure-varying kinematic chains [102, 71]. The algorithm is applied to a simulator for a humanoid robot [70], and the computational complexity is improved from $O(N^3)$ to $O(N)$

in serial computation and to $O(\log N)$ in parallel computation, where N are the degrees of freedom of the kinematic chain [106].

When we treat a humanoid robot with many degrees of freedom in a closed loop, it is preferable to use a simplified model rather than to treat such a complex structure directly. Models simplified by focusing only on trajectories of the CM are often used since complex models are hard to treat. One of the most useful concepts for discussing the movement of the CM is a ZMP. The ZMP proposed by Vukobratović et al. [93, 94], is the point at which all the ground reaction is regarded as acting. By using a ZMP, it is possible to treat the motion of a robot as the relationship between the CM and the ZMP. In addition, the concept of a ZMP can also be used to test whether a designed motion can be executed by a robot without falling down. For an example of the use of a ZMP, Goswami proposed the concept of a foor rotation indicator (FRI) point, which is a extension of a ZMP to indicate the degree of stability (or instability) of the motion. [22]

Many methods to generate motion of a humanoid robot considering the CM and the ZMP have been proposed so far. Kagami et al. proposed a real-time algorithm to generate dynamically-stable compensation motion for a given input motion [38]. In this method, a "dynamic balance compensator" generates the compensation motion by solving a second order nonlinear programming optimization problem containing a ZMP constraint. Nishiwaki et al. developed a real-time system to generate humanoid walking motion [77] based on the motion pattern generation technique that follows the desired ZMP proposed by Kagami et al. [39]. Sugihara st al. proposed a real-time motion generation method that controls the CM by indirect manipulation of the ZMP by "the COG Jacobian" [89]. Kurazume et al. utilized the method of a "sway compensation trajectory" designed for a quadruped walking robot, and developed the method to generate biped walking motion [56]. In this method, a ZMP is specified as the diagonal line between supporting legs. Kajita et al. proposed a dynamic model for real-time walking control called 3D-LIPM (Three-Dimensional Linear Inverted Pendulum Model) [44, 42, 43]. It simplifies the relationship between the CM and the ZMP to a three-dimensional inverted pendulum in which motion is constrained to move along an arbitrarily defined plane. Software to control a humanoid robot was also developed based on the model [108].

In most of the walking pattern generators, including the above methods, only linear momentum of the CM is considered. Angular momentum is seldom considered except in the case that its time-differentiation, moment, is indirectly considered in the ZMP calculation. However, because induced moment around the yaw-axis cannot be dealt with by consideration of a ZMP, undesired "slip"

around the yaw-axis is unavoidable, particularly in high-speed motion. To mitigate this problem, methods considering not only linear momentum but also angular momentum have been proposed. Yamaguchi et al. proposed a control method of dynamic biped walking in which a robot was stabilized by a trunk motion compensating for the three-axis moment on an arbitrary planned ZMP [99, 100]. Kajita et al. proposed a method to generate whole-body motion of a humanoid robot so that the resulting total linear and angular momenta became specified values [41]. In the method, first, a linear equation that calculates the momenta is derived, and then the whole-body motion is generated. Goswami et al. studied the fundamental mechanics of rotational stability of multi-body systems, and proposed three control strategies that can recover stability in a biped robot [23].

In the methods that have been introduced so far, a robot executes biped walking actuated by motors. On the other hand, a method in which biped walking is realized without a motor is proposed. A robot can be actuated only by gravity, and this is called "passive walking," while biped walking actuated by a motor is called "active walking." The concept of passive walking was originally proposed by McGeer [64] as a two-legged walking mechanism on a two-dimensional plane. Once it starts on a shallow slope, it settles into a steady gait. The motion is quite comparable to human walking. Originally the mechanism had no knees and moved like a compass, but a mechanism with knees in the swing leg was proposed later [65]. Although a model actuated by only gravity is simple, the resulting motion is quite comparable to human walking. Thus it was to be expected that analysis of passive walking leads to understanding of human walking mechanisms. After that, some researchers analyzed the feature of passive walking [54, 88], and other researchers produced passive walking on a flat floor by applying minimum torque to the joints with a motor [4, 5, 55]. Passive walking is easy to treat analytically if we consider two-dimensional passive walking. However, when considering three-dimensional passive walking, the analytical approach becomes quite complex. Formerly, most research was performed in two-dimensional space. Recently, Collins et al. studied passive walking in three-dimensional space [10].

Because there are many difficulties in producing stable motion by a humanoid robot, even walking has been a challenging problem for long time. In fact, most of the studies about a humanoid robot make stable walking their subject. However, in order for a humanoid robot to execute expected work in our living space, it has to move in a more complex way than merely walking. As a study of such complex motion, the way for a humanoid robot to fall down safely is studied, in contrast to the previous study where a humanoid robot was controlled to avoid falling down.

With regard to a humanoid robot that is the same size as a human, Fujiwara et al. proposed a method to minimize damage to a humanoid robot when it falls over on the ground by controlling the posture of the robot so that it lands first on its the shock-absorbing parts [17, 20]. They also developed a system that allows a humanoid robot to get up from the floor. They produced a humanoid robot that can lie down on the floor and get up from the floor [46]. Recently, they produced a humanoid robot that can safely fall over by reducing the impact of falling and can stand up by itself [18, 19]. Terada et al. also produced a humanoid robot that can get up by "roll-and-rise motion" [92]. In their method, a robot stands up in a single motion from the state of lying down flat. Like a human, it first swings both of its legs up high, swings them down, rolling forward and up on both feet, then extends its legs to achieve a standing posture.

Running motion has also been studied. Running is a gait in which there is a moment when both feet are in the air, while walking is a gait in which one foot is always in contact with the ground. Nagasaka et al. succeeded in producing humanoid running with QRIO, which is a humanoid robot 580 mm tall [66]. Nagasaki et al. also succeeded in this with HRP-2, which is the same size as a human [68, 45, 67]. For other studies about complex motion, Wooten et al. proposed a technique for generating transitions between simulated behaviors [98]. They parameterized various behaviors, such as leaping, tumbling, landing, balancing, and so on, and designed control systems to concatenate them, maintaining dynamic consistency. Faloutsos et al. proposed a framework for composing motor controllers into autonomous composite reactive behaviors for physically-simulated humanoid robots based on Support Vector Machine (SVM) learning theory [15].

As we have seen, humanoid motion has been generated in constructive ways in many research projects involving a humanoid robot. Some researchers also proposed a method to generate humanoid motion by converting captured human motion or created motion by an animator. Yamane et al. proposed the concept of "dynamics filter", which transforms a physically inconsistent motion into a consistent one [103, 105]. Nakaoka et al. developed a system to generate the whole-body motion of a humanoid robot imitating human motion captured by a motion-capturing system [72].

In robotics, the most important thing is that a humanoid robot actually moves, thus robotics researchers have paid attention to only this goal for a robot. However, because the most important characteristic of a humanoid robot is that it has a similar structure to a human and achieves verisimilitude, it is important to observe human motion carefully and to make use of that knowledge to control a humanoid robot. Recently, Nakamura et al. developed a detailed musculoskeletal

human model and estimated the somatosensory information of a human during whole-body motions [69]. Applying the model to the dynamics computation algorithms for kinematic chains, they analyzed various characteristics of human motion from the point of view of muscle power. Kagami et al. compared humanoid walking to human walking using a motion-capturing system and force plates [40].

The method proposed in this thesis also makes use of knowledge from the observation of human motion. Besides analyzing captured human motion, we construct a model of balance maintenance and generate motion of a human-like character.

In robotics, although many researchers have tried to produce well-balanced motion by a humanoid robot, there are few studies that consider the effect of large external perturbation. In studies mentioned above, Sugihara et al. [89] and Fujiwara et al. [18, 19]treated it.

Sugihara et al. generated stepping motion against external perturbation. They controlled the CM by indirect manipulation of the ZMP. Since the objective of the study is real-time motion generation, the algorithm takes care of only generating dynamically consistent motion effectively. It is not concerned with how a human takes a step when he or she receives external perturbation.

Fujiwara et al. dealt in larger external perturbation. Against such perturbation, they did not try to maintain balance, but tried to safely fall down so as to reduce damage to the hardware. Such a strategy is necessary when we consider using a humanoid robot in real life. However, if it is possible to maintain balance without falling down, that would be even better. In this thesis, we discuss maintaining balance without falling down.

Comparing our study to studies in robotics, there are a lot of things in common for individual methods or concepts that are used in generating motion. In particular, the concepts of a ZMP and an inverted pendulum model, which are significant concepts for our method, are ordinary concepts in robotics.

However, our objective is different from that in robotics. Since the interest of robotics researchers is to make a humanoid robot actually move, it can be said that generating well-balanced motion is the major part of their objective. On the other hand, it is only one condition of generating human-like motion in our method. Dynamically consistency of motion is employed to constrain the probability of motion. The objective of our study is to extract essential mechanisms of human motion by observing human motion and to make a model of it.

2.4 Biomechanics

In biomechanics, many studies that examine human motion precisely from the viewpoint of dynamics have been undertaken. With regard to balance maintenance, researchers have measured human motion under various condition, and have modeled it in various ways.

Balance maintenance during upright posture is a major topic in biomechanics. A human maintains balance by feedback from the ground reaction, causing the human to sway the upper body. Many researchers have measured and modeled this movement precisely [9, 95, 82, 1, 13].

With regard to balance maintenance against perturbations, the body's response to external forces has been examined by applying forces experimentally. In particular, the relationship of the position of the CM and the posture of the lower body in response to perturbation has been studied precisely. Gu et al. measured the difference of postural adjustment between young children and adults [25]. Rietdyk et al. and Matjačić et al. designed special equipment to specify conditions such as the position and the strength of forces applied to a human with corresponding measurements of the human response [85, 63].

Studies of maintaining balance by stepping have also been made. An inverted pendulum model is often used here [11, 80, 33, 81]. It is often used in robotics in order to deal with the complex structure of a humanoid robot. The inverted pendulum model is also useful to analyze human motion by abstracting it. Pai et al. examined cases where feet slipped and proved that a model designed for cases where no slipping occurs and be applied in cases where slipping does occur [79]. While the CM is mainly focused on studies with an inverted pendulum model, there have also been studies that consider the structure of the lower body. Tagawa et al. and Kepple et al. measured the torque and the moment at joints induced by stepping [90, 47]. Bauby et al. and Donelan et al. modeled human walking based on passive walking, which was proposed in robotics, and compared it to human walking [6, 12].

The objective of our study is to model the mechanism of maintaining human balance with whole-body motion. It is very similar to the objective of studies in biomechanics. As mentioned above, many researchers have measured human motion precisely and have modeled it. However, the model that we try to make is not only one that describes human motion, but also one that can reproduce whole-body motion. In biomechanics, since the important thing is to understand human motion as precisely as possible, the measurement is performed for restrained motion under restrained situations. For that reason, researchers have

not studied large-scale whole-body motion to maintain balance, which is a main topic in our study, because it is difficult to measure such motion precisely under a restrained situation. Our objective is not to make precise model of human motion, but to show that an apparently complex human motion to maintain balance is representable by a simple model.

Chapter3

Overview of the Model of Balance Maintenance

3.1 Overview

In this chapter, the basic concept of the proposed model of balance maintenance is described. As mentioned in Chapter 1, the model is constructed based on the following concepts:

- The model is based on the observation of human motion.
- The model is made as simple a model as is possible.

Regarding the first concept, we capture human motion using a motion-capturing system and force plates, and analyze it in order to extract essential characteristics from it. We construct a model of balance maintenance based on it. Regarding the second concept, our model consists of a simple structure like an inverted pendulum model, the extracted parameters, and optimization calculation. It is controlled via global quantities, such as the CM and the ZMP. The advantage of a simple model is as follows:

- One can pay attention to only the essential part of motion.
- Effective whole-body motion can be generated even if the posture momentarily gets far away from a stable posture.
- Motion of maintaining balance can be decoupled from other motion.

In the following sections, we describe how to construct such a model. First, the outline of the whole system is presented. Next, the human model and its

notation are defined. Third, a ZMP, which is a key concept of dynamic balance maintenance, is described. Finally, balance maintenance when the character is in a stable state is described. The other models of balance maintenance, keeping feet on the ground and stepping, are major topics of this thesis; thus, they are detailed later in separate chapters.

3.2 Outline of the Model

In this study, we focus on large-scale whole-body motion against large perturbation. We capture such motion by a motion-capturing system, and abstract a fundamental structure of motion and parameters controlling the structure from it. When we generate motion, we use optimization calculation about angular acceleration of joints based on the structure with the parameters. We call the framework the model of balance maintenance in this thesis. The model of balance maintenance has two modes: balance maintenance by keeping feet on the ground and balance maintenance by stepping.

In addition, when the human-like character is in a stable state, its posture is adjusted by PD control. The definition of "stable posture" is discussed later. To simplify the description, the initial posture is assumed to be standing upright, which is a stable state. An example of another initial posture is described in a later chapter (Chapter 6).

The flowchart of the system is shown in Figure 3.1. In a stable state, the character maintains its balance by PD control. When a small perturbation is applied, it can be dealt with by PD control. If the perturbation is too large for PD control to cope with, balance maintenance by keeping the feet on the ground is employed. If balance is recovered by it, PD control is again adopted for final postural adjustment to the upright posture. If balance maintenance by keeping the feet on the ground fails, that is, no possible motion without stepping is found, balance maintenance by stepping is adopted.

In PD control, torque is applied to the joints so that the posture of the character gets closer to the target posture. This works well only when perturbation is small.

In balance maintenance by keeping the feet on the ground, the angular acceleration of the joints is optimized using optimization calculation. The motion to make the CM return to the initial position as soon as possible is generated here, and posture itself is not directly considered. Therefore, the motion that is effective for recovering balance can be generated even if the posture momentarily gets farther away from the target posture.

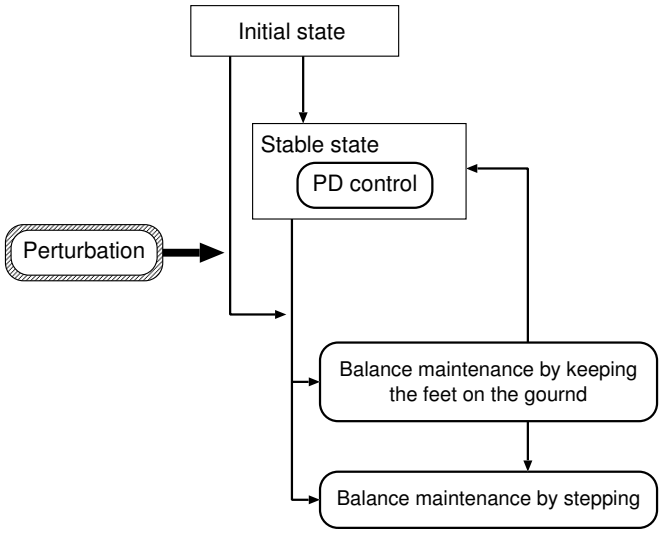

Figure 3.1: Overview of the system

In balance maintenance by stepping, the character prevents its body from falling down by taking a step, thereby widening its base of support for the feet. The largest perturbation can be handled by this method. However, the character does not return to the initial posture after it takes a step.

In this model, motion of maintaining balance is generated frame by frame. An advantage of this method is computational cost, which is less than a global method. A global method, which considers the whole sequence of motions at the same time, requires heavy computation because the data size increases depending on the number of time frames. Another advantage of this method is that a human way to move is based on local strategy. Generating human-like motion is one of the main goals of this study, and therefore, human-like strategy is desirable. However, a disadvantage of frame-by-frame strategy is a risk of falling a local minimum. For avoiding a local minimum, constraints based on observation of human motion are utilized when optimization calculation is performed. For dynamic calculation of an articulated object, we use SD/FAST by Symbolic Dynamics, Inc.

3.3 Human Body Model

The human body model, depicted in Figure 3.2, consists of fifteen linked rigid body parts, and has fourteen joints and thirty-four degrees of freedom. Two types of joints are used in this model: pin joints, which have one degree of freedom, and ball joints, which have three degrees of freedom. The coordinate system in this paper is defined as in the figure. The x- and z-axes are on a horizontal plane, and the y-axis is perpendicular to the horizontal plane.

When the model stands on both feet, there is a closed-loop structure in the legs. Because of it, the actual degrees of freedom of the lower body are reduced from fourteen to eight. Figure 3.3 shows the degrees of freedom considering the closed-loop constraint. Now, two variables of $\boldsymbol{\theta}$ and $\boldsymbol{\varphi}$ are defined. The former is a vector whose elements represent the angles of the joints, and the latter is a vector whose elements represent the actual degrees of freedom of the model. When the model is supported by both feet, $\boldsymbol{\varphi}$ means the reduced degrees of freedom; when it is supported by one foot and there is no closed-loop structure, it is the same as $\boldsymbol{\theta}$. The optimization is always done about the actual degrees of freedom $\boldsymbol{\varphi}$.

3.4 Zero Moment Point

A zero moment point (ZMP) is a key concept of dynamic balance maintenance, which is proposed by Vukobratović et al. [93, 94]. It is the point where the moment (strictly speaking, the horizontal elements of the moment) induced by the ground reaction becomes zero. Because the concept of a ZMP plays a vital role in the proposed method, we describe it minutely in this section.

When we consider static balance, the condition of equilibrium is that the projection of the CM is inside the supporting area by the feet. If it goes out of the area, the static balance is broken and the human begins to fall down. However, when we consider dynamic balance, the human does not lose his or her control unless the ZMP is inside the support area, even if the projection of the CM goes out of the area. If the ZMP is on the boundary of the area, the human begins to fall down. Contrary to the projection of the CM in static balance, the ZMP stays on the boundary during falling down and never gets out of the area (Figure 3.4).

Now, consider a flat floor. The x- and z-axes of the coordinates are on the floor and the y-axis is a vertical axis. If a human stands on the floor, the moment

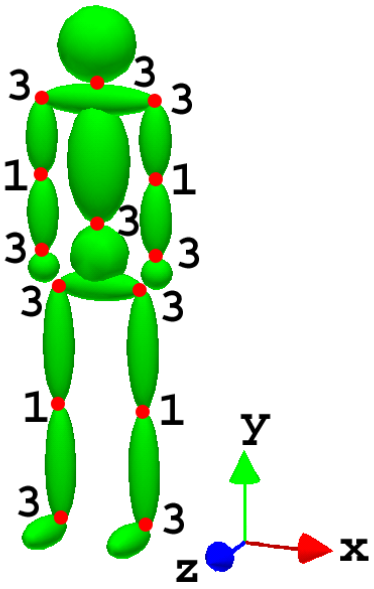

Figure 3.2: Human body model: Numbers at joints are degrees of freedom of the joint.

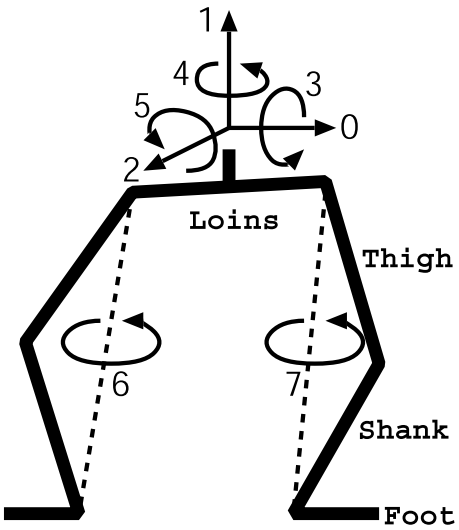

Figure 3.3: Closed loop in the legs

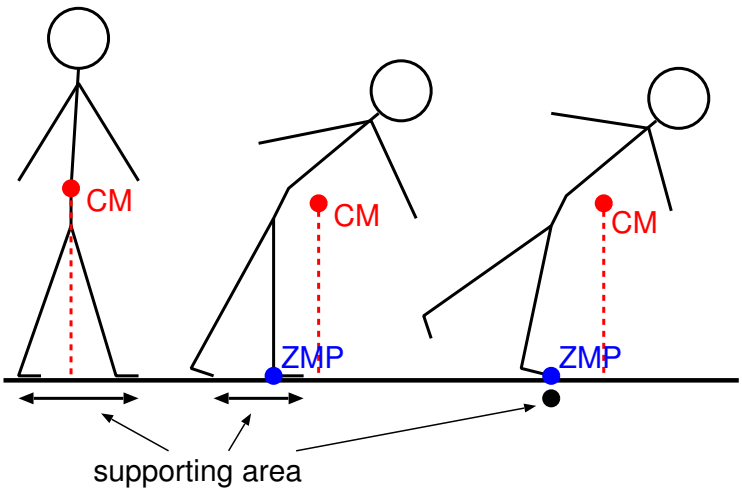

Figure 3.4: ZMP vs. Projection of the CM: The projection of the CM is inside the supporting area when the static balance is kept (the left figure). If it goes out of the area but the ZMP is still inside the area, the dynamic balance is kept (the middle figure). If the ZMP reaches the boundary of the area, which shrinks to a point in the figure, the dynamic balance is lost and the human begins to fall down (the right figure).

induced by the ground reaction with respect to a point $\boldsymbol{p}$ is written as

$$\begin{aligned}\boldsymbol{n_p} &= \int_X (\boldsymbol{x} - \boldsymbol{p}) \times \boldsymbol{f}(\boldsymbol{x}) d\boldsymbol{x} \\ &= \int_X \boldsymbol{x} \times \boldsymbol{f}(\boldsymbol{x}) d\boldsymbol{x} - \boldsymbol{p} \times \int_X \boldsymbol{f}(\boldsymbol{x}) d\boldsymbol{x},\end{aligned} \tag{3.1}$$

where $\boldsymbol{n_p}$ is the moment, X is the area where the feet contact the ground, $\boldsymbol{x}$ is a point in X, and $\boldsymbol{f}(\boldsymbol{x})$ is the force acting on $\boldsymbol{x}$. According to the above equation, if $\boldsymbol{p}$ is on the floor (*i.e.* $\boldsymbol{p} = (p_x, 0, p_z)^T$), $\boldsymbol{p}$ can be determined so that the horizontal elements (x- and z- elements) of $\boldsymbol{n_p}$ are zero (*i.e.* $\boldsymbol{n_p} = (0, n_{py}, 0)^T$). Such $\boldsymbol{p}$ is called a ZMP.

Let $\boldsymbol{s}$ be the CM of the body, and the moment around the CM when no external force except the ground reaction acts is written as

$$\begin{aligned}\boldsymbol{n} &= \int_X (\boldsymbol{x} - \boldsymbol{s}) \times \boldsymbol{f}(\boldsymbol{x}) d\boldsymbol{x} \\ &= \int_X \{(\boldsymbol{x} - \boldsymbol{p}) + (\boldsymbol{p} - \boldsymbol{s})\} \times \boldsymbol{f}(\boldsymbol{x}) d\boldsymbol{x} \\ &= \boldsymbol{n_p} + (\boldsymbol{p} - \boldsymbol{s}) \times \boldsymbol{F},\end{aligned} \tag{3.2}$$

where $\boldsymbol{n}$ is the moment and

$$\boldsymbol{F} = \int_X \boldsymbol{f}(\boldsymbol{x}) d\boldsymbol{x} \tag{3.3}$$

is the integration of all ground reaction. Therefore, we can consider only the force $\boldsymbol{F}$ and the moment $\boldsymbol{n_p}$, instead of the ground reaction (Figure 3.5).

When no external force except the ground reaction acts, Newton's equation is written as

$$\boldsymbol{F} = m(\ddot{\boldsymbol{s}} - \boldsymbol{g}), \tag{3.4}$$

where m is the mass of the body and $\boldsymbol{g}$ $(= (0, g_y, 0)^T)$ is the gravity acceleration. Substituting this, the equation (3.2) can be solved about the ZMP $\boldsymbol{p}$ $(= (p_x, 0, p_z)^T)$:

$$p_x = \frac{n_y + s_x m(\ddot{s}_y - g_y) - s_y m \ddot{s}_x}{m(\ddot{s}_y - g_y)} \tag{3.5a}$$

$$p_z = -\frac{n_y - s_z m(\ddot{s}_y - g_y) + s_y m \ddot{s}_z}{m(\ddot{s}_y - g_y)}. \tag{3.5b}$$

As mentioned above, the ground reaction is replaceable to the force acting at the ZMP; thus, the ZMP is always within the area where the foot or feet contact the ground or within the convex hull constructed by the feet (see Figure 3.6). This fact can be used as the test of dynamic consistency of synthesized motion.

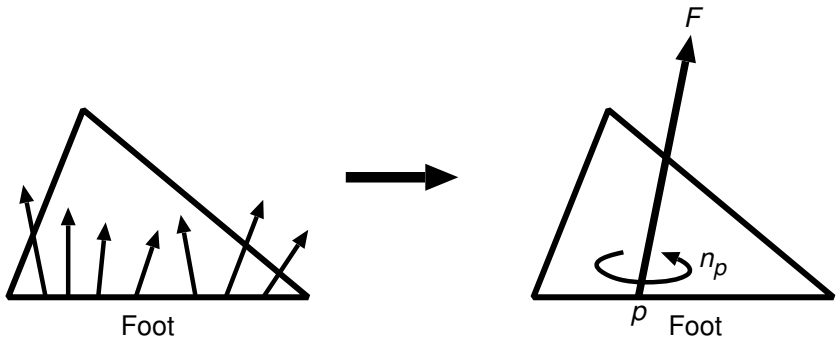

Figure 3.5: Zero moment point: The ground reaction can be replaced by the same force acting on the ZMP ($\boldsymbol{F}$) and the moment of the vertical element around the ZMP ($\boldsymbol{n_p}$).

If a motion is generated by an animator or a computer program, the acceleration of the CM ($\boldsymbol{s}$) and the moment around the CM ($\boldsymbol{n}$) can be calculated from the motion and the knowledge about the body that is given beforehand, such as the mass, the inertia tensor, and the kinematics of the body. Substituting these $\boldsymbol{s}$ and $\boldsymbol{n}$ in the equations (3.5), the trajectory of the ZMP corresponding to the generated motion is calculated. If the ZMP gets out of the foot support area even momentarily, the motion is dynamically inconsistent, and then it can be said that the motion is impossible in practice.

3.5 Balance Maintenance in Stable State (PD Control)

First, we define the "stable state". It is judged by the position of the projection of the CM of the body. The stable area is specified as Figure 3.7, and if the projection is inside the area, the state is judged as the stable state. The area is specified to be similar to the supporting area, and the scale factor can be set by a user freely. In the following experiment, we use the 1/2 for it.

In the stable state, the postural adjustment by PD control is executed. In practice, a human maintains balance in a complex way. A human sways his or her upper body slightly during stance and performs feedback balance maintenance.

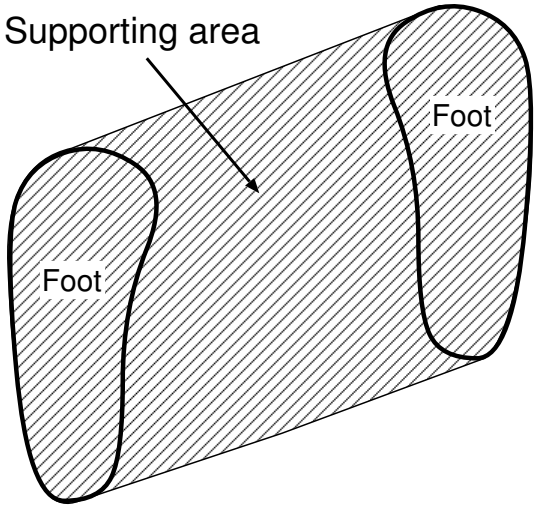

Figure 3.6: Supporting area by the feet: When a human stands on two feet, the supporting area in which the ZMP has to exist is the convex hull constructed by the feet.

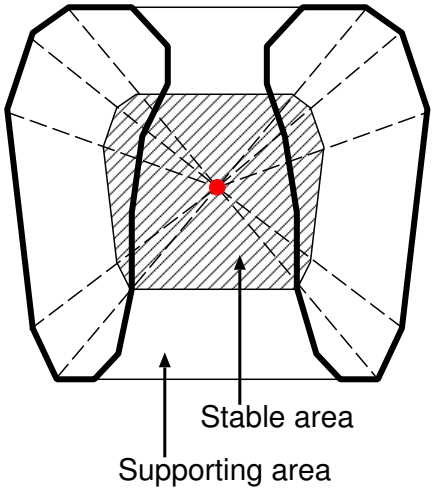

Figure 3.7: Stable area: The stable area is similar to the supporting area. If the projection of the CM is inside the area, the state is judged as the stable state.

In biomechanics, this complex balancing can be measured and modeled precisely [9, 95, 82, 1, 13]. However, because our study focuses on large motions for maintaining balance, this complex balance maintenance is not simulated. Instead, simple PD control is employed during the stable state.

The strategy of PD control is adopted for small perturbations and for the final postural adjustment, with the goal of returning the posture of the model to the initial posture. Proper torque for the joints is calculated by the following formula:

$$\boldsymbol{\tau} = -K_p(\boldsymbol{\theta} - \boldsymbol{\theta}_0) - K_d(\dot{\boldsymbol{\theta}} - \dot{\boldsymbol{\theta}}_0), \tag{3.6}$$

while $\boldsymbol{\theta}_0$ and $\dot{\boldsymbol{\theta}}_0$ are the target angle and angular velocity, and $K_p(> 0)$ and $K_d(> 0)$ are constants. The reason why the torque is calculated rather than the acceleration ($\ddot{\boldsymbol{\varphi}}$) is that the closed-loop problem need not be considered when applying torque. Because PD control is performed in the stable state and the required motion is not large, this simple strategy works well. But when balance is maintained by the large motions involved in keeping feet on the ground or by stepping, this simple strategy does not work well. Motion has to be generated by considering varying degrees of freedom ($\ddot{\boldsymbol{\varphi}}$).

The constants in the above formula are determined adaptively under constraint to keep the ZMP in the support area. First, the ZMP is calculated by the initial values of K_p and K_d. If the ZMP is outside the supporting area, the values are decreased and the ZMP is calculated again. When the ZMP is within the supporting area, the corresponding torque is adopted. The initial values are determined empirically. The result is not sensitive for these values, but it becomes stable when the larger value is set for K_p compared to K_d.

Chapter4

Obtaining Human Motion

4.1 Overview

In this chapter, the way to capture human motion is described. A characteristic of our model is that it is based on observation of human motion. Thus, capturing human motion and abstracting essential mechanisms from it are key procedures in our model. A motion-capturing system and force plates are used for this purpose. First, detailed descriptions of this equipment are presented. Then, the method of obtaining physical quantities, such as the CM, the ZMP, and so on, is described. Finally, the kinds of motions that are captured in practice are described.

4.2 Motion-Capturing System

In order to capture human motion, the motion-capturing system at Aizu University is used in this study. It consists of a three-dimensional optical motion capture by VICON Motion and force plates by Kistler Japan. The motion capture records the position of markers attached to a human body. The markers are made of a material that reflects infrared rays, eight infrared cameras take images of them, and the position is calculated from the images. The force plates record the position, the magnitude, and the direction of the ground reaction. The size of one plate is 1200 mm by 600 mm, and for every plate, the resultant force is obtained. The algorithm used to calculate the resultant force is detailed in Appendix C. The data from the motion capture and the force plates are automatically synchronized. The frame rate is 250 frames per second.

Figure 4.1 shows the process of capturing motion. The red lights near the ceiling are the infrared cameras, and the silver balls on the subject's body are the markers. Figure 4.2 shows the captured motion. The green pyramids stand for the markers, the red lines stand for the ground reaction force, and the white rectangles on the floor stand for the force plates.

4.3 Extracting Physical Parameters

As mentioned in the previous sections, the motion-capturing system records the position of the markers attached to the subject's body, and the force plates record the direction and the magnitude of the ground reaction. For analyzing human motion, various quantities, such as the CM and the ZMP, have to be calculated from the data. In this section, the way to obtain such quantities is described.

4.3.1 Local Coordinates

First, we divide a human body into several elements, and determine the local coordinates for them. The body is treated as an articulated object consisting of elements. A body is depicted as Figure 4.3. The positions of the elements are determined from data of the motion-capturing system in three ways. First, the positions of several joints are determined from the position of the markers. Second, the CM of the elements is determined. Third, employing the CM as the origin, the local coordinates are determined. The local coordinates are illustrated in Figure 4.4. The details of calculating them are described in Appendix A.

For every element, the mass and inertia have to be determined. These cannot be determined from data gathered by the motion-capturing system and the force plates, but there is research about mass and inertia of humans, for example, [37]. In this study, a standard mass distribution is used and displayed in the following table (Table 4.1).

With regard to the inertia, each element is approximated with a cylinder, and the inertia is calculated. The mass and the length of the elements are determined already, then the radius of the cylinder is calculated as

$$r = \sqrt{\frac{m}{\rho \pi h}}, \tag{4.1}$$

where r is the radius, m is the mass, h is the length, and ρ is the density. In this

Figure 4.1: Scene of capturing motion: The red lights near the ceiling are the infrared cameras, and the silver balls on the subject body are the markers.

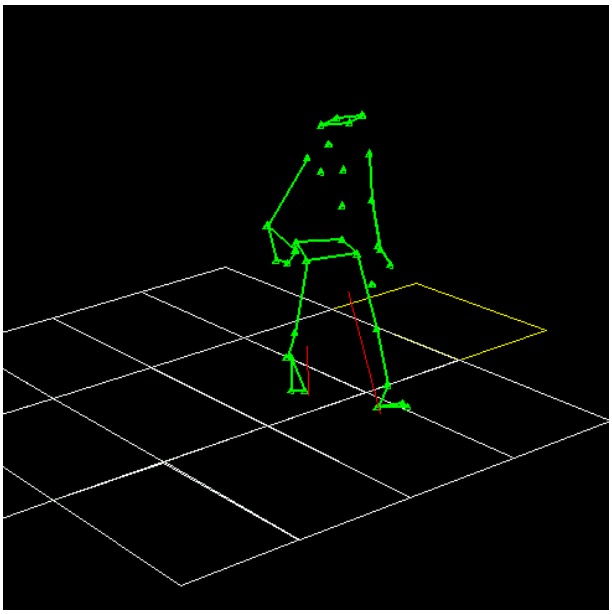

Figure 4.2: Captured motion: The green pyramids stand for the markers, the red lines stand for the ground reaction force, and the white rectangles on the floor stand for the force plates.

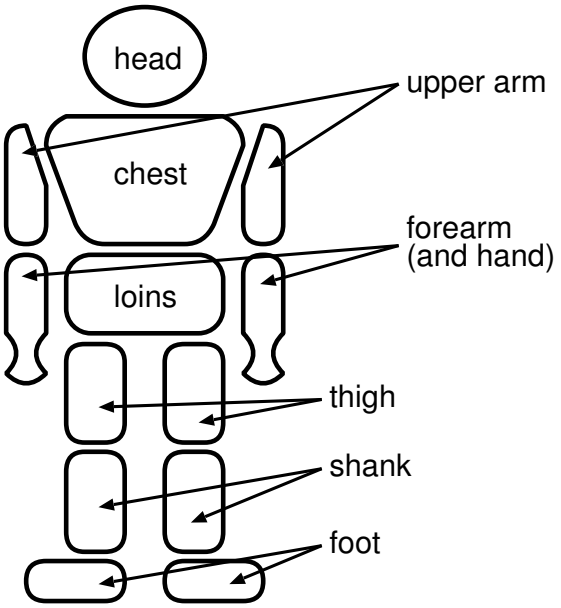

Figure 4.3: The body elements: The body is divided into thirteen elements.

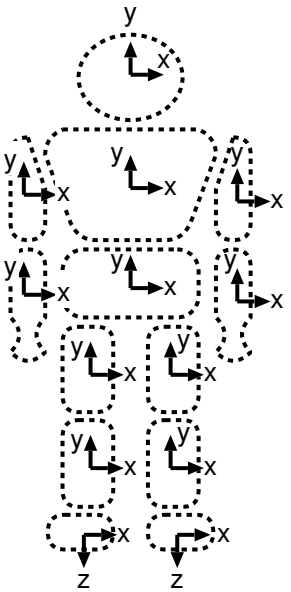

Figure 4.4: Local coordinates of the body elements: The x axis is basically set to be parallel to the pivot of the joints. The y axis is basically set to point the upward direction.

Element	Mass (%)		
head	7.0		7.0
chest	25.8		25.8
loins	17.2		17.2
upper arm	3.6	x2	7.2
forearm	2.2	x2	4.4
hand	0.7	x2	1.4
thigh	11.4	x2	22.8
shank	5.3	x2	10.6
foot	1.8	x2	3.6
total			100.0

Table 4.1: Standard mass distribution of a body

thesis, $\rho = 1.0$. Therefore, the inertia is calculated as

$$I_h = \frac{mr^2}{2} \tag{4.2a}$$

$$I_r = \frac{m(3r^2 + h^2)}{12}, \tag{4.2b}$$

where I_h and I_r are the inertia of the height direction and the perpendicular direction, respectively.

4.3.2 Center of Mass

Now, let m_i and $\boldsymbol{s}_i$ denote the mass and the CM of the i-th elements, respectively. The CM of the whole body ($\boldsymbol{s}$) is obtained as

$$\boldsymbol{s} = \frac{\sum_i m_i \boldsymbol{s}_i}{\sum_i m_i}. \tag{4.3a}$$

The velocity and the acceleration of the CM are obtained in the same way:

$$\dot{\boldsymbol{s}} = \frac{\sum_i m_i \dot{\boldsymbol{s}}_i}{\sum_i m_i} \tag{4.3b}$$

$$\ddot{\boldsymbol{s}} = \frac{\sum_i m_i \ddot{\boldsymbol{s}}_i}{\sum_i m_i}, \tag{4.3c}$$

therefore, these are calculated based on the time-difference of the position of the CM between frames:

$$\dot{\boldsymbol{s}}_i(t) = \frac{\boldsymbol{s}_i(t+\Delta t) - \boldsymbol{s}_i(t-\Delta t)}{2\Delta t} \tag{4.4a}$$

$$\ddot{\boldsymbol{s}}_i(t) = \frac{\boldsymbol{s}_i(t+\Delta t) - 2\boldsymbol{s}_i(t) + \boldsymbol{s}_i(t-\Delta t)}{\Delta t^2}. \tag{4.4b}$$

However, when the difference is calculated, errors included in the captured data are integrated and the result is not always reliable.

On the other hand, with regard to the acceleration of the CM, it can be calculated from the data of force plates. If any external force except the ground reaction does not act, the equation of motion is written as

$$\boldsymbol{f}_g = m\ddot{\boldsymbol{s}} + m\boldsymbol{g}, \tag{4.5}$$

where $\boldsymbol{f}_g$ is the ground reaction, m is the total mass of the body, and $\boldsymbol{g}\,(= (0, g_y, 0)^T)$ is the acceleration of the gravity. Therefore, the acceleration of the CM is calculated as

$$\ddot{\boldsymbol{s}} = \frac{\boldsymbol{f}_g}{m} - \boldsymbol{g}. \tag{4.6}$$

This value is more reliable than the value calculated from the time-difference of the positions of the CM.

In practice, when no external force except the ground reaction is applied, the value from the data of the force plates is taken, and when external force is applied, the value from the difference of positions is taken. Figure 4.5 shows the value of the acceleration of the CM calculated by the two methods. The red points show the acceleration calculated from the difference of the positions. The green points show the acceleration calculated from the data of the force plates. The values are basically similar, but high frequency noise is observed on the red points because of the integrated error by the calculation of difference. Thus the values from the force plates are more reliable. However, from 0.2 sec to 0.7 sec, the values returned by the two methods are definitely different because external force is applied in this period and the values from the force plates include the external force. Thus the values from the difference are taken as the acceleration in this period.

4.3.3 Zero Moment Point

A ZMP is a point on the floor, and the all ground reaction is replaceable as the equivalent force acting to the point. It is very important to treat the dynamic

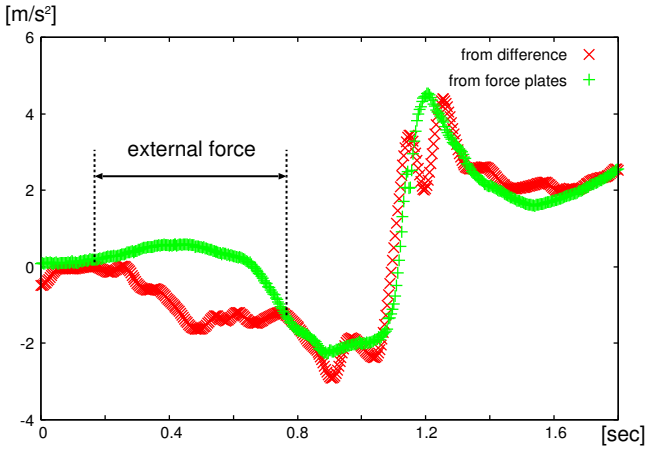

Figure 4.5: Two ways to calculate the acceleration of the CM: The red points show the acceleration calculated from the difference of the position. The green points show the acceleration calculated from the data of the force plates.

stability. The detail about a ZMP is discussed in 3.4. In this section, the way to obtain the ZMP from the captured data is described.

The ZMP can be determined by data of the force plates. If a subject is standing on only one plate, the data of the plate, the point where the force acts, can be directly used as the ZMP. If a subject is standing over more than one plate, the ZMP is calculated by the following equation which is derived from the definition of a ZMP:

$$\sum_i (\boldsymbol{p}_i - \boldsymbol{p}) \times \boldsymbol{f}_i = \boldsymbol{n}_p, \tag{4.7}$$

where $\boldsymbol{p}(= (p_x, 0, p_z)^T)$ is the ZMP, $\boldsymbol{n}_p(= (0, n_{py}, 0))$ is the moment around $\boldsymbol{p}$, which has only the vertical element, $\boldsymbol{f}_*$ and $\boldsymbol{p}_*$ are the force and the point where the force acts for each plate.

4.4 Experiments

In this study, human motion to deal with external perturbation is captured for four subjects. All of them are students and their properties are shown in Table 4.2. The reason why we chose only students is that they are considered

Subject	Age	Height (m)	Weight (kg)	Sex
1	29	1.68	74	male
2	27	1.66	71	male
3	25	1.72	95	male
4	24	1.69	59	male

Table 4.2: Properties of subjects

ideal subjects to maintain balance with whole-body motion. For children, it is too complex to maintain balance with whole-body motion. For aged persons, it is difficult to move forcefully and quickly because of the decline of muscle power and flexibility. In this experiment, in order to extract the fundamental essence of human motion for maintaining balance, we observed the only motion of the ideal persons who have similar properties, and thus we were able to extract common characteristics.

Perturbation is applied to them by pulling a rope that is attached to the trunk of the subjects. The person who applies perturbation must perform the operation far from the subjects; a person near the subjects causes occlusion for the optical motion capture and noise for the force plates. The three experiments are performed as described below.

With regard to the results of the experiments, it is not possible to show the captured motion here, but the results are used in the following chapters to design the model of balance maintenance based on human motion.

Experiment 1

Perturbation was applied to the four subjects. The direction of it was from front to back and from back to front. The subjects stood upright initially. When perturbation was applied, they were allowed to maintain their balance freely: they could keep their feet on the ground, or they could take a step if they wanted to do so. The strength of the perturbation changed with every trial. For every subject, the trials were performed twenty or thirty times for perturbation from back to front, and ten or twenty times for perturbation from front to back.

Experiment 2

Perturbation was applied to the four subjects who were walking forward. Because the subjects walked forward in this experiment, perturbation was applied from the back to the front. The trials were performed five or ten times for every subject.

Experiment 3

Perturbation was applied to the backward direction, the forward direction, the side direction, and the diagonal direction. A strain gage was adapted to the rope so that the strength of the applied force was recorded. In this experiment, the measurement was preformed for one subject. The subject, a male, stood upright at the initial time, and he was told to keep his feet on the ground as much as possible. The trial performed five or ten times for every direction.

Chapter5

Balance Maintenance by Keeping Feet on the Ground

5.1 Overview

In this chapter, the model of balance maintenance by keeping feet on the ground is described. It is used when the perturbations are too large to maintain balance by PD control. Rather than focusing on posture, this model focuses on the CM and the ZMP. The aim of this model is to make the trajectory of the CM the same for a human-like character as for a human. In this strategy, an effective motion to maintain balance is generated even if the posture of the character momentarily deviates considerably from the target position. Optimization calculation using the quadratic programming method is performed, and motion is generated frame by frame. If the character returns to a stable state after maintaining balance by keeping feet on the ground, PD control is again adopted.

This chapter is organized as follows. First, the quadratic programming method is described and linearization of physical parameters is detailed as preliminary. These are necessary to generate motion by optimization calculation. Next, the observation of human motion to maintain balance is described, and the characteristics of it are extracted. Third, the model of balance maintenance is constructed based on the observation, and then the simulation results using the model are shown.

5.2 Preliminary

5.2.1 Quadratic Programming Method

In this study, motion is generated by optimization calculation based on the quadratic programming method. This is a type of mathematical programming method. It consists of one objective function and constraints that are represented as equations and inequations, and finds the solution that minimizes the objective function satisfying the constraints. It is a suitable method to implement our model that generates whole-body motion satisfying conditions represented by macro quantities, such as the CM, the ZMP, and so on.

The simplest method in mathematical programming is the linear programming method. It receives only linear formulae such as the objective function and the constraints. The solution of this method is always on the boundary of the constraints. Since the constraints in the proposed method represent extreme cases of the motion, the feature is not disabled for the proposed method.

The second simplest method is the quadratic programming method. It receives a quadratic formula as the objective function and linear equations and inequations as the constraints. The solution is not always on the boundary of the constraints. Moreover, conditions about the CM and the ZMP can be represented as a quadratic programming problem, as detailed in the following section. Therefore, the quadratic programming method is adopted to implement the proposed method.

5.2.2 Linearization of Physical Parameters

As mentioned above, the quadratic programming method is used to obtain the optimal angular acceleration. The ZMP, the acceleration of the CM, and the moment around the CM are used in the optimization. Because the quadratic programming method allows a quadratic formula as an objective function and linear formulae as constraints, the ZMP, the acceleration of the CM, and the moment around the CM have to be expressed as linear formulae about the variable $\ddot{\boldsymbol{\varphi}}$.

The joint angles, which are elements of $\boldsymbol{\theta}$, are functions of the degrees of freedom of the body $\boldsymbol{\varphi}$:

$$\theta_i = \theta_i(\boldsymbol{\varphi}) \qquad (i = 1, \ldots, N_{\text{joints}}). \tag{5.1}$$

Differentiating the equation, the acceleration of the joint angles can be expressed

as a linear formula about $\ddot{\boldsymbol{\varphi}}$ as follows:

$$\ddot{\theta}_i = \sum_j^{N_{\mathrm{DOF}}} \frac{\partial \theta_i}{\partial \varphi_j} \ddot{\varphi}_j + \sum_{j,k}^{N_{\mathrm{DOF}}} \frac{\partial^2 \theta_i}{\partial \varphi_j \partial \varphi_k} \dot{\varphi}_j \dot{\varphi}_k. \tag{5.2}$$

In the quadratic programming problem, a variable is only $\ddot{\boldsymbol{\varphi}}$. Because $\boldsymbol{\varphi}$ and $\dot{\boldsymbol{\varphi}}$ are not variables here, these can be treated as constants. Therefore, the acceleration of the joint angles can be expressed as a linear formula:

$$\ddot{\theta}_i = \sum_j^{N_{\mathrm{DOF}}} c_{\theta_i j}\, \ddot{\varphi}_j + d_{\theta_i}, \tag{5.3}$$

where $c_{\theta_i j}$ and d_{θ_i} are coefficients and a constant, respectively.

In the same way, because the position of the CM ($\boldsymbol{s}$) is a function of $\boldsymbol{\varphi}$ as

$$s_* = s_*(\boldsymbol{\varphi}) \qquad (* = x, y, z), \tag{5.4}$$

the acceleration of the CM ($\ddot{\boldsymbol{s}}$) is expressed as:

$$\ddot{s}_* = \sum_j^{N_{\mathrm{DOF}}} \frac{\partial s_*}{\partial \varphi_j} \ddot{\varphi}_j + \sum_{j,k}^{N_{\mathrm{DOF}}} \frac{\partial^2 s_*}{\partial \varphi_j \partial \varphi_k} \dot{\varphi}_j \dot{\varphi}_k. \tag{5.5}$$

Therefore, it can be expressed as a linear formula:

$$\ddot{s}_* = \sum_j^{N_{\mathrm{DOF}}} c_{s_* j}\, \ddot{\varphi}_j + d_{s_*}, \tag{5.6}$$

where $c_{s_* j}$ and d_{s_*} are coefficients and a constant, respectively.

The angular momentum of the whole body ($\boldsymbol{l}$) around a point $\boldsymbol{r}$ is formulated as

$$\boldsymbol{l} = \sum_i^{N_{\mathrm{body}}} m_i (\boldsymbol{s}_i - \boldsymbol{r}) \times \dot{\boldsymbol{s}}_i + I_i \boldsymbol{\omega}_i, \tag{5.7}$$

where I_i is the inertia tensor of the i-th body and $\boldsymbol{\omega}_i$ is the vector of angular velocity of the i-th body. Because $\boldsymbol{s}_i$ and I_i depend on $\boldsymbol{\varphi}$, and $\dot{\boldsymbol{s}}_i$ and $\boldsymbol{\omega}_i$ depend on $\boldsymbol{\varphi}$ and $\dot{\boldsymbol{\varphi}}$, the angular momentum $\boldsymbol{l}$ can be written as a function of $\boldsymbol{\varphi}$ and $\dot{\boldsymbol{\varphi}}$:

$$l_* = l_*(\boldsymbol{\varphi}, \dot{\boldsymbol{\varphi}}) \qquad (* = x, y, z). \tag{5.8}$$

Therefore, the moment around the CM ($\boldsymbol{n}$), which is the derivative of the angular momentum, is expressed as

$$n_* = \dot{l}_* = \sum_j^{N_{\mathrm{DOF}}} \frac{\partial l_*}{\partial \varphi_j} \dot{\varphi}_j + \sum_j^{N_{\mathrm{DOF}}} \frac{\partial l_*}{\partial \dot{\varphi}_j} \ddot{\varphi}_j, \tag{5.9}$$

and then, it can be expressed as a linear formula:

$$n_* = \sum_{j}^{N_{\mathrm{DOF}}} c_{n_* j}\, \ddot{\varphi}_j + d_{n_*}, \tag{5.10}$$

where $c_{n_* j}$ and d_{n_*} are coefficients and a constant, respectively.

As shown in (5.3), (5.6), and (5.10), the angular acceleration of the joints, the acceleration of the CM, and the moment of the whole body around the CM are expressed as linear functions about $\ddot{\boldsymbol{\varphi}}$. On the other hand, these quantities are determined by inverse dynamics calculation if $\boldsymbol{\varphi}$, $\dot{\boldsymbol{\varphi}}$, and $\ddot{\boldsymbol{\varphi}}$ are given:

$$\ddot{\boldsymbol{\theta}} = \ddot{\boldsymbol{\theta}}(\boldsymbol{\varphi}, \dot{\boldsymbol{\varphi}}, \ddot{\boldsymbol{\varphi}}) \tag{5.11a}$$

$$\ddot{\boldsymbol{s}} = \ddot{\boldsymbol{s}}(\boldsymbol{\varphi}, \dot{\boldsymbol{\varphi}}, \ddot{\boldsymbol{\varphi}}) \tag{5.11b}$$

$$\boldsymbol{n} = \boldsymbol{n}(\boldsymbol{\varphi}, \dot{\boldsymbol{\varphi}}, \ddot{\boldsymbol{\varphi}}). \tag{5.11c}$$

Using the above three equations, the coefficients and the constants in the equations (5.3), (5.6), and (5.10) are determined by $N_{\mathrm{DOF}} + 1$ times of dynamic calculation.

Now, we take the case of $\ddot{\boldsymbol{\theta}}$ for an example. Let $\mathbf{0}$ be a null vector and $\mathbf{1}^j$ be the vector whose elements are zero except the j-th element:

$$\mathbf{1}^j = (0, \ldots, 0, \overset{j\text{-th}}{\overset{\vee}{1}}, 0, \ldots) \quad (j = 1, \ldots, N_{\mathrm{DOF}}). \tag{5.12}$$

First, $\ddot{\boldsymbol{\theta}}(\boldsymbol{\varphi}, \dot{\boldsymbol{\varphi}}, \mathbf{0})$ is calculated based on (5.11a). The variable is only $\ddot{\boldsymbol{\varphi}}$ here. and $\boldsymbol{\varphi}$ and $\dot{\boldsymbol{\varphi}}$ are given beforehand and cannot be changed. Let $\boldsymbol{b}$ denote the value:

$$\boldsymbol{b} = \ddot{\boldsymbol{\theta}}(\boldsymbol{\varphi}, \dot{\boldsymbol{\varphi}}, \mathbf{0}). \tag{5.13}$$

Substituting $\ddot{\boldsymbol{\varphi}} = \mathbf{0}$ to (5.3),

$$\ddot{\theta}_i = d_{\theta_i}, \tag{5.14}$$

therefore, the constant d_{θ_i} is determined as

$$d_{\theta_i} = b_i. \tag{5.15}$$

Next, $\ddot{\boldsymbol{\theta}}(\boldsymbol{\varphi}, \dot{\boldsymbol{\varphi}}, \mathbf{1}^j)$ is calculated based on (5.11a). Let $\boldsymbol{a}$ denote the value:

$$\boldsymbol{a} = \ddot{\boldsymbol{\theta}}(\boldsymbol{\varphi}, \dot{\boldsymbol{\varphi}}, \mathbf{1}^j). \tag{5.16}$$

Substituting $\ddot{\boldsymbol{\varphi}} = \mathbf{1}^j$ to (5.3),

$$\ddot{\theta}_i = c_{\theta_i j} + d_{\theta_i}, \tag{5.17}$$

$\boldsymbol{b} = \ddot{\boldsymbol{\theta}}(\boldsymbol{\varphi}, \dot{\boldsymbol{\varphi}}, \mathbf{0})$
for $(i = 1;\ i \leq N_{\text{joint}};\ ++i)$
    $d_{\theta_i} = b_i$
for $(j = 1;\ j \leq N_{DOF};\ ++j)$ {
    $\boldsymbol{a} = \ddot{\boldsymbol{\theta}}(\boldsymbol{\varphi}, \dot{\boldsymbol{\varphi}}, \mathbf{1}^j)$
    for $(i = 1;\ i \leq N_{\text{joint}};\ ++i)$
        $c_{\theta_i j} = a_i - b_i$
}

Figure 5.1: Procedure for determining the coefficients and the constant of $\ddot{\boldsymbol{\theta}}$

therefore, the constant $c_{\theta_i j}$ is determined as

$$c_{\theta_i j} = a_i - b_i. \tag{5.18}$$

All coefficients in (5.3) are determined by calculating this for

$$j = 1, \ldots, N_{\text{DOF}}. \tag{5.19}$$

The flowchart of this procedure is shown in Figure 5.1. In the same way, the coefficients and the constants of the acceleration of the CM ($\ddot{\boldsymbol{s}}$) and the moment around the CM ($\boldsymbol{n}$) can be calculated.

The above discussion proves that the acceleration of the joint angles, the acceleration of the CM, and the moment acting around the CM can be expressed as the linear formulae about $\ddot{\boldsymbol{\varphi}}$. Substituting these formulae in the equation (3.5), the numerators and the denominators in these equations are also written as linear formulae about $\ddot{\boldsymbol{\varphi}}$:

$$p_x = \frac{\boldsymbol{c}_x^T \ddot{\boldsymbol{\varphi}} + d_x}{\boldsymbol{c}_c^T \ddot{\boldsymbol{\varphi}} + d_c} \tag{5.20a}$$

$$p_z = \frac{\boldsymbol{c}_z^T \ddot{\boldsymbol{\varphi}} + d_z}{\boldsymbol{c}_c^T \ddot{\boldsymbol{\varphi}} + d_c}, \tag{5.20b}$$

where

$$\boldsymbol{c}_x = \boldsymbol{c}_{n_y} + ms_x\boldsymbol{c}_{s_y} - ms_y\boldsymbol{c}_{s_x} \tag{5.21a}$$

$$d_x = d_{n_y} + ms_x(d_{s_y} - g_y) - ms_y d_{s_x} \tag{5.21b}$$

$$\boldsymbol{c}_z = -\boldsymbol{c}_{n_y} + ms_z\boldsymbol{c}_{s_y} - ms_y\boldsymbol{c}_{s_z} \tag{5.21c}$$

$$d_x = -d_{n_y} + ms_z(d_{s_y} - g_y) - ms_y d_{s_z} \tag{5.21d}$$

$$\boldsymbol{c}_c = m\boldsymbol{c}_{s_y} \tag{5.21e}$$

$$d_c = m(d_{s_y} - g_y). \tag{5.21f}$$

Per the above discussion, the ZMP is not formulated as a linear formula about $\ddot{\boldsymbol{\varphi}}$, but formulated as a fraction of linear formulae. However, the condition that the ZMP is within an area can be formulated as a set of linear inequations as follows. First, we represent the boundary of the area by N_{boundary} lines:

$$\alpha_i x + \beta_i z + \gamma_i < 0 \quad (i = 1, 2, \ldots, N_{\text{boundary}}), \tag{5.22}$$

and then, substituting the equations (5.20) for this, the condition is written as:

$$(\alpha_i\boldsymbol{c}_x + \beta_i\boldsymbol{c}_z + \gamma_i\boldsymbol{c}_c)^T\ddot{\boldsymbol{\varphi}} + (\alpha_i d_x + \beta_i d_z + \gamma_i d_c) < 0. \tag{5.23}$$

If the denominator in (5.20) is negative, the sign of inequality in the above inequation have to be reversed. However, according to the equation (3.5), the denominator is

$$m(\ddot{s}_y - g_y). \tag{5.24}$$

If it becomes negative, it means that the character is jumping. Because we do not consider such a case in our method, the condition that the denominator is always positive has to be added as a constraint. It can be written as a linear inequation of $\ddot{\boldsymbol{\varphi}}$ as

$$\boldsymbol{c}_{s_y}^T\ddot{\boldsymbol{\varphi}} + d_{s_y} - g_y > 0. \tag{5.25}$$

5.3 Observing Human Motion

For maintaining balance by keeping the feet on the ground, it is important that the CM moves properly. Because the support area by the feet is small when the feet are kept on the ground, it is difficult to control the CM to return a stable position properly. In this section, the captured human motion is observed from the viewpoint of the behavior of the CM.

Figure 5.2 shows a typical relationship among the position, the velocity, and the acceleration of the CM in the sagittal plane. The end points, in which the

Subject	Average	Standard deviation
1	—	—
2	-11.8	1.42
3	—	—
4	-11.2	0.47
total	-11.6	1.16

Table 5.1: Average and standard deviation of the slope of the regression line

velocity and the acceleration are near zero, are stable positions. Because only acceleration is a variable in this method, the relationship between acceleration and the other values is observed. Figure 5.3 shows the relationship between the position and the acceleration of the CM. A linear relationship is observed from the graph. In particular, when the CM is far from the stable position (the left side of the graph), the relationship appears to become stronger. The green line is the regression line. Figure 5.4 shows the relationship between the velocity and the acceleration of the CM. From this graph, no relationship, including linear relationship, is observed. Therefore, it can be said that the acceleration of the CM has a linear relationship only to the position.

Table 5.1 shows the average and the standard deviation of the slope of the regression line for every subject. With regard to Subjects 1 and 3, because they almost always took a step and seldom maintained their balance by keeping their feet on the ground even if the perturbation was not very large, we could not obtain a sufficient number of samples about them. According to the table, it is observed that the values of the slope converge well. The value is about -11.6 for every subject.

Based on the observation, the motion of the CM when a large perturbation is applied is modeled as Figure 5.5. When the CM is at the position of s in the sagittal plane, the acceleration applied to the CM is

$$\ddot{s} = k_{\mathrm{CM}}(s - s_0), \tag{5.26}$$

where s_0 is the stable position and $k_{\mathrm{CM}} \approx 11.6$.

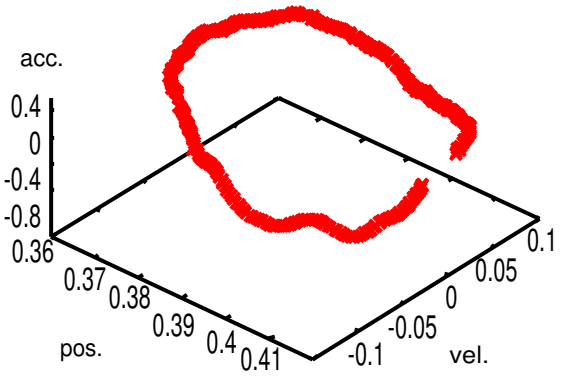

Figure 5.2: Relationship among the position(m), the velocity(m/s), and the acceleration(m/s^2) of the CM in the sagittal plane

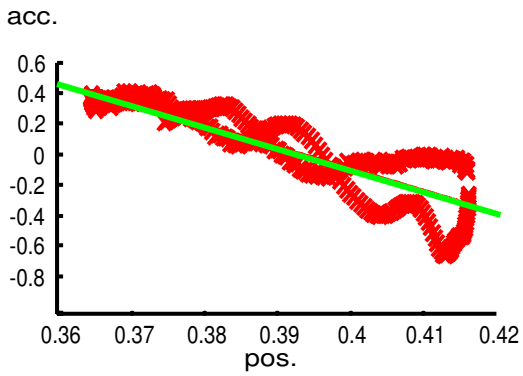

Figure 5.3: Relationship between the position(m) and the acceleration(m/s^2) of the CM: The green line is the regression line of the red points.

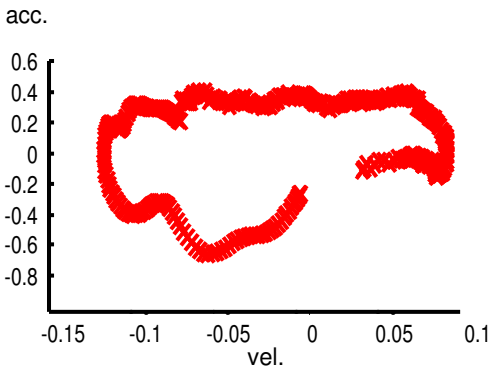

Figure 5.4: Relationship between the velocity(m/s) and the acceleration(m/s^2) of the CM: No linear relation appears.

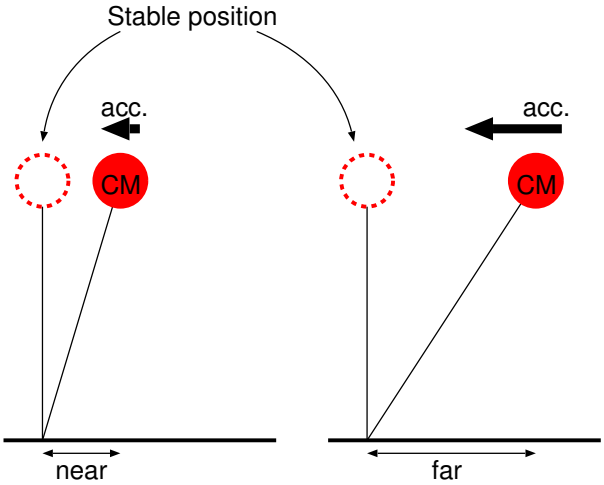

Figure 5.5: Model of the motion of the CM for maintaining balance by keeping the feet on the ground: If the CM is near the stable position, the acceleration required to return the CM to the stable position is small. If the CM gets farther from the stable position, acceleration also gets larger. The relationship between acceleration and position obeys the equation (5.26).

5.4 Model of Balance Maintenance

Based on the observation of the captured human motion, the model of balance maintenance by keeping feet on the ground is constructed. In the model, the following points are considered:

- generating low-cost motion,
- controlling the CM in the same way as humans do,
- generating dynamically consistent motion, and
- generating symmetric motion.

With regard to the first point, low-cost motion means motion that requires little muscle power. Because a human body has many of degrees of freedom, it is important to select the criterion to determine a motion from many possible motions. In this model, minimizing muscle power is selected. However, because muscle power cannot be handled directly, the square sum of the angular acceleration of the joints is employed instead. There are two reasons why torque is not used for this criterion. One is the redundancy about the torque. The torque acting at leg joints is not determined uniquely because of the closed-loop problem at the legs. On the other hand, acceleration is determined uniquely. The other reason is the difference of the maximum torque. Because the maximum torque is different for every joint, the importance of torque is not same among joints even if torque has the same value; thus, torque is not a good criterion. Generally, the joint that needs to generate large torque has large muscles. Because of this, it can be considered that the importance of the torque is canceled by the muscle power and that the load for the joints is measured by angular acceleration (see Figure 5.6).

The second point, controlling the CM the same way humans do, is one of the most important features of the model in generating human-like motion. This control is based on the observation of human motion discussed in the previous section.

The third point concerns the dynamic consistency of the motion. It is judged based on the position of the ZMP. As mentioned before, a ZMP is the point on which all ground reaction is considered as acting, and it is always within the supporting area if the motion is dynamically consistent. In this model, because both feet contact the ground, the supporting area is the convex hull constructed by the feet.

The fourth point concerns the symmetry of motion. It is based on the observation of human motions. When humans maintain their balance by keeping

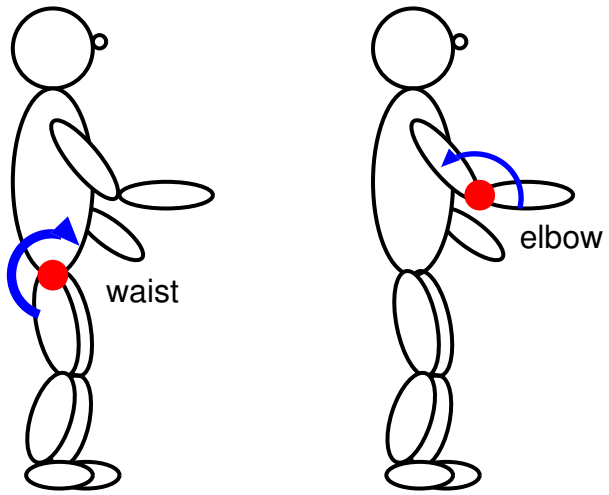

Figure 5.6: Torque vs. acceleration: The left character moves the waist joint and the right character moves the elbow. Even if the angular acceleration of both motions is the same, the torque acting at the joints is not the same: the torque at the waist joint is larger. However, because the waist joint has more muscle power than the elbow, the load of the waist joint is not much larger.

their feet on the ground, they prefer to take symmetric motion. For example, when humans rotate their arms to maintain their balance, they move their arms in the same way, rather than separately. For another example, and this is particularly true when humans maintain their balance by keeping their feet on the ground, they move to reduce the yaw rotation. In this way, humans tend to make symmetrical motions when they maintain their balance. Symmetrical motion is efficient not only for generating human-like motion, but also for reducing possible motions. Because motion is generated frame by frame in this method, it is difficult to produce global stability. Therefore, it is helpful to reduce possible motions.

In this model, motion is generated frame by frame. If the stability of the state is broken by a perturbation, the system receives the state, the posture, and the angular velocity, as the input. Optimization calculation is performed on the input, and the acceleration for every degree of freedom ($\ddot{\boldsymbol{\varphi}}$) satisfying the above condition is calculated. Integrating the state of the character with acceleration, the next state is obtained, and then optimization calculation is performed again on the new state. This operation is continued until the state reverts to the stable state. The process is illustrated in Figure 5.7.

In this model, the above points are represented using a quadratic programming problem. As mentioned before, a quadratic programming problem consists of one objective function, which is a quadratic function, and constraints, which are linear equations and inequations. Thus the above points have to be formulated as such a function, equations, and inequations about $\ddot{\boldsymbol{\varphi}}$, which is the variable of the model. The first point, which is "generating low-cost motion," is formulated as the objective function, and other points are formulated as the constraints.

In practice, some other constraints are required for the model. One constraint is the limitation of the joint structure. For example, the elbows and the knees bend in only one direction; they cannot be bent in the opposite direction, so this is a limitation of the joint angle. In the same way, there is limitation of velocity and acceleration.

Another constraint is that the character tries to keep an upright posture. Without this constraint, the character often tends to sit down because the posture of sitting down is more stable than the posture of standing upright. When the character sits down, the distance between the CM and the ground is small; thus the moment acting on the body is reduced and the projection of the CM to the ground tends to converge to the center of the supporting area. Although sitting down contributes to the stability of motion, this is not what humans do to

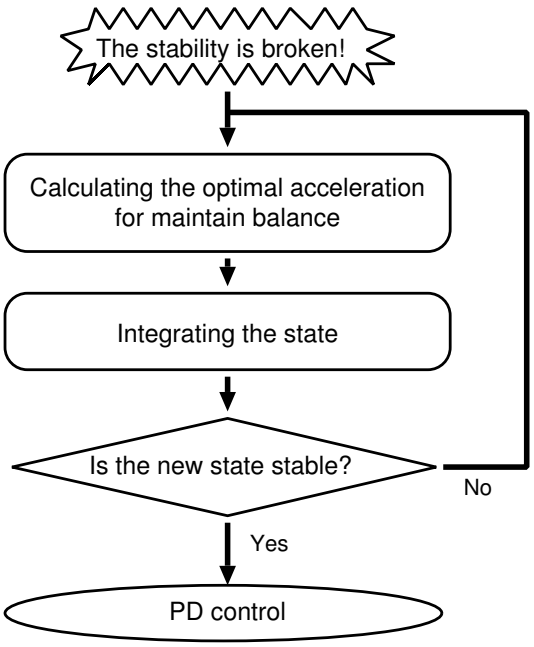

Figure 5.7: Flowchart of balance maintenance by keeping feet on the ground

maintain balance. Therefore, constraints to keep the character standing upright are required. In this model, the constraint is not implemented as a constraint of the quadratic programming problem, but as a part of the objective function. This constraint needs to be implemented as a soft constraint; an objective function is suitable to a soft constraint.

The objective function is formulated for two purposes. One is to generate low-cost motion, and the other is to make the character keep an upright posture. It is formulated as

$$\min \quad \ddot{\boldsymbol{\theta}}^T A_\theta \, \ddot{\boldsymbol{\theta}} - \ddot{s}_y, \tag{5.27}$$

where A_θ is a constant matrix and $\ddot{s}_y$ is the y-element of the acceleration of the CM. The first term is the square sum of the angular acceleration of the joints. As mentioned above, low-cost motion is generated by reducing this term. The constant A_θ is a diagonal matrix and represents the weight of the joints. The value of A_θ, which is determined from mass distribution of the body, is detailed in Appendix D. Influence of A_θ on the generated motion is discussed later in Chapter 7. The second term requires the character to keep an upright posture. It is implemented by generating motion where the y-element of the acceleration of the CM is larger.

In order to use the formula (5.27) for the objective function, it has to be rewritten as the quadratic formula about $\ddot{\boldsymbol{\varphi}}$. Substituting (5.3) and (5.6), the formula (5.27) is written as

$$(C_\theta \ddot{\boldsymbol{\varphi}} + \boldsymbol{d}_\theta)^T A_\theta \, (C_\theta \ddot{\boldsymbol{\varphi}} + \boldsymbol{d}_\theta) - (\boldsymbol{c}_{s_y} \ddot{\boldsymbol{\varphi}} + d_{s_y}), \tag{5.28}$$

where

$$\boldsymbol{c}_{\theta_i} = (c_{\theta_i 0}, c_{\theta_i 1}, \ldots, c_{\theta_i N_{\mathrm{DOF}}})^T \tag{5.29a}$$

$$C_\theta = (\boldsymbol{c}_{\theta_0}^T, \boldsymbol{c}_{\theta_1}^T, \ldots, \boldsymbol{c}_{\theta_{N_{\mathrm{joint}}}}^T)^T \tag{5.29b}$$

$$\boldsymbol{d}_\theta = (d_{\theta_0}, d_{\theta_1}, \ldots, d_{\theta_{N_{\mathrm{joint}}}})^T \tag{5.29c}$$

$$\boldsymbol{c}_{s_*} = (c_{s_* 0}, c_{s_* 0}, \ldots, c_{s_* N_{\mathrm{DOF}}})^T. \tag{5.29d}$$

Arranging the above formula, the objective function is written as

$$\min \quad \ddot{\boldsymbol{\varphi}}^T (C_\theta^T A_\theta C_\theta) \ddot{\boldsymbol{\varphi}} + (2\boldsymbol{d}_\theta - \boldsymbol{c}_{s_y}) \ddot{\boldsymbol{\varphi}}. \tag{5.30}$$

The constant in (5.28) is omitted because it is no use in the objective function.

The first constraint is about the trajectory of the CM. According to the observation of human motion, the acceleration of the CM has a linear relationship to the position of the CM. It is written as

$$\ddot{s}_z = k_{CM}(s_z - s_{z0}), \tag{5.31}$$

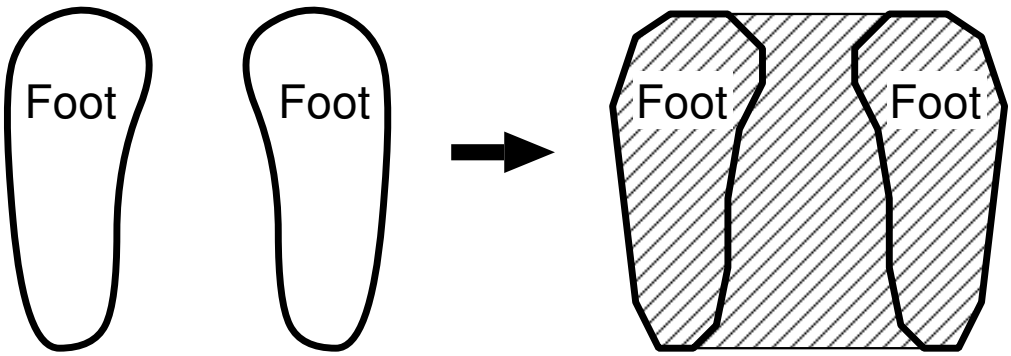

Figure 5.8: Supporting area by the feet: The boundaries of the feet are approximated by the lines. The convex hull of the lines is the supporting area.

where k_{CM} is the constant obtained by observation and s_{z0} is the stable position of the CM, which is the position when the character stands upright. The sagittal axis of the character is set to be parallel to the z axis here, thus only the z-element of the CM is considered. Substituting (5.6) in the above equation results in this equation:

$$\boldsymbol{c}_{s_z}\ddot{\boldsymbol{\varphi}} + d_{s_z} = k_{CM}(s_z - s_{z0}). \tag{5.32}$$

The second constraint is about the position of the ZMP. In this model, both feet contact the ground and the supporting area is the convex hull of the feet. First, the boundary of the area is approximated by lines (Figure 5.8). Let the number of the lines be N_{boundary}, the boundary is written as

$$\alpha_i x + \beta_i z + \gamma_i < 0 \quad (i = 1, 2, \ldots, N_{\text{boundary}}), \tag{5.33}$$

and then, as mentioned in section 5.2.2, the condition that the ZMP is within the area is written as:

$$(\alpha_i \boldsymbol{c}_x + \beta_i \boldsymbol{c}_z + \gamma_i \boldsymbol{c}_c)^T \ddot{\boldsymbol{\varphi}} + (\alpha_i d_x + \beta_i d_z + \gamma_i d_c) < 0 \tag{5.34a}$$

$$\boldsymbol{c}_{s_y}^T \ddot{\boldsymbol{\varphi}} + d_{s_y} - g_y > 0. \tag{5.34b}$$

The third constraint is to generate symmetric motion. In this model, symmetric motion is realized by controlling the legs and the arms to move symmetrically. In practice, the x-axis of the shoulder joints, the knee joints, and the x-axis of

the ankle joints are considered. With regard to these joints, the acceleration of the corresponding pairs is constrained to make the angles close:

$$\begin{cases} \ddot{\theta}_{\text{right}} < \ddot{\theta}_{\text{left}} & (\theta_{\text{right}} > \theta_{\text{left}}) \\ \ddot{\theta}_{\text{right}} > \ddot{\theta}_{\text{left}} & (\theta_{\text{right}} < \theta_{\text{left}}), \end{cases} \tag{5.35}$$

where θ_{right} and θ_{left} are the corresponding pairs of the joints.

The last constraint is about the range of the angles, the angular velocity, and the angular acceleration of the joints. It is written as

$$\boldsymbol{\theta}_{\min} \leq \boldsymbol{\theta} \leq \boldsymbol{\theta}_{\max} \tag{5.36a}$$

$$\dot{\boldsymbol{\theta}}_{\min} \leq \dot{\boldsymbol{\theta}} \leq \dot{\boldsymbol{\theta}}_{\max} \tag{5.36b}$$

$$\ddot{\boldsymbol{\theta}}_{\min} \leq \ddot{\boldsymbol{\theta}} \leq \ddot{\boldsymbol{\theta}}_{\max}. \tag{5.36c}$$

The maximum and minimum values are described in Appendix D. These constraints have to be written as the constraints about $\ddot{\boldsymbol{\varphi}}$ as the following:

$$\xi_{\min i} < \ddot{\theta}_i < \xi_{\max i} \quad (1, 2, \ldots, N_{\text{joint}}), \tag{5.37}$$

where

$$\xi_{\min i} = \begin{cases} 0 & (\theta_i < \theta_{\min i} \text{ or } \dot{\theta}_i < \dot{\theta}_{\min i}) \\ \ddot{\theta}_{\min i} & (\text{otherwise}) \end{cases} \tag{5.38a}$$

$$\xi_{\max i} = \begin{cases} 0 & (\theta_i > \theta_{\max i} \text{ or } \dot{\theta}_i > \dot{\theta}_{\max i}) \\ \ddot{\theta}_{\max i} & (\text{otherwise}). \end{cases} \tag{5.38b}$$

This means that if the angle or the angular velocity of a joint is out of the range, angular acceleration is generated only in the direction to make the motion slow. These have to be rewritten again to accommodate the constraints about $\ddot{\boldsymbol{\varphi}}$ as follows:

$$\boldsymbol{c}_{\theta_i}^T \ddot{\boldsymbol{\varphi}} + d_{\theta_i} \geq \xi_{\min i} \tag{5.39a}$$

$$\boldsymbol{c}_{\theta_i}^T \ddot{\boldsymbol{\varphi}} + d_{\theta_i} \leq \xi_{\max i}. \tag{5.39b}$$

In summary, the quadratic programming problem is as follows:

$$\min \quad \ddot{\boldsymbol{\varphi}}^T (C_\theta^T A_\theta C_\theta) \ddot{\boldsymbol{\varphi}} + (2\boldsymbol{d}_\theta - \boldsymbol{c}_{s_y}) \ddot{\boldsymbol{\varphi}} \tag{5.40a}$$

subject to

$$\boldsymbol{c}_{s_z}^T \ddot{\boldsymbol{\varphi}} + d_{s_z} = k_{CM}(s_z - s_{z0}) \tag{5.40b}$$

$$(\alpha_j \boldsymbol{c}_x + \beta_j \boldsymbol{c}_z + \gamma_j \boldsymbol{c}_c)^T \ddot{\boldsymbol{\varphi}} + (\alpha_j d_x + \beta_j d_z + \gamma_j d_c) < 0 \tag{5.40c}$$

$$\boldsymbol{c}_{s_y}^T \ddot{\boldsymbol{\varphi}} + d_{s_y} - g_y > 0 \tag{5.40d}$$

$$\ddot{\theta}_{\text{right}} < \ddot{\theta}_{\text{left}} \qquad (\theta_{\text{right}} > \theta_{\text{left}}) \tag{5.40e}$$

$$\ddot{\theta}_{\text{right}} > \ddot{\theta}_{\text{left}} \qquad (\theta_{\text{right}} < \theta_{\text{left}}) \tag{5.40f}$$

$$\boldsymbol{c}_{\theta_i}^T \ddot{\boldsymbol{\varphi}} + d_{\theta_i} \geq \xi_{\min i} \tag{5.40g}$$

$$\boldsymbol{c}_{\theta_i}^T \ddot{\boldsymbol{\varphi}} + d_{\theta_i} \leq \xi_{\max i}, \tag{5.40h}$$

where $i = 1, \ldots, N_{\text{joint}}$ and $j = 1, \ldots, N_{\text{boundary}}$.

Solving this quadratic programming problem, the motion of maintaining balance is generated. However, the solution is not always found. If no solution is found, it means that the perturbation is too large to maintain balance by this method. In that case, the strategy is switched to balance maintenance by stepping.

5.5 Experiments

In this section, results of simulation are shown when several types of perturbation are applied to the character. The generation of motion is performed every 0.01 second. Perturbation is applied to a point near the CM of the model and control begins 0.2 second after perturbation is applied in order to simulate the response delay in a human case.

Figure 5.9 shows the result when a force of 300N is applied for 0.1 second from the backward direction. The model keeps its balance by rotating its arms. Humans also make these kinds of motions when they receive a sudden large perturbation, because it is an effective motion to reduce the effect of the induced angular momentum that makes them fall down forward.

Figure 5.10 shows the result when a force of 300N is applied for 0.1 second from the forward direction. The model also rotates its arms to keep its balance, but the direction of the rotation is opposite to that of the previous case. In this case, the arms are swung harder than in the previous case, because the waist cannot be bent backward as far as it can be bent forward.

Figure 5.11 shows the result when a force of 200N is applied for 0.1 second from the right direction. The model can cope with the smaller force because there are fewer degrees of freedom in the side direction. Furthermore, it cannot take any steps in this case because the ZMP is under the left foot here although that leg is expected to be a swing leg.

Figure 5.12 shows the result when the force of a sinusoidal wave such as

$$100 \sin 2\pi t \ [\mathrm{N}] \tag{5.41}$$

acts constantly on the model. In this case, PD control is usually chosen. When the model cannot keep its balance by PD control, the optimization method is chosen and the arms are quickly moved to adjust the angular momentum acting on the model.

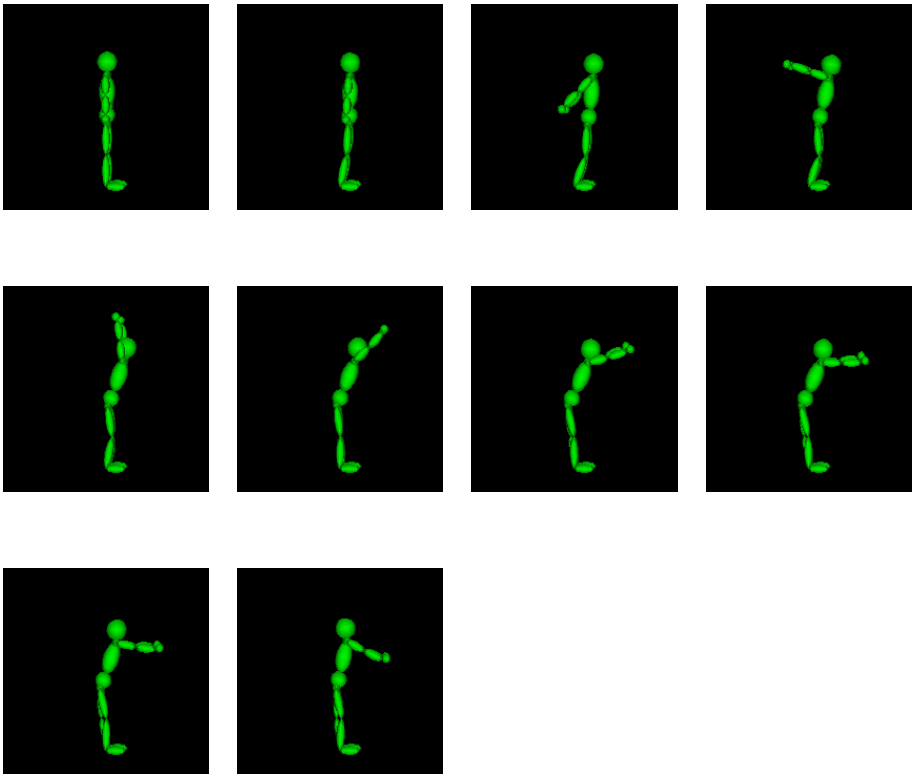

Figure 5.9: Force applied from the backward direction

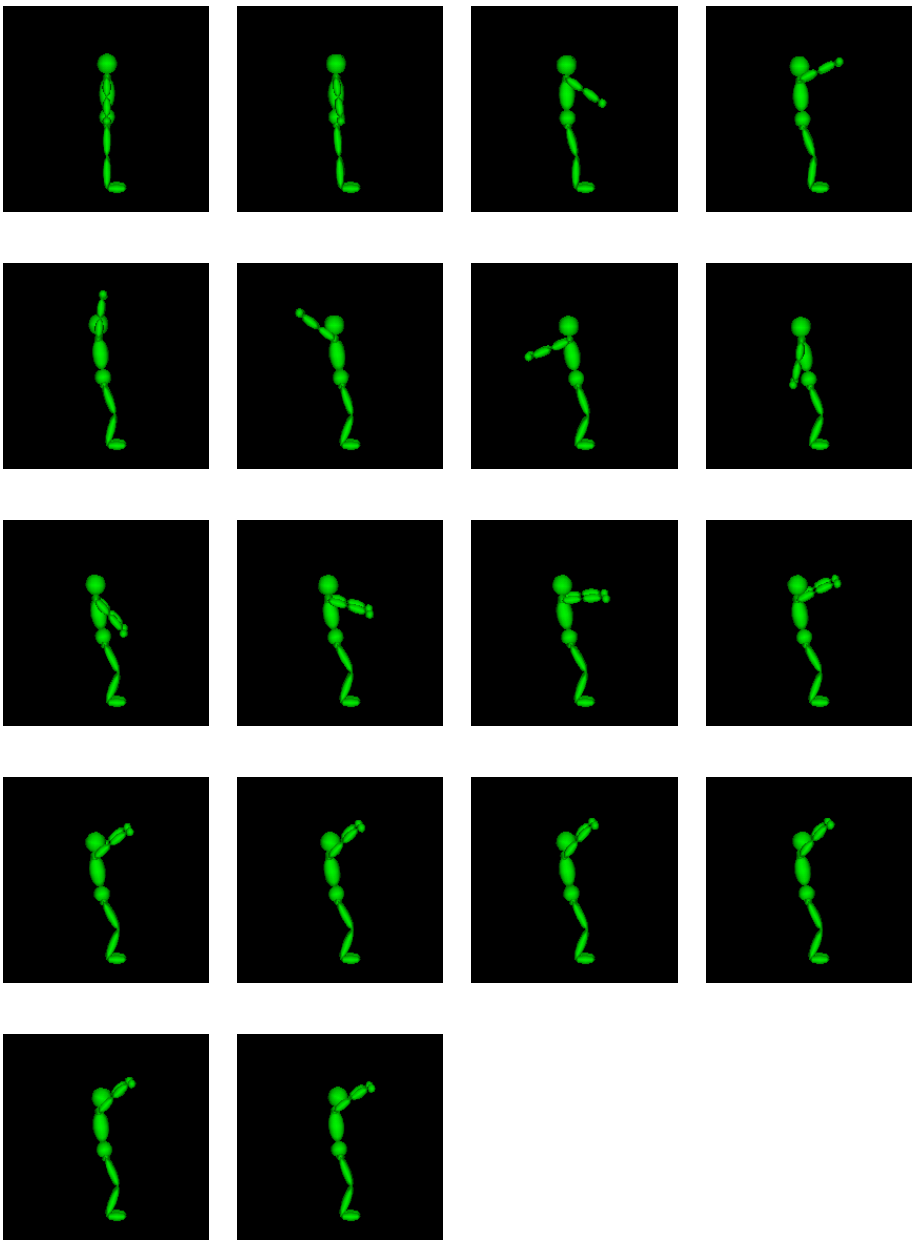

Figure 5.10: Force applied from the forward direction

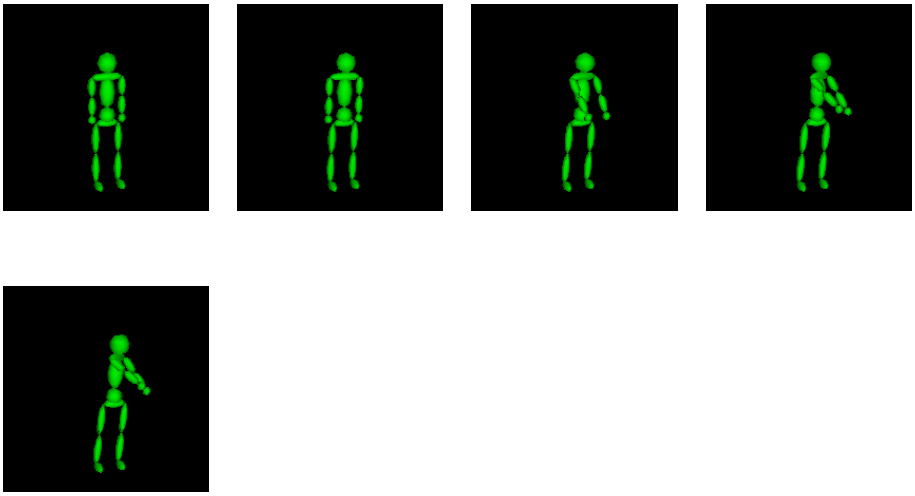

Figure 5.11: Force applied from the side direction: The force of 200 N is applied from the right of the figure for 0.2 second.

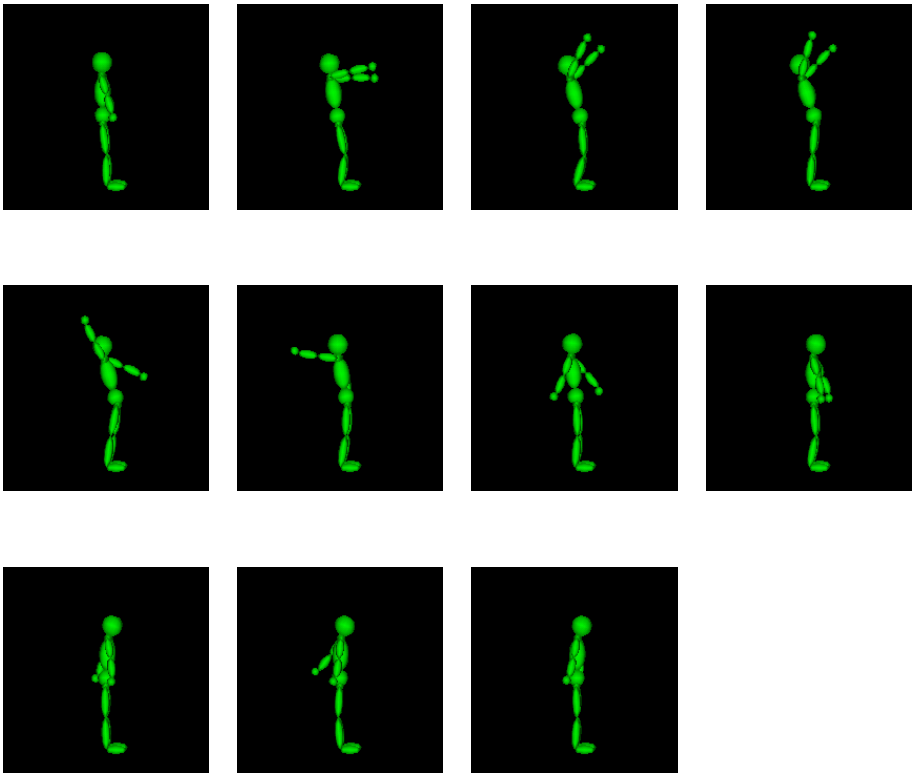

Figure 5.12: Sinusoidal force applied back and forward: The sinusoidal force which is formulated as $100 \sin 2\pi t$ N is applied continuously.

Chapter6

Balance Maintenance by Stepping

6.1 Overview

In the previous chapter, the model of balance maintenance by keeping feet on the ground was described. That method can deal with a large perturbation by controlling the CM as humans do. However, that method stipulates that the character cannot move its feet, while humans usually take a step to keep from falling down when a large perturbation is applied. In this chapter, the model of balance maintenance by stepping is described.

The model consists of three phases: determining the trajectory of the CM using the inverted pendulum model, generating lower body motion by inverse kinematics, and generating whole-body motion by optimization calculation. In the first phase, the focus is on the trajectory of the CM; this is determined using a simple structure like an inverted pendulum model and parameters extracted from observation of human motion. In the second phase, the lower body motion is generated based on the trajectory. Dynamic consistency is still not considered in this phase. In the last phase, dynamic consistency is satisfied using the redundancy of the upper body, and whole-body motion is generated.

This chapter is organized as follows: First, the observation of human motion is described. We observe the captured motion and extract essential parameters from it. The human body is approximated to an inverted pendulum model. Next, the proposed model of balance maintenance by stepping is detailed. It is based on the observation of human motion. Finally, simulation of generating motion by the model is performed and the results are shown.

6.2 Observing Human Motion

6.2.1 Inverted Pendulum Model

When we treat the motion in which a biped character is supported by one leg, such as stepping, an inverted pendulum model is suitable for use. It consists of a mass point that stands for the CM of the character and a connection from the mass point to the supporting feet (Figure 6.1). It is a simple model, but it can deal with dominant dynamics of stepping motion because the relationship between the CM and the ZMP is represented by using it. In biomechanics, many researchers use it for analyzing and modeling a stepping motion [11, 80, 33, 81], and the validity of it is confirmed.

In this section, we use it in order to analyze the captured human motion. The model that we use is depicted in Figure 6.2. It is an extension of a normal inverted pendulum model, and has two states: One is the state from the time when a swinging leg leaves the ground to when it again comes in contact with the ground. In this state, a human is supported by one leg. The other is a state after foot contact, when a human is supported by both legs (Figure 6.2). In the former state, a rotational spring is assumed to be attached at the base of the inverted pendulum model in order to generate torque to prevent the model from falling down. In the latter state, the stepping leg is assumed to be a spring that absorbs the shock of foot contact. In this model, m denotes the mass of the character, θ denotes the lean angle of the body, l denotes the distance between the CM and the supporting foot, α denotes the angle between the two legs, x denotes the distance between the CM and the swing foot, and a denotes the distance between the two feet. l and a are regarded as constants, and the value of x and α at foot contact are written as x_c and α_c, respectively. x_c is considered as the natural length of the swing leg spring. The constants of the springs are k_a and k_b, respectively.

The behavior of the CM is calculated as follows:

$$ml^2\ddot{\theta} = mlg\sin\theta - k_a\theta \qquad \text{(before the foot contact)} \tag{6.1a}$$

$$ml^2\ddot{\theta} = mlg\sin\theta - k_b l(x_c - x) \qquad \text{(after the foot contact).} \tag{6.1b}$$

Although some parameters, such as m, l, are determined by the information of the character, undetermined parameters still remain. They are determined in the following section.

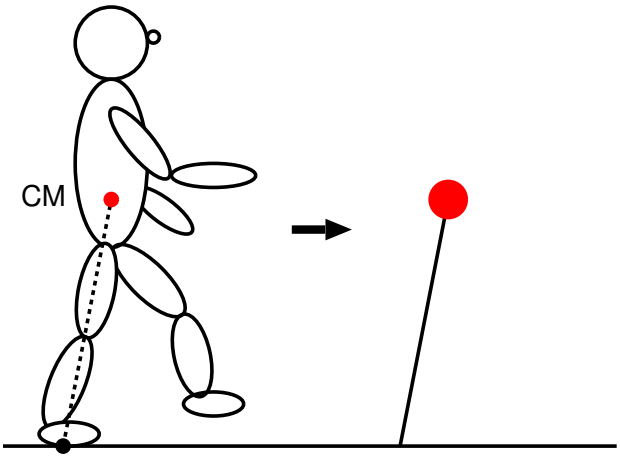

Figure 6.1: Inverted pendulum model: It consists of a mass point that stands for the CM of the character and a connection from the mass point to the supporting feet.

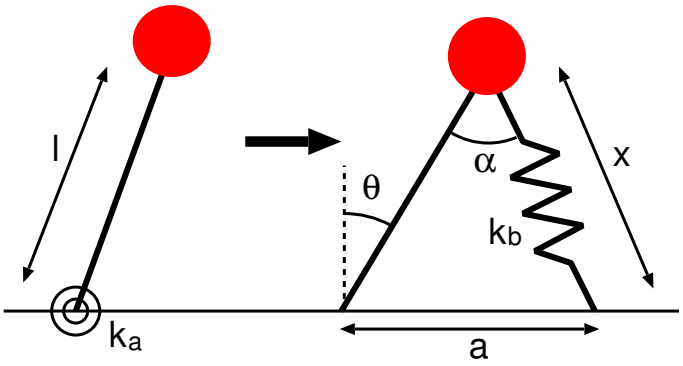

Figure 6.2: Inverted pendulum model in this method: There are two states; before and after the foot contact. The left figure illustrates the state before the foot contact, and the right figure illustrates the state after the foot contact.

6.2.2 Extracting Parameters

In this section, human motion is analyzed based on the structure that is designed in the previous section. We have to perform the two things here:

- Examining validity of the model
- Extracting parameters of the model

For the purpose of it, we apply the structure to the captured human motion and examine whether it is fitting or not. Then, parameters controlling the structure are extracted.

First, the stepping, the phase before the foot contact, is examined. In this phase, the inverted pendulum model obeys (6.1a). Applying the captured human motion to this equation, k_a is calculated and Table 6.1 shows the result. It is observed that the value of k_a is always very small, so we can regard $k_a = 0$.

The duration of stepping, which is defined as the duration from when the swing foot leaves the floor to when it contacts the floor again, is shown in Table 6.2, with values stated in milliseconds. The values converge well, and individual variation is not observed. Therefore, we can consider that the duration of stepping is always the same for all subjects.

Next, the state at the time when the stepping leg contacts the ground is examined. With regard to the position where the stepping foot contacts the ground, a strong relationship is observed in the ratio of the stepping angle, α_c, to the lean angle, θ_c. Table 6.3 shows the ratio for every subject. The value converges on a constant of 1.20 independent of the subjects.

Combining the observation of the stepping duration and the observation of the stepping angle, the position where the swing foot contacts the floor is calculated. First, θ_c is calculated from the duration and (6.1a), α_c is calculated by the ratio of θ_c and α_c, and then the contact position (the distance of the feet) is calculated:

$$a = \frac{\sin \alpha_c}{\cos(\theta_c - \alpha_c)} l. \tag{6.2}$$

Finally, the state after foot contact is examined. Before calculating k_b, it must be confirmed that human motion obeys the proposed model, in which the former stepping leg is regarded as a spring. In the model, the relationship between the length of the former stepping leg and the ground reaction is written as

$$f_g = k_b(x - x_c), \tag{6.3}$$

where f_g is the ground reaction, x is the length of the stepping leg, x_c is the length of the stepping leg at the foot contact, and k_b is the spring constant. The

equation shows that x and f_g have a linear relationship. For human motion, x is calculated from the captured motion data, and f_g is calculated from the force plates data. Therefore, when plotting (x, f_g) for human motion, the points lie on a line if the model is valid. The graphs plotting (x, f_g) for every subject are shown in Figure 6.3. The horizontal axis stands for the distance between a foot contact point and the CM, and the vertical axis stands for the ground reaction force acting on the swing foot. It is observed that the points lie on a line in all the graphs. The green lines are the regression lines.

As (6.3) shows, k_b is a gradient of the lines. The values are shown in Figure 6.4. Although the values converge for each subject, they are different among individuals. Accordingly, it can be said that k_b is a parameter that has individual variation.

6.3 Model of Balance Maintenance

The model consists of three phases; determining the trajectory of the CM using the inverted pendulum model, generating the lower body motion by inverse kinematics, and generating the whole-body motion by optimization calculation. Motion of maintaining balance is generated as follows: First, the trajectory of the CM is determined using the simplified model which is proposed in the previous section. The trajectory is calculated for all the frames. Next, the posture of the lower body is determined by inverse kinematics. The calculation is performed for the first frame. Then, the posture of the upper body is determined by optimization calculation for the frame. In this way, the posture of the first frame is generated. Using it as the initial posture, the postures of the following frames are generated frame by frame.

6.3.1 Determining Trajectory of the CM

The trajectory of the CM is calculated by (6.1). In the equations, m and l are determined by the information of the character. k_a, k_b, x_c, and the time of the foot contact are determined by observing human motion in the previous section.

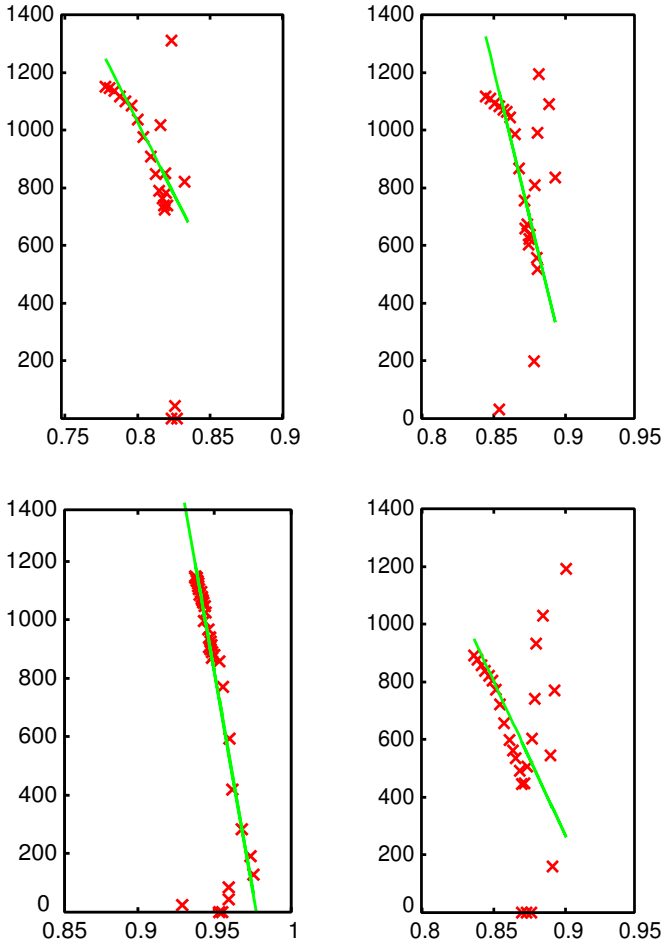

Figure 6.3: Relationship between the length of the leg spring and the ground reaction: The horizontal axis stands for the distance between a foot contact point and the CM (m), and the vertical axis stands for the ground reaction force acting on the swing foot (N). The green line is the regression line. The graphs show typical stepping by every subject.

Subject	Average	Std. deviation
1	79.9	184.4
2	101.8	273.6
3	-83.5	560.7
4	-96.6	264.9
total	15.8	356.3

Table 6.1: (Left table) Average and standard deviation of the value k_a

Subject	Average	Std. deviation
1	243.2	26.7
2	224.0	27.8
3	233.2	26.7
4	215.2	23.0
total	231.2	28.3

Table 6.2: (Right table) Average and standard deviation of the stepping duration (msec)

Subject	Average	Std. deviation
1	1.29	0.215
2	1.07	0.221
3	1.30	0.167
4	1.16	0.300
total	1.20	0.256

Table 6.3: (Left table) Average and standard deviation of the value α_c/θ_c

Subject	Average	Std. deviation
1	25100	5400
2	17900	7000
3	12700	4200
4	13500	4300

Table 6.4: (Right table) Average and standard deviation of the value k_b: The total is not calculated for k_b because individual variation is observed.

6.3.2 Generating Lower Body Motion

This section describes the way to generate lower body motion from the designed trajectories of the CM based on the inverted pendulum model discussed in the previous sections. In order to generate lower body motion, inverse kinematics is used. In this phase, it is not necessary to consider dynamic consistency. This is considered in the next phase.

The calculation is performed frame by frame. For every frame, the inverse kinematics calculation is performed twice, first for the CM and next for the swing foot. In the former, the link structure from the ankle of the support leg to the CM is considered and in the latter, the link structure from the hip joint of the swing leg to the heel is considered (Figure 6.4). The reason why inverse kinematics calculation is performed twice is for stability. If the two calculations are performed simultaneously, the result is not stable because of the high degree of freedom.

The way to solve inverse kinematics is as follows. Let $\boldsymbol{\theta} = (\theta_0, \ldots, \theta_n)^T$ be angles of the joints related to the link structure for considering inverse kinematics, $\boldsymbol{p}_i$ and $\boldsymbol{z}_i$ be the position and the rotational axis of each degree of freedom, and $\boldsymbol{r} = (\boldsymbol{P}^T, \boldsymbol{\Omega}^T)^T$ be the position and the rotation of the ends of the link structure, such as the CM and the swing foot. The rotation of joints that have three degrees of freedom is expressed by the Euler angle. The relationship between $\boldsymbol{r}$ and $\boldsymbol{\theta}$ is written as

$$\Delta \boldsymbol{r} = J \Delta \boldsymbol{\theta}, \tag{6.4}$$

where J is the Jacobian:

$$J(\boldsymbol{\theta}) = \begin{pmatrix} \dfrac{\partial P_1}{\partial \theta_1} & \dfrac{\partial P_1}{\partial \theta_2} & \cdots & \dfrac{\partial P_1}{\partial \theta_n} \\ \vdots & \vdots & & \vdots \\ \dfrac{\partial P_3}{\partial \theta_1} & \dfrac{\partial P_3}{\partial \theta_2} & \cdots & \dfrac{\partial P_3}{\partial \theta_n} \\ \dfrac{\partial \Omega_1}{\partial \theta_1} & \dfrac{\partial \Omega_1}{\partial \theta_2} & \cdots & \dfrac{\partial \Omega_1}{\partial \theta_n} \\ \vdots & \vdots & & \vdots \\ \dfrac{\partial \Omega_3}{\partial \theta_1} & \dfrac{\partial \Omega_3}{\partial \theta_2} & \cdots & \dfrac{\partial \Omega_3}{\partial \theta_n} \end{pmatrix}. \tag{6.5}$$

Now, because the relationship among $\boldsymbol{P}$, $\boldsymbol{\Omega}$, $\boldsymbol{p}_i$, and $\boldsymbol{z}_i$ is as shown in Figure 6.5,

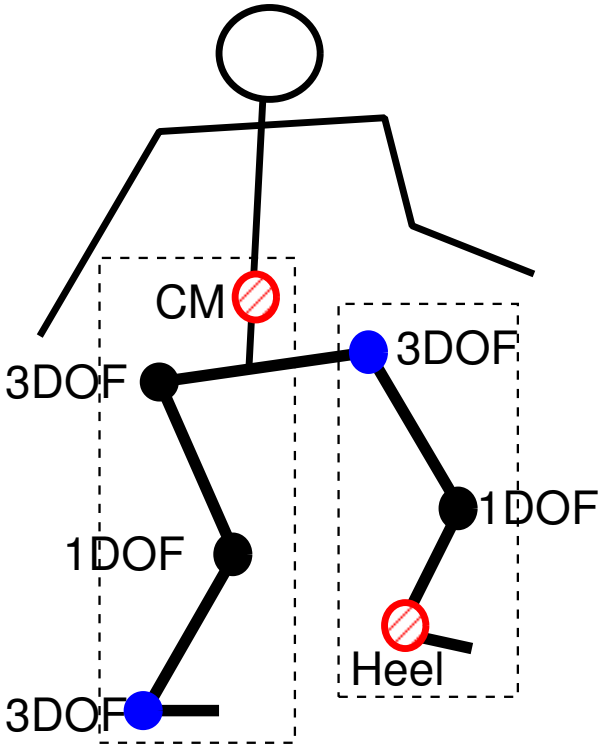

Figure 6.4: Link structures for solving inverse kinematics: first, inverse kinematics for the CM is solved and then inverse kinematics for the swing foot is solved.

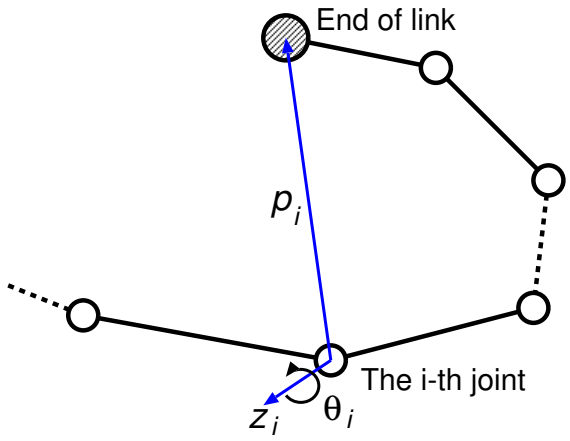

Figure 6.5: Relationship among $\boldsymbol{P}$, $\boldsymbol{\Omega}$, $\boldsymbol{p}_i$, and $\boldsymbol{z}_i$

the elements of the Jacobian matrix are written as

$$\frac{\partial \boldsymbol{P}}{\partial \theta_i} = (\boldsymbol{z}_i \times (\boldsymbol{P} - \boldsymbol{p}_i))\Delta\theta_i \tag{6.6a}$$

$$\frac{\partial \boldsymbol{\Omega}}{\partial \theta_i} = \boldsymbol{z}_i \Delta\theta_i, \tag{6.6b}$$

therefore the Jacobian is written as

$$J = \begin{pmatrix} \boldsymbol{z}_0 \times (\boldsymbol{P} - \boldsymbol{p}_0) & \boldsymbol{z}_1 \times (\boldsymbol{P} - \boldsymbol{p}_1) & \cdots & \boldsymbol{z}_n \times (\boldsymbol{P} - \boldsymbol{p}_n) \\ \boldsymbol{z}_0 & \boldsymbol{z}_1 & \cdots & \boldsymbol{z}_n \end{pmatrix}. \tag{6.7}$$

The inverse kinematics problem is solved using the pseudo-inverse matrix, $J^T(JJ^T)^{-1}$, iteratively. The actual procedure of solving inverse kinematics is as shown in Figure 6.6

6.3.3 Generating Whole-Body Motion

Lower body motion was generated by the inverse kinematics operation in the previous section. Next, the upper body motion must be determined. The generated motion here is well-balanced motion making use of the freedom remaining in the upper body. Optimization calculation by the quadratic programming method is used for this purpose.

```
set r for initial θ
while (‖r_dest − r‖ > δ) {
    obtain J for θ
    Δθ = J^T(JJ^T)^{-1}(r_dest − r)
    renew θ as θ + Δθ
    renew r for new θ
}
```

Figure 6.6: Procedure for solving inverse kinematics

In this case, the following two points are considered:

- Generating low-cost motion, and
- generating dynamically consistent motion.

Compared to balance maintenance by keeping the feet on the ground, the number of items that have to be considered is small. This is because the trajectory of the CM and the lower body motion are already determined in this model, and so the behavior of the CM and symmetry of motion are not necessary to be considered in the quadratic programming problem.

As in the case of balance maintenance by keeping the feet on the ground, the first item of "generating low-cost motion" is formulated in the objective function as follows:

$$\min \quad \ddot{\boldsymbol{\theta}}_{\text{upper}}^{T} A_{\theta_{\text{upper}}} \ddot{\boldsymbol{\theta}}_{\text{upper}}, \tag{6.8}$$

where $A_{\theta_{\text{upper}}}$ is a weight constant and $\boldsymbol{\theta}_{\text{upper}}$ represents the joint angles in the upper body. In contrast to balance maintenance by keeping the feet on the ground, keeping the character in an upright posture is not necessary because the lower body motion is determined beforehand in this model. This formula is rewritten as the formula about $\ddot{\boldsymbol{\varphi}}$:

$$\min \quad \ddot{\boldsymbol{\varphi}}^{T}(C_{\theta_{\text{upper}}}^{T} A_{\theta_{\text{upper}}} C_{\theta_{\text{upper}}})\ddot{\boldsymbol{\varphi}} + 2\boldsymbol{d}_{\theta_{\text{upper}}}^{T} A_{\theta_{\text{upper}}} C_{\theta_{\text{upper}}} \ddot{\boldsymbol{\varphi}}, \tag{6.9}$$

where $C_{\theta_{\text{upper}}}$ is the submatrix of the C_θ, which is defined in (5.29b), and its elements correspond to the upper body angle.

With regard to dynamic consistency, the constraint about the ZMP is employed. As with balance maintenance by keeping the feet on the ground, the boundary of the supporting area is approximated by the lines:

$$\alpha_i x + \beta_i z + \gamma_i < 0 \quad (i = 1, 2, \ldots, N_{\text{boundary}}), \tag{6.10}$$

and then, the condition that the ZMP is within the area is written as:

$$(\alpha_i \boldsymbol{c}_x + \beta_i \boldsymbol{c}_z + \gamma_i \boldsymbol{c}_c)^T \ddot{\boldsymbol{\varphi}} + (\alpha_i d_x + \beta_i d_z + \gamma_i d_c) < 0 \tag{6.11a}$$

$$\boldsymbol{c}_{s_y}^T \ddot{\boldsymbol{\varphi}} + d_{s_y} - g_y > 0. \tag{6.11b}$$

When the character is supported by one leg, the supporting area is the same as the supporting foot. Otherwise, the supporting area is the convex hull of the two feet.

Additionally, constraints about the limitation of the joint angle, velocity, and acceleration have to be considered. These are the same as for balance maintenance by keeping the feet on the ground:

$$\boldsymbol{c}_{\theta_i}^T \ddot{\boldsymbol{\varphi}} + d_{\theta_i} \geq \xi_{\min i} \tag{6.12a}$$

$$\boldsymbol{c}_{\theta_i}^T \ddot{\boldsymbol{\varphi}} + d_{\theta_i} \leq \xi_{\max i}, \tag{6.12b}$$

where ξ_* is defined in (5.37).

In summary, the quadratic programming problem is as follows:

$$\min \quad \ddot{\boldsymbol{\varphi}}^T (C_{\theta_{\text{upper}}}^T A_{\theta_{\text{upper}}} C_{\theta_{\text{upper}}}) \ddot{\boldsymbol{\varphi}} + 2\boldsymbol{d}_{\theta_{\text{upper}}}^T A_{\theta_{\text{upper}}} C_{\theta_{\text{upper}}} \ddot{\boldsymbol{\varphi}}, \tag{6.13a}$$

subject to

$$(\alpha_j \boldsymbol{c}_x + \beta_j \boldsymbol{c}_z + \gamma_j \boldsymbol{c}_c)^T \ddot{\boldsymbol{\varphi}} + (\alpha_j d_x + \beta_j d_z + \gamma_j d_c) < 0 \tag{6.13b}$$

$$\boldsymbol{c}_{s_y}^T \ddot{\boldsymbol{\varphi}} + d_{s_y} - g_y > 0 \tag{6.13c}$$

$$\boldsymbol{c}_{\theta_i}^T \ddot{\boldsymbol{\varphi}} + d_{\theta_i} \geq \xi_{\min i} \tag{6.13d}$$

$$\boldsymbol{c}_{\theta_i}^T \ddot{\boldsymbol{\varphi}} + d_{\theta_i} \leq \xi_{\max i}, \tag{6.13e}$$

where $i = 1, \ldots, N_{\text{joint}}$ and $j = 1, \ldots, N_{\text{boundary}}$.

6.4 Experiments

In this section, the results of the simulation are shown. Motions are generated under two conditions: The case in which the character takes a step immediately

after losing its balance, and the case in which the character takes a step after trying to maintain its balance without stepping.

Figure 6.7 shows the result when a force of 300N is applied for 0.1 second from the backward direction. It is the same as in the experiment of balance maintenance by keeping the feet on the ground (Figure 5.9), but in this case, balance maintenance by keeping the feet on the ground is not used. Instead, balance maintenance by stepping is taken directly after PD control. Compared with the previous experiment, balance can be maintained with a smaller motion although the position of the feet changes after the motion. Yellow bars in the figures stand for the inverted pendulum model used for generating steps.

Figure 6.8 shows the result when a force of 300N is applied for 0.4 second from the backward direction. Compared with the experiment of balance maintenance by keeping the feet on the ground (Figure 5.9), the magnitude of the applied force is the same, but the duration is four times as long as in the first experiment. At first, balance maintenance by keeping the feet on the ground is employed, and the character rotates its arms to keep its balance. At last, however, it becomes impossible to maintain its balance by using that method; then, balance maintenance by stepping is applied.

We also apply the method to the situation where perturbation is applied during walking. The model of balance maintenance holds in the case of walking. However, a parameter of α_c/θ_c is different. It is $\sim$1.4 during walking while it is $\sim$1.3 during standing upright. It means that a human takes a larger step when perturbation is applied during walking. Figure 6.9 shows the result. The three figures in the top row are walking motion from the captured motion. From the figure at the middle left, our method is applied. The velocity of the joints in the initial state is calculated from the captured data. A force of 300 N is applied for 0.4 second from the backward direction. After the perturbation, the character keeps stepping but the distance of stepping gets larger than normal walking and the waist is bent down.

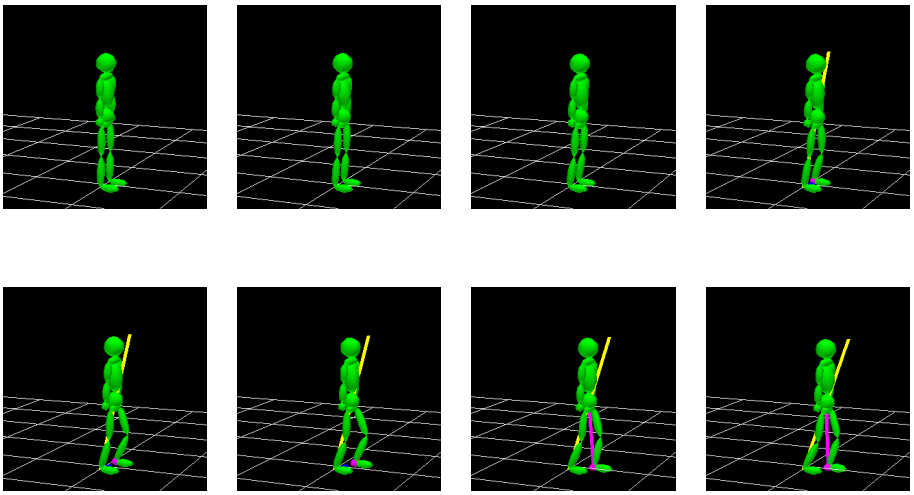

Figure 6.7: Balance maintenance by stepping: A force of 300 N is applied for 0.1 second from the backward direction. The character takes a step directly after it lost stability.

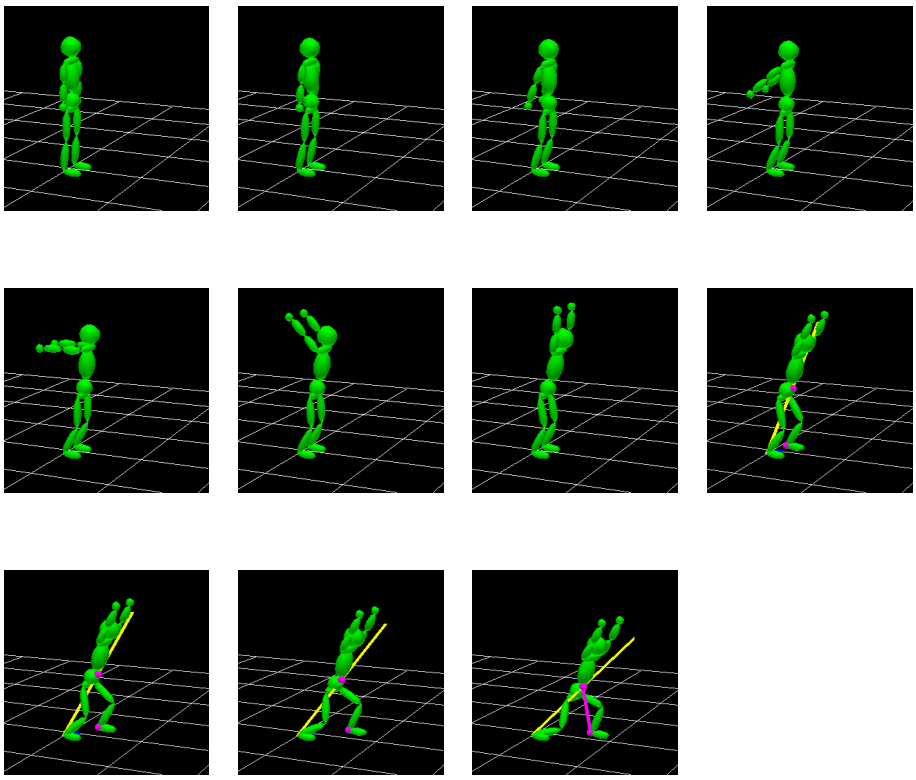

Figure 6.8: Combination of the two methods of balance maintenance: A force of 300 N is applied for 0.4 second. First, the character tries to maintain its balance by keeping its feet on the ground, but because the perturbation is too large, it takes a step to avoid falling down.

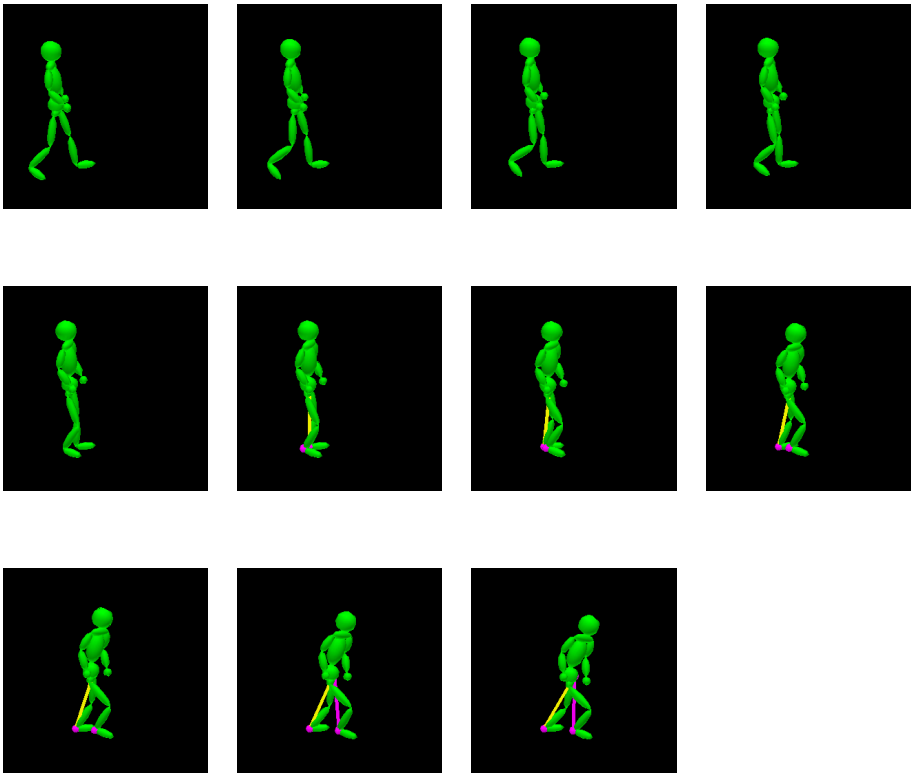

Figure 6.9: Balance Maintenance during Walking: The force of 300 N is applied for 0.4 second from the backward direction. The figures in the top row are the captured figures without modification. The method is applied from the figure at the middle left.

Chapter7

Discussion

7.1 Overview

So far, we have described the model of balance maintenance based on the observation of human motion, and have generated motion of a human-like character against various external perturbation. In this chapter, we examine the results and discuss the validity of our model.

First, we compare the generated motion with human motion. We extract apparent characteristics of human motion by hand based on observing it, and compare the generated motion with it. In addition to the qualitative comparison, we perform quantitative comparison in an aspect of dynamic property. As the criterion, the magnitude of impulse that can be handled without stepping is taken up. For human motion, the magnitude is calculated from the experiment using a strain gage. We compare the simulation result with it, and see the correspondence between the generated motion and human motion.

Next, we discuss the relationship between parameters and the generated motion. In particular, we focus on A_θ, which is the only parameter whose value is not determined based on human motion, and discuss the influence of it on the generated motion. As the result, we show that the correspondence between the generated motion and human motion is not because of appropriate tuning of parameters but because our model approximates the essence of human motion well.

7.2 Comparison of the Generated Motion and Human Motion

In this section, the results of simulation are compared with human motion. However, motions are different in every person, and, moreover, motions of the same person are different at different times. Therefore, it would not make sense to simply compare motions. In this study, we abstract essential parameters from captured human motion, make the model of balance maintenance based on the parameters, and reproduce whole-body motion from the behavior of the simplified model. If the characteristics of human motion, which are not modeled in the simplified model, appear in the reproduced motion, we may say that this is evidence that our model is reasonable.

First, we compare the results of simulation with human motion in an aspect of appearance. Next, we compare them in an aspect of a dynamic property.

7.2.1 Appearance

First, we examine the motion generated by balance maintenance by keeping the feet on the ground. In Figure 7.1, the upper figures are the captured human motions of maintaining balance when a force is applied from the backward direction. The middle figures illustrate these characteristics as follows: When a force is applied to a subject, who is a male, from his backward direction, his body leans forward and he begins to rotate his arms. It is effective in preventing humans from falling down because the momentum induced by this motion reduces the momentum of the whole body and prevents it from falling down. Next, he stretches his legs and bends down to move his waist backward, and then, he can recover his balance. The lower figures show a result of simulation. We can see that the above characteristics are well represented in it.

Next, we examine the motion of maintaining balance by stepping. Figure 7.2–7.4 shows the comparisons involved in three different cases. For every case, the upper figures are the captured human motion, the middle figures illustrate its characteristics, and the lower figures are results of simulation.

The first one (Figure 7.2) is the case when a human and a human-like character take a step immediately after losing its balance. In this case, perturbation is not so large that one cannot maintain balance without stepping. The human takes a step against the perturbation, but the step is small and his upper body keeps upright.

The next one (Figure 7.3) is the case when a human and a human-like character take a step after trying to maintain its balance without stepping. In this case, perturbation is large. When the perturbation is applied to the human, his body leans forward. He begins to rotate his arms and to bend down in order to maintain balance by keeping his feet on the ground. However, the perturbation is too large to allow his CM to return to the stable position. Therefore, he takes a step to prevent himself from falling down.

The last one (Figure 7.4) is the case when perturbation is applied during walking. The force is applied from the backward direction when a human and a human-like character support their bodies by their left feet during walking. When the perturbation is applied, the human takes a larger step to prevent himself from falling down. At the same time, he takes the counter action, moving his left shoulder and his left arm forward, to maintain his balance in a right-left direction.

In these three cases, the characteristics of human motion are also observed in the generated motion by simulation.

As shown in above, the characteristics of human motion are well reproduced in the generated motion in both modes. An important point to emphasize is that only macro parameters, such as the CM and the ZMP, are considered in the model of balance maintenance; thus, such characteristics are not motions programmed in advance, but are rather the results of optimization calculation. The fact that the motion similar to a human is generated as the result of optimization calculation based on the simple model means that the model correctly represents the essential part of balance maintenance of a human.

7.2.2 Dynamic Property

Next, we compare results of simulation to human motion in an aspect of dynamics. In this subsection, we focus on the magnitude of perturbation that can be handled without stepping.

As mentioned in the previous chapter, we performed an experiment in which perturbation was applied to a subject who was told to maintain his balance by keeping his feet on the ground as much as possible. A strain gage was used then in order to record the applied force. The recorded force is shown as Figure 7.5. The magnitude of the impulse that is applied in each trial is calculated from the graphs. Table 7.1 shows the calculated impulse and whether the subject could maintain balance without stepping or not.

According to the table, we can estimate the limit of the impulse for which

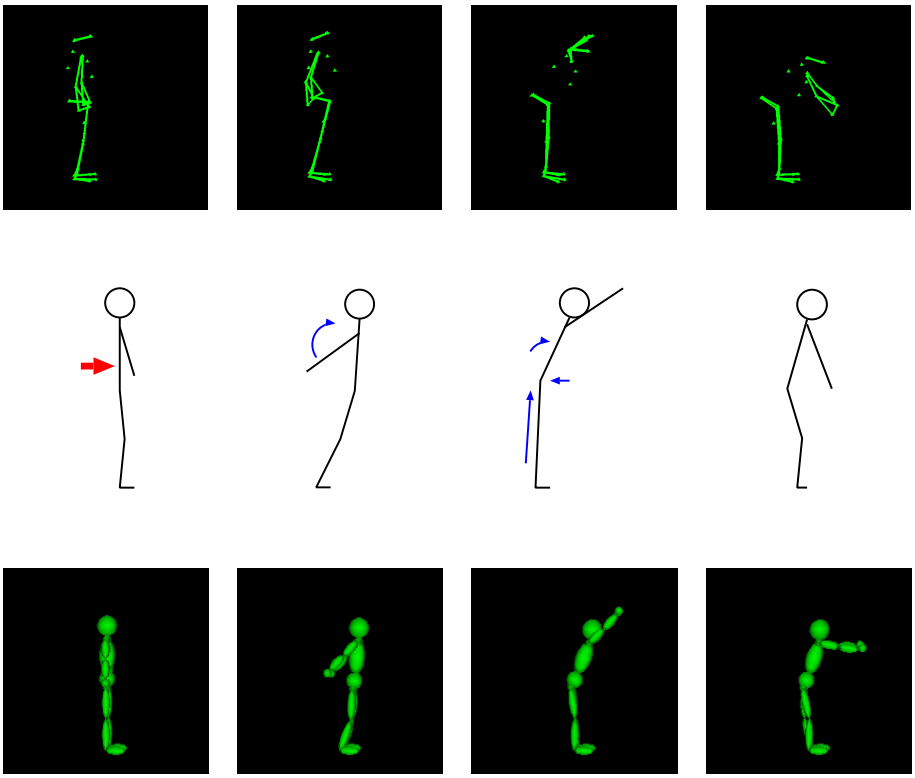

Figure 7.1: Human motion vs. generated motion (Balance maintenance by keeping feet on the ground): The upper figures show the captured human motion when the force is applied from the backward direction; the middle figures show the characteristics of it; and the lower figures show the result of simulation.

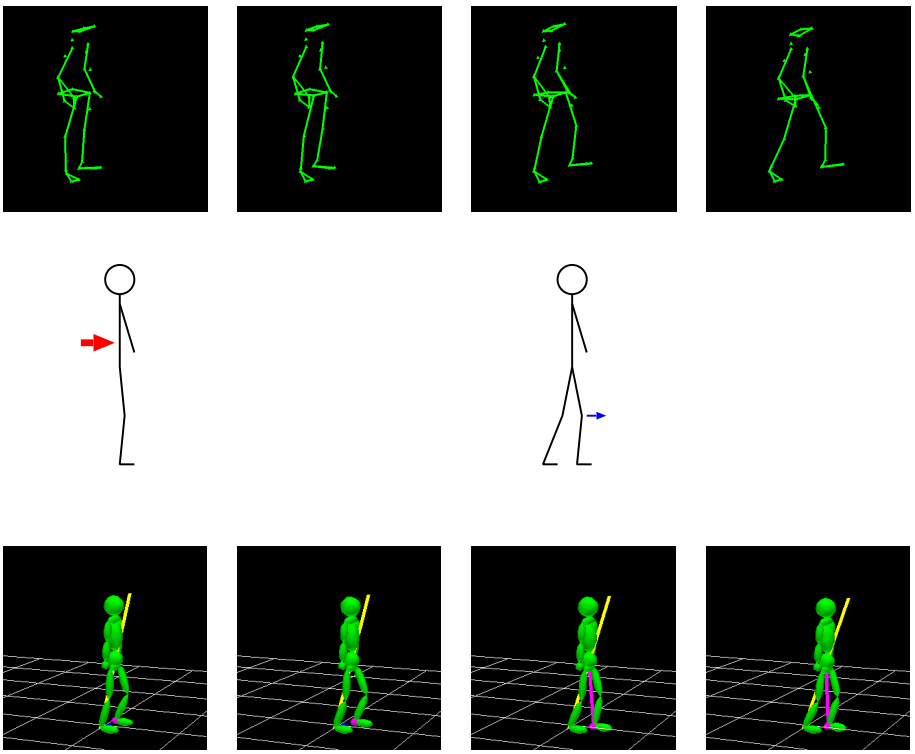

Figure 7.2: Human motion vs. generated motion (Balance maintenance by stepping): The upper figures show the captured human motion when the human takes a step directly after the perturbation. The middle figures show its characteristics. The lower figures show a result of simulation.

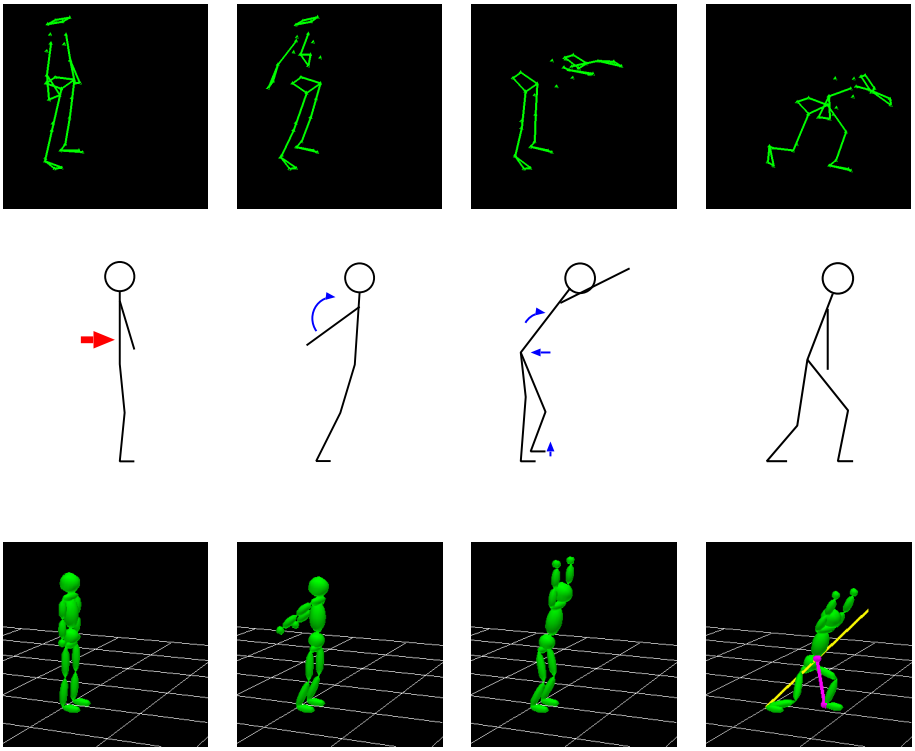

Figure 7.3: Human motion vs. generated motion (Combination of two modes): The upper figures show the captured human motion when the human first keeps his or her feet on the ground as much as possible, but finally takes a step. The middle figures show its characteristics. The lower figures show a result of simulation.

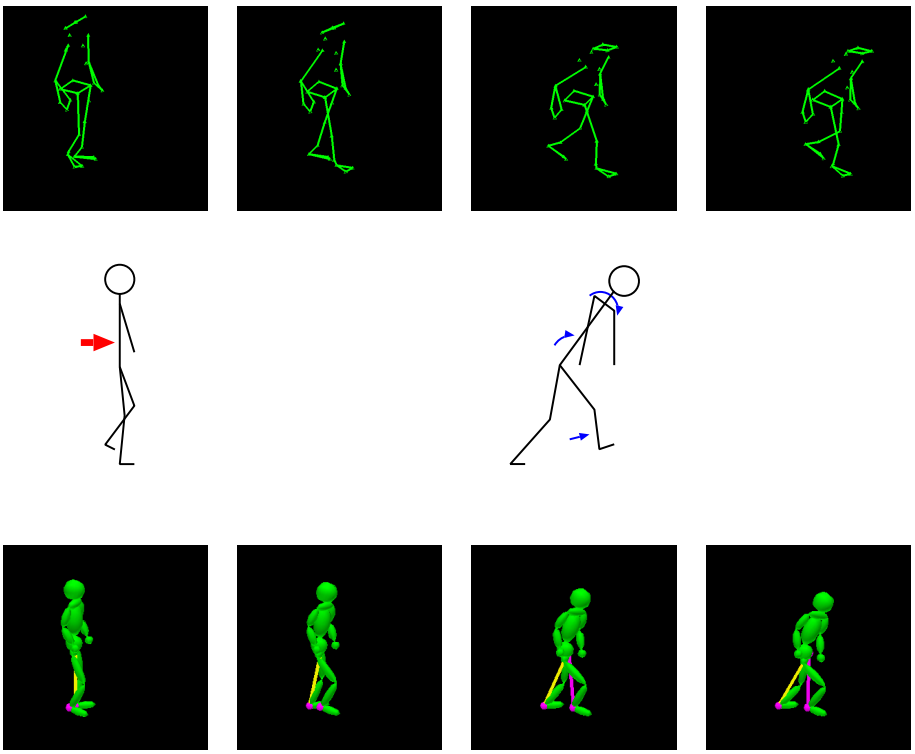

Figure 7.4: Human motion vs. generated motion (Balance maintenance during walking): The upper figures show the captured human motion when perturbation is applied during walking. The middle figures show its characteristics. The lower figures show the simulation result.

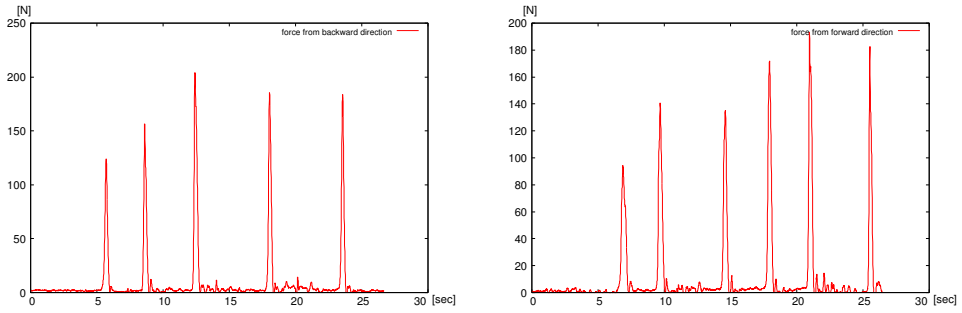

Figure 7.5: Applied force: The perturbation by the forward force (the left) and the backward force (the right). The horizontal axis represents the time (second) and the vertical axis represents the magnitude of perturbation[N].

the subject could maintain balance without stepping. For perturbation from the backward direction, the limit is estimated as ∼40 Ns, and for perturbation from the forward direction, it is estimated as ∼35 Ns. In the latter case, the subject could maintain balance without stepping in the fourth trial although the larger perturbation of 44.5 Ns was applied. However, the subject's success in maintaining balance occurred mainly because the subject by mistake made a counter motion before perturbation was applied.

Comparing this, the proposed model generates stable motion against perturbation from backward and forward directions for the perturbation of ∼35 Ns and ∼30 Ns respectively. If the perturbation is increased, the result becomes unstable. For an impulse of 40 Ns from the backward direction, the method could not find a solution. For an impulse of 35 Ns from the forward direction, the method also could not find the solution.

Figure 7.6 is a graph to compare the result of simulation with the human case. The upper band represents the case when perturbation is applied from a backward direction, and the lower band represents the case when perturbation is applied from a forward direction. The horizontal axis represents the applied impulse. The green area shows the range of impulse in which a solution of the optimization calculation is stably found, while the red area shows the range of impulse in which no solution is found without stepping. The mark '◯' means that the subject could maintain his balance without stepping for the impulse, while the mark '×' means that he could not. According to the graph, it can be said

Trial	Impulse (Ns)	Step
1	29.4	no step
2	35.9	no step
3	54.7	step
4	43.5	step
5	38.4	no step

Trial	Impulse (Ns)	Step
1	29.1	no step
2	39.0	step
3	34.0	no step
4	44.5	no step
5	47.8	step
6	36.7	step

Table 7.1: Impulse applied to the subject: The tables show the magnitude of the impulse applied to the subjects when the force applied from the backward direction (the left) and from the forward direction (the right). The column "Step" shows whether the subject could maintain balance without stepping or not. "no step" means he could and "step" means he could not.

that the human character under the proposed method shows the similar dynamic property to a human about the limitation of impulse that can be handled without stepping.

7.3 Influence of Parameters on the Result

In the previous section, we have seen that not only apparent characteristics but also dynamic characteristics, that is, the limitation of impulse which can be handled without stepping, are reproduced in generated motion by our method. However, we did not discuss influence of parameters on the result. There are various parameters in our model and generated motion changes depending on them. In this section, we examine the influence of them on the generated motion and discuss the condition of the qualitative and quantitative correspondence between the generated motion and human motion.

Although there are many parameters in our model, most of them are extracted from human motion. Because their values are determined so as to be the same as humans and cannot be changed freely, we do not discuss them in this section. What we discuss here is a parameter that is not determined from human

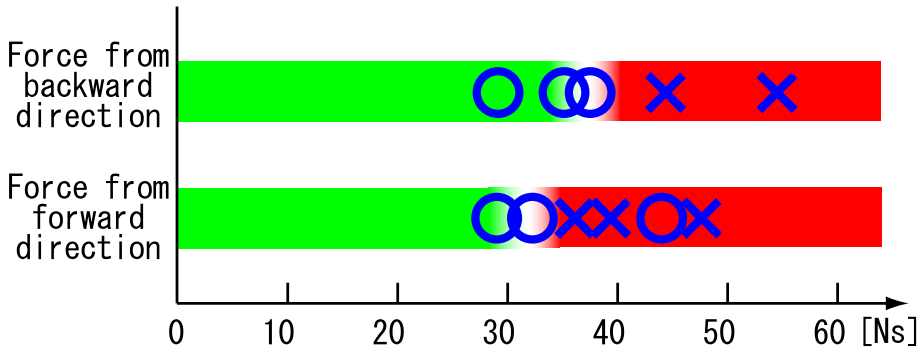

Figure 7.6: Comparison of impulse that can be handled without stepping: The horizontal axis represents applied impulse. The green/red area shows the range of impulse in which the optimization problem can/cannot be solved. The mark ◯/× means that the subject could/could not maintain his balance without stepping.

motion. Concretely, we focus on a parameter A_θ in equation (5.27), which is a coefficient in the objective function of the quadratic programming problem. It determines weight of joints, and therefore it influences the generated motion significantly. As described above, the value of A_θ is determined empirically. In this section, we generate motion for different values of A_θ and examine the results.

Figure 7.7 shows the generated motion for three different A_θ, in which the elements corresponding to shoulder joints (a_{shoulder}) are varied. The same force is applied from the backward direction for every case. The upper figures are the case of $a_{\text{shoulder}} = 1.5$, the middle figures are the case of $a_{\text{shoulder}} = 0.15$, which is the value used in the previous chapters, and the lower figures are the case of $a_{\text{shoulder}} = 0.015$. Because the optimization problem is solved to minimize the objective function, a joint tends to move easily if a smaller value is set on the corresponding element. In the simulation, the character rotates its arms largely in the lower figures. In the upper case, it bends down further instead of rotating its arms to maintain balance. In this way, generated motion changes depending on the value of A_θ. However, the characteristics of the motion do not change even if the parameter A_θ changes. With regard to this case, the characteristics of "rotating arms" and "bending down" appear in every case. Only the magnitude of each characteristic changes.

Next, we examine the trajectory of the CM. Figure 7.8 shows the position

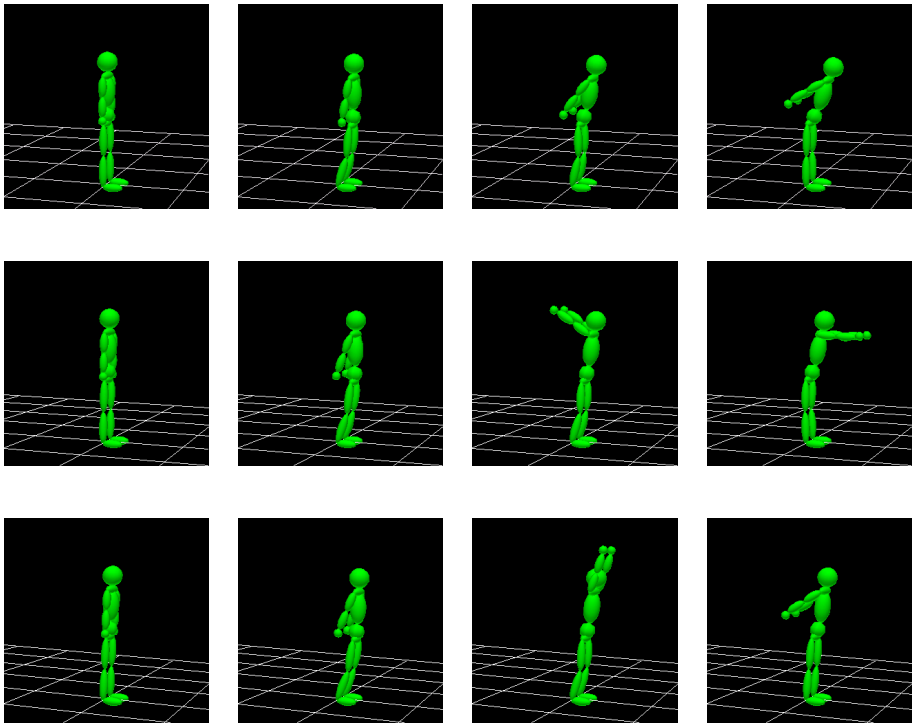

Figure 7.7: Motion for various A_θ: The elements of A_θ that corresponds to shoulder joints are changed. The values are 1.5 in the upper figures, 0.15 in the middle figures, and 0.015 in the lower figures. Force is applied from the backward direction.

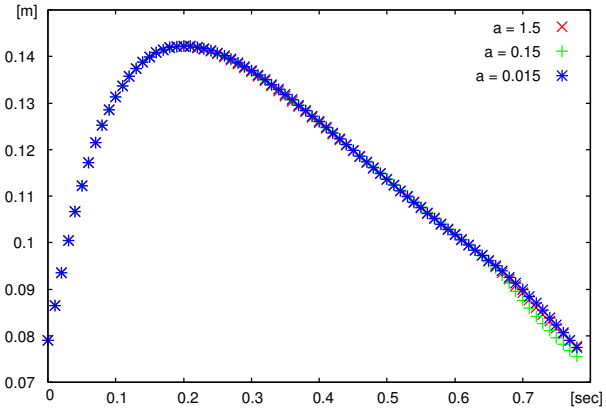

Figure 7.8: Trajectory of the CM for various A_θ: The horizontal axis represents the time after beginning balance maintenance. The vertical axis represents the distance of the CM from the initial position.

of the CM in the three cases. The horizontal axis means time. Time 0 is the time when the character begins to maintain its balance. The vertical axis means the distance between the position of the CM and its initial position. Observing the graph, we can see that the trajectory is always the same without regard to the value of A_θ. This result is reasonable because the behavior of the CM is constrained by the constraints of the optimization problem. The posture of the character is determined so as to satisfy the constrained trajectory of the CM, and A_θ relates only to determining the posture.

In the previous section, we have examined the situation when the stepping motion is generated. In practice, it is generated when no solution that satisfies the constraints, including the constraint about trajectory of the CM, is found. Therefore, the value of A_θ has little influence on the limitation of impulse that can handle without stepping because it is a coefficient in the objective function. In the above simulation, the difference of the limitation is not observed among the three cases. According to the fact, it can be said that the reason why the limitation of impulse corresponds between simulated motion and human motion is not the correct tuning of A_θ. The reason is considered as follows: Practically, a human does not have such a large degree of freedom to move effectively when he or she tries to maintain balance against large perturbation. Therefore, a human maintaining balance can be modeled sufficiently using a model with small degrees

of freedom, such as an inverted pendulum model.

In summary, it is found that the qualitative and quantitative characteristics of motion are conserved when the value of A_θ changes. From this fact, it can be said that A_θ is not a parameter that determines the fundamental characteristics of motion but a parameter that realizes minor variation of motion. The reason why generated motion by the proposed model of balance maintenance corresponds to human motion is not that value of parameters are set correctly but that the proposed simple model well approximates the essence of human balance maintenance.

Chapter8

Conclusion

8.1 Summary

In this thesis, we have discussed balance maintenance with whole-body motion of a human-like character. In most previous research, methods to reproduce pre-designed motion, sometimes with a few modifications, have been proposed. However, it is also important to generate motion actively in order to respond to interaction with the environment. Therefore, we proposed a method to generate active motion to maintain balance against large and sudden perturbations. We focused on large-scale whole-body motion in maintaining balance, which a human usually takes in order to realize high-quality balance maintenance. We modeled it with a simple structure based on observation of human motion.

We captured human motion by a motion-capturing system and force plates, and analyzed it. In this method, the captured motion was not used directly. Instead, the essential parameters of maintaining balance were extracted, and a model of balance maintenance was designed based on them. The model has a simple structure similar to an inverted pendulum model, and macro quantities, such as the position of the CM and the ZMP, were considered in it. By means of treating motion with our simplified model, we concentrated on only the essential elements for maintaining balance. In order to reconstruct whole-body motion from the simplified model, we used optimization calculation. Our method does not require any reference motion or prior knowledge about the whole-body motion. Without them, it can reproduce complex whole-body motion from a simple model. It is the most important feature of our method.

In practice, we modeled two types of whole-body motion of maintaining bal-

ance: keeping the feet on the ground, and stepping.

Balance maintenance by keeping the feet on the ground was for generating the motion whereby a character maintains its balance by keeping its feet firmly on the ground without stepping. When designing this model, we focused on the human way to control the position of its CM. We analyzed the captured motion and extracted the essential parameters. Based on these parameters, we constructed a quadratic programming problem and generated the motion.

In balance maintenance by stepping, motion was generated through three phases. First, trajectory of the CM was determined using the simple model similar to an inverted pendulum model. It was designed based on the result of observing human motion. The way to take a step was also modeled based on the result. Next, motion of the lower body was determined satisfying the trajectory of the CM and inverse kinematics calculations using a Jacobian were performed. Finally, the upper body motion was calculated to realize dynamic consistency using optimization calculation, and the whole-body motion was generated.

In our simulation, we generated whole-body motion to maintain balance under various perturbations. Motions that a human often takes, such as rotating the arms and bending down, were generated. Such motion was not programmed beforehand, but obtained as a result of our optimization calculations. In addition, our model was applied to other cases besides standing upright. We generated the motion of maintaining balance during walking, which was an advantage of abstracting a simple model from human motion. In the abstraction, the motion of maintaining balance was decoupled from other motions, and it could be re-coupled to another motion when generating motion.

We also compared the generated motion by our method with human motion. It was shown that characteristics of human motion are reproduced in the generated motion, such as rotating arms and bending down. Moreover, the correspondence between generated motion and human motion was observed with regard to the magnitude of perturbation that can be handled without stepping. This showed that our model correctly represented the human motion of maintaining balance with whole-body motion not only in a qualitative aspect but also in a quantitative aspect.

In summary, the contribution of this thesis is considered as follows: (1) It is shown that characteristics of complex human whole-body motion against large perturbation can be represented using a simple structure with parameters extracted for human motion and optimization calculation. (2) It is found that the threshold to choose the mode can be represented by the model. (3) Various motions that are similar to human motion can be generated using the model.

8.2 Future Work

Generating realistic motion for a human-like character is increasing in importance, and I hope to deal with realistic motion in greater detail in future work.

The computing and actuation hardware of a humanoid robot is rapidly improving, so that the idea that a humanoid robot could coexist with people in a living space is becoming increasingly realistic. But because accidents cannot be avoided in a practical environment, it is important to cope with accidents by executing corresponding corrective actions automatically.

In computer graphics, the required quality of animation is becoming higher and higher. In order to reduce the load of a creator when generating animation of a human figure, it is not enough to use captured motion directly. One must also have a method to edit and synthesize motion flexibly.

The method proposed in this thesis matches these needs. And in the future, by extending our proposed model, it will be possible to describe and generate even more types of motion. Notably, because transitions from one motion trajectory to another trajectory are not included in our proposed model, we did not deal with the motions that need to be generated after maintaining balance to the original state. If such transitions were added to our model, the kinds of motion that could be generated would be enormously extended.

Even in regards to maintaining balance, there is room for all models to improve. In this thesis, we have attempted to improve current methodology by modeling the motion of keeping feet on the ground as well as stepping. In the future, our model could be extended to a broader range of human activities such as running and jumping.

It remains a valuable goal to describe, edit, and synthesize the modeling of human motion.

Appendix A

Determining Local Coordinates

This appendix explains the way to determine the local coordinates of the body elements from motion data by a motion-capturing system. First, some points on the body are determined from the marker position, and then the local coordinates are defined using the points.

A.1 Determining Points

For defining the local coordinates, thirty-two points are determined on the body. The points are indexed with numbers from 0 to 31 and the point indexed with i is written as $\langle i \rangle$. Figure A.1 illustrates the points. In this figure, the white points are determined by directly using the marker positions, and the black points are determined based on the markers' positions. The way to determine the position of the points is described in Table A.1.

The point $\langle 31 \rangle$ is on the line that is through $\langle 30 \rangle$ and is perpendicular to the plane formed by $\langle 12 \rangle$, $\langle 13 \rangle$, $\langle 18 \rangle$, and $\langle 19 \rangle$. The perpendicular line from $\langle 31 \rangle$ to the line formed by $\langle 25 \rangle$ and $\langle 30 \rangle$ divides the latter line in the ratio of $\alpha : 1$. Figure A.2 illustrates it. If $\boldsymbol{n}$ denotes the normal vector of the plane formed by $\langle 12 \rangle$, $\langle 13 \rangle$, $\langle 18 \rangle$, and $\langle 19 \rangle$, $\langle 31 \rangle$ is formulated using a parameter t as

$$\langle 31 \rangle = t\boldsymbol{n} + \langle 30 \rangle. \tag{A.1}$$

On the other side, because the line formed by $\langle 25 \rangle$ and $\langle 30 \rangle$ is divided in the ratio of $\alpha : 1$ by the perpendicular line form $\langle 31 \rangle$,

$$\left(\frac{\langle 25 \rangle - \langle 30 \rangle}{|\langle 25 \rangle - \langle 30 \rangle|}, \langle 31 \rangle - \langle 30 \rangle \right) : |\langle 25 \rangle - \langle 30 \rangle| = 1 : 1 + \alpha. \tag{A.2}$$

From the above two equations, the parameter t is solved as

$$t = \frac{|\langle 25\rangle - \langle 30\rangle|^2}{(\alpha+1)(\langle 25\rangle - \langle 30\rangle, \boldsymbol{n})}, \tag{A.3}$$

and therefore the position of $\langle 31\rangle$ is determined. In this thesis, $\alpha = 2$.

A.2 Determining Coordinates

As described in 4.3.1, the local coordinates are defined as Figure A.3. The x-axis of each element is basically set to be parallel to the pivot of the joint. The y-axis points basically toward an upper direction. In this section, the way to define the local coordinates is described.

First, a function named `make_axis` is defined. In order to make an axis from vectors that are not exactly perpendicular, `make_axis` receives two vectors as its arguments and returns a vector $\boldsymbol{y}'$ such that

$$\boldsymbol{y}' = (\boldsymbol{x} \times \boldsymbol{y}) \times \boldsymbol{x}. \tag{A.4}$$

$\boldsymbol{y}'$ is exactly perpendicular to $\boldsymbol{x}$, and therefore, $\boldsymbol{x}$ and $\boldsymbol{y}'$ can be used for the coordinates. The rest of the axis is calculated by $\boldsymbol{x} \times \boldsymbol{y}'$.

The coordinates of the elements are defined as follows.

Head First, the x-axis is defined, and then the y-axis is defined:

$$\boldsymbol{x} = \frac{\langle 0\rangle + \langle 1\rangle}{2} - \frac{\langle 2\rangle + \langle 3\rangle}{2} \tag{A.5a}$$

$$\boldsymbol{y} = \texttt{make\_axis}(\boldsymbol{x},\ \langle 24\rangle - \langle 25\rangle). \tag{A.5b}$$

Chest First, the x-axis is defined, and then the y-axis is defined:

$$\boldsymbol{x} = \langle 4\rangle - \langle 8\rangle, \tag{A.6a}$$

$$\boldsymbol{y} = \texttt{make\_axis}(\boldsymbol{x},\ \langle 31\rangle - \langle 30\rangle). \tag{A.6b}$$

Loins First, the x-axis is defined, and then the y-axis is defined:

$$\boldsymbol{x} = \langle 28\rangle - \langle 29\rangle, \tag{A.7a}$$

$$\boldsymbol{y} = \text{tt make\_axis}(\boldsymbol{x},\ \langle 31\rangle - \langle 30\rangle). \tag{A.7b}$$

Left upper arm First, the y-axis is defined, and then the x-axis is defined:

$$\boldsymbol{y} = \langle 4\rangle - \langle 5\rangle, \tag{A.8a}$$

$$\boldsymbol{x} = \texttt{make\_axis}((\langle 5\rangle - \langle 26\rangle) \times \boldsymbol{y},\ \boldsymbol{y}). \tag{A.8b}$$

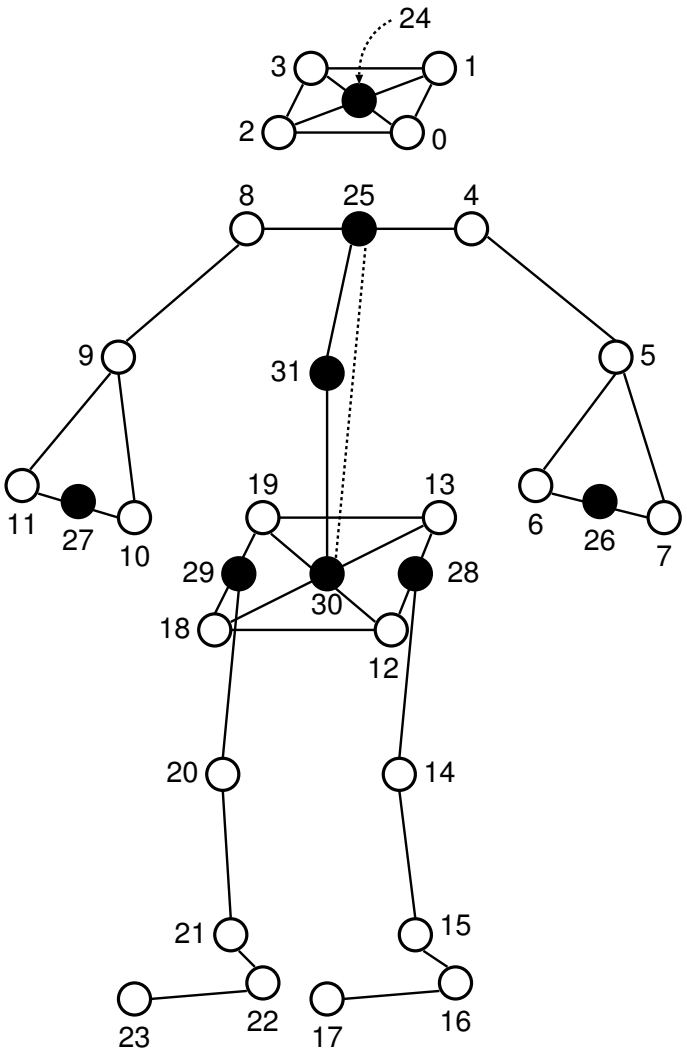

Figure A.1: Points on the body: The white points are determined by directly using the marker positions. The black points are determined based on the markers' positions.

Point	Marker
$\langle 0 \rangle$	LFHD (left forward head)
$\langle 1 \rangle$	LBHD (left backward head)
$\langle 2 \rangle$	RFHD (right forward head)
$\langle 3 \rangle$	RBHD (right backward head)
$\langle 4 \rangle$	LSHO (left shoulder)
$\langle 5 \rangle$	LELB (left elbow)
$\langle 6 \rangle$	LWRA (left wrist A — radius side)
$\langle 7 \rangle$	LWRB (left wrist B — ulna side)
$\langle 8 \rangle$	RSHO (right shoulder)
$\langle 9 \rangle$	RELB (right elbow)
$\langle 10 \rangle$	RWRA (right wrist A — radius side)
$\langle 11 \rangle$	RWRB (right wrist B — ulna side)
$\langle 12 \rangle$	LFWT (left forward waist)
$\langle 13 \rangle$	LBWT (left backward waist)
$\langle 14 \rangle$	LKNE (left knee)
$\langle 15 \rangle$	LANK (left ankle)
$\langle 16 \rangle$	LHEE (left heel)
$\langle 17 \rangle$	LTOE (left toe)
$\langle 18 \rangle$	RFWT (right forward waist)
$\langle 19 \rangle$	RBWT (right backward waist)
$\langle 20 \rangle$	RKNE (right knee)
$\langle 21 \rangle$	RANK (right ankle)
$\langle 22 \rangle$	RHEE (right heel)
$\langle 23 \rangle$	RTOE (right toe)
$\langle 24 \rangle$	$(\langle 0 \rangle + \langle 1 \rangle + \langle 2 \rangle + \langle 3 \rangle)/4$
$\langle 25 \rangle$	$(\langle 4 \rangle + \langle 8 \rangle)/2$
$\langle 26 \rangle$	$(\langle 6 \rangle + \langle 7 \rangle)/2$
$\langle 27 \rangle$	$(\langle 10 \rangle + \langle 11 \rangle)/2$
$\langle 28 \rangle$	$(\langle 12 \rangle + \langle 13 \rangle)/2$
$\langle 29 \rangle$	$(\langle 18 \rangle + \langle 19 \rangle)/2$
$\langle 30 \rangle$	$(\langle 28 \rangle + \langle 29 \rangle)/2$
$\langle 31 \rangle$	described in the body

Table A.1: Description of the points

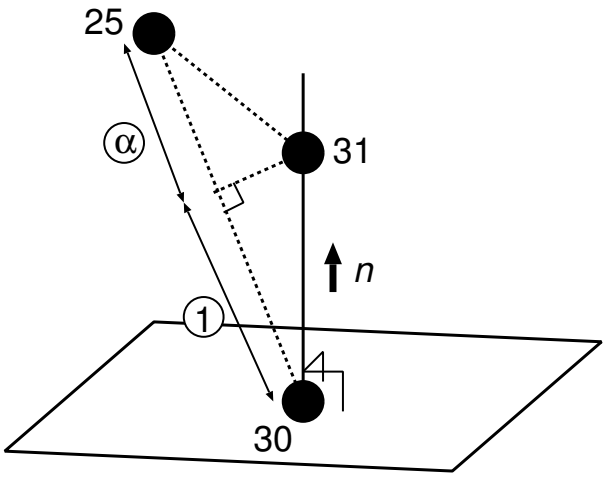

Figure A.2: Point ⟨31⟩: Point ⟨31⟩ is the point that connects the chest and the waist.

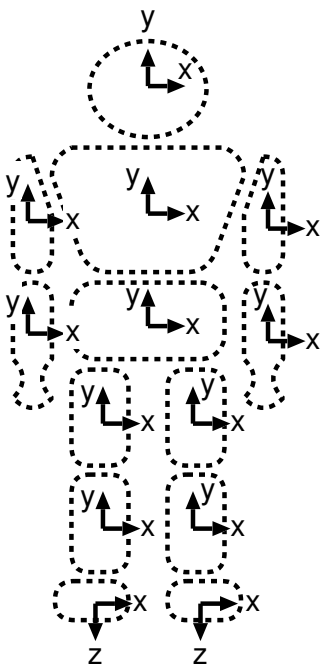

Figure A.3: Local coordinates of the body elements

Left forearm First, the y-axis is defined, and then the x-axis is defined:

$$\boldsymbol{y} = \langle 5 \rangle - \langle 26 \rangle, \tag{A.9a}$$

$$\boldsymbol{x} = \texttt{make\_axis}(\langle 6 \rangle - \langle 7 \rangle, \boldsymbol{y}). \tag{A.9b}$$

Right upper arm First, the y-axis is defined, and then the x-axis is defined:

$$\boldsymbol{y} = \langle 8 \rangle - \langle 9 \rangle, \tag{A.10a}$$

$$\boldsymbol{x} = \texttt{make\_axis}((\langle 9 \rangle - \langle 27 \rangle) \times \boldsymbol{y}, \boldsymbol{y}). \tag{A.10b}$$

Right forearm First, the y-axis is defined, and then the x-axis is defined:

$$\boldsymbol{y} = \langle 9 \rangle - \langle 27 \rangle, \tag{A.11a}$$

$$\boldsymbol{x} = \texttt{make\_axis}(\langle 11 \rangle - \langle 10 \rangle, \boldsymbol{y}). \tag{A.11b}$$

Left thigh In order to define the coordinates of the left thigh, the pivot of the left knee has to be obtained. However, the knee is often stretched and its pivot cannot be calculated properly. If the knee is stretched, the pivot of the ankle about the pitch rotation is used. First, the pivot of the knee is obtained:

$$\boldsymbol{p} = \begin{cases} (\langle 14 \rangle - \langle 15 \rangle) \times (\langle 17 \rangle - \langle 16 \rangle) & \text{If the knee is stretched,} \\ (\langle 28 \rangle - \langle 14 \rangle) \times (\langle 14 \rangle - \langle 15 \rangle) & \text{otherwise.} \end{cases} \tag{A.12}$$

Next, the y-axis is defined, and then the x-axis is defined:

$$\boldsymbol{y} = \langle 28 \rangle - \langle 14 \rangle, \tag{A.13a}$$

$$\boldsymbol{x} = \texttt{make\_axis}(\boldsymbol{p}, \boldsymbol{y}). \tag{A.13b}$$

Left shank First, the y-axis is defined, and then the x-axis is defined:

$$\boldsymbol{y} = \langle 14 \rangle - \langle 15 \rangle, \tag{A.14a}$$

$$\boldsymbol{x} = \texttt{make\_axis}((\langle 14 \rangle - \langle 15 \rangle) \times (\langle 17 \rangle - \langle 16 \rangle), \boldsymbol{y}). \tag{A.14b}$$

Left foot First, the x-axis is defined, and then the y-axis is defined:

$$\boldsymbol{x} = (\langle 14 \rangle - \langle 15 \rangle) \times (\langle 17 \rangle - \langle 16 \rangle), \tag{A.15a}$$

$$\boldsymbol{y} = \texttt{make\_axis}(\boldsymbol{x}, (\langle 17 \rangle - \langle 16 \rangle) \times \boldsymbol{x}). \tag{A.15b}$$

Right thigh As in the case of the left thigh, first, the pivot of the right knee is obtained:

$$\boldsymbol{p} = \begin{cases} (\langle 20\rangle - \langle 21\rangle) \times (\langle 23\rangle - \langle 22\rangle) & \text{If the knee is stretched,} \\ (\langle 29\rangle - \langle 20\rangle) \times (\langle 20\rangle - \langle 21\rangle) & \text{otherwise.} \end{cases} \tag{A.16}$$

Next, the y-axis is defined, and then the x-axis is defined:

$$\boldsymbol{y} = \langle 29\rangle - \langle 20\rangle, \tag{A.17a}$$

$$\boldsymbol{x} = \texttt{make\_axis}(\boldsymbol{p}, \boldsymbol{y}). \tag{A.17b}$$

Right shank First, the y-axis is defined, and then the x-axis is defined:

$$\boldsymbol{y} = \langle 20\rangle - \langle 21\rangle, \tag{A.18a}$$

$$\boldsymbol{x} = \texttt{make\_axis}((\langle 20\rangle - \langle 21\rangle) \times (\langle 23\rangle - \langle 22\rangle), \boldsymbol{y}). \tag{A.18b}$$

Right foot First, the x-axis is defined, and then the y-axis is defined:

$$\boldsymbol{x} = (\langle 20\rangle - \langle 21\rangle) \times (\langle 23\rangle - \langle 22\rangle), \tag{A.19a}$$

$$\boldsymbol{y} = \texttt{make\_axis}(\boldsymbol{x}, (\langle 23\rangle - \langle 22\rangle) \times \boldsymbol{x}). \tag{A.19b}$$

Appendix B

Markers of Motion-Capturing System

This appendix describes the markers that are attached to a human body when its motion is captured by a motion-capturing system. They are attached as illustrated in Figure B.1. The detailed description of the position is shown in Table B.1.

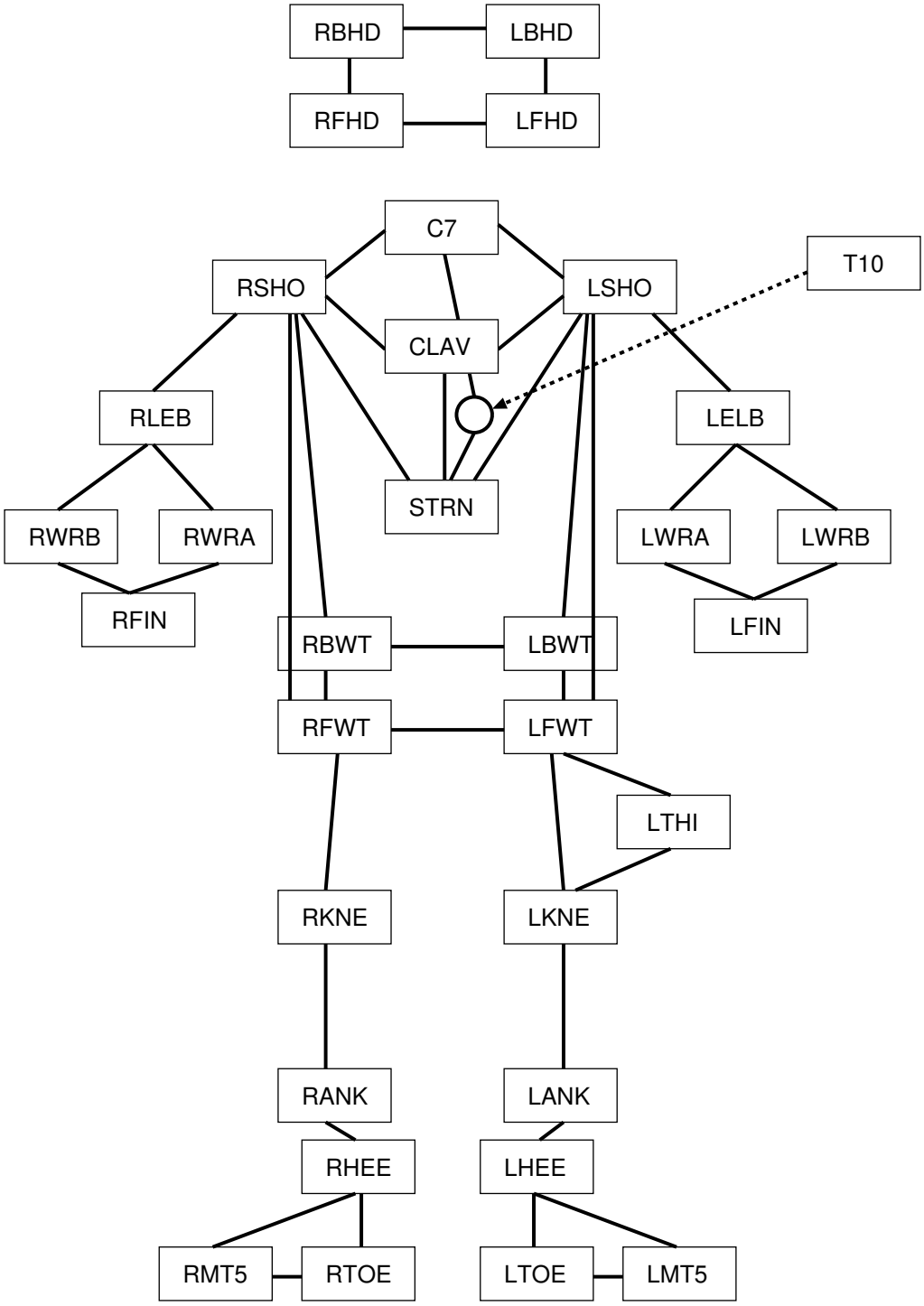

Figure B.1: Marker labels of the motion-capturing system

Marker	Position
LFHD	the left front of the head
LBHD	the left back of the head
RFHD	the right front of the head
RBHD	the right back of the head
CLAV	the middle of the two clavicle
STRN	the pit of the stomach
T10	the spine opposite to STRN
C7	the back of the neck
LSHO	the left shoulder
LELB	the left elbow
LWRA	the left wrist (the radius side)
LWRB	the left wrist (the ulna side)
LFIN	the center of the back of the left hand
RSHO	the right shoulder
RELB	the right elbow
RWRA	the right wrist (the radius side)
RWRB	the right wrist (the ulna side)
RFIN	the center of the back of the right hand
LFWT	the left front of the waist
LBWT	the left back of the waist
LTHI	the left thigh
LKNE	the left knee
LANK	the left ankle
LHEE	the left heel
LTOE	the left toe
LMT5	the left little toe
RFWT	the right front of the waist
RBWT	the right back of the waist
RKNE	the right knee
RANK	the right ankle
RHEE	the right heel
RTOE	the right toe
RMT5	the right little toe

Table B.1: Position of the markers

Appendix C

Force Plate

Each force plate returns the direction, the magnitude, and the position of the resultant force acting on the plate. The mechanism of it is described in this appendix.

As shown in Figure C.1, four force sensors are attached to every force plate. The length of the sensor from the center of a plate is w and d, and the height of the surface from the sensor is h. The origin of the local coordinates is at the center of the surface. Each sensor returns the magnitude of force acting on it. Let the force be $\boldsymbol{f}_i$ $(i = 1, 2, 3, 4)$. The resultant force $\boldsymbol{F}$ is calculated as

$$\boldsymbol{F} = \sum_i \boldsymbol{f}_i. \tag{C.1}$$

The resultant moment $\boldsymbol{N}$ is calculated as

$$\boldsymbol{N} = \sum_i \boldsymbol{r}_i \times \boldsymbol{f}_i, \tag{C.2}$$

where $\boldsymbol{r}_*$ is the vector from the center of the surface to the sensors:

$$\begin{aligned} \boldsymbol{r}_1 &= (w, 0, d) \qquad \boldsymbol{r}_2 = (w, 0, -d) \\ \boldsymbol{r}_3 &= (-w, 0, d) \quad \boldsymbol{r}_4 = (-w, 0, -d). \end{aligned} \tag{C.3}$$

Thus, let the position where the resultant force acts be $\boldsymbol{a} = (a_x, h, a_z)$, it is calculated as

$$a_x = \frac{-N_z + hF_x}{F_y} \tag{C.4a}$$

$$a_z = \frac{N_x + hF_x}{F_y}. \tag{C.4b}$$

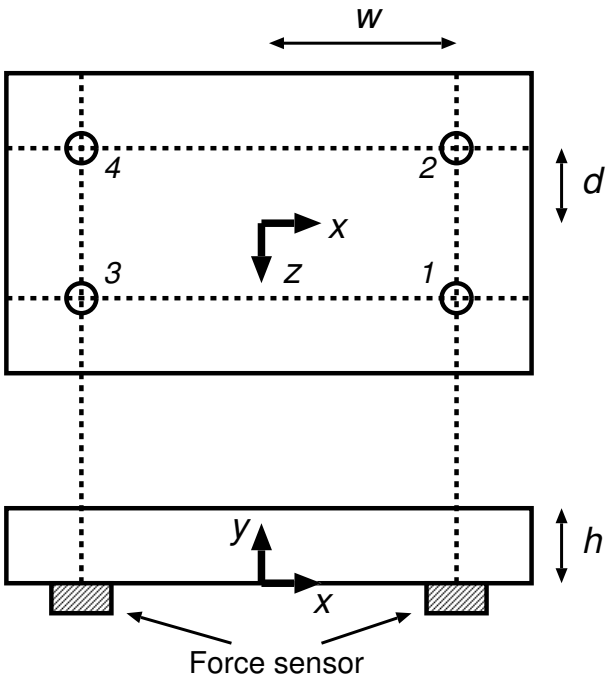

Figure C.1: Force plate: Four force sensors are attached under every force plate. The length of the sensor from the center of a plate is w and d, and the height of the surface from the sensor is h.

Appendix D

Weight Matrix and Range of Motion for Joints

In this chapter, we describe two constants that are used when generating motion. One is A_θ, which is a constant in the objective function of the quadratic programming problem. It is a weight matrix that determines the importance of the joints in generating motion. The other is a range of motion for the joints. It is used as the constraint of the quadratic programming problem.

A_θ is a diagonal matrix, and each diagonal element corresponds to a degree of freedom of the joints. Its value is determined as Table D.1 based on the distribution of mass in the body. First, the summation of mass for the child links regarding the feet as the root is calculated for every joint, and then, the inverse of it is used as the value of the corresponding element. Since the objective function is minimized in the optimization, a joint tends to move farther if a smaller value is set on the corresponding element. In this case, joints near the root are easier to move. Empirically, we can obtain good results from this A_θ. Setting high priority to joints near the root is considered reasonable to generate low-cost motion because the effect of moving a joint near the root is larger than that of moving other joints.

However, the value is not very significant to generate human-like motion. As mentioned in Chapter 7, varying A_θ has little influence on the fundamental characteristics of motion. Moreover, generated motion is not so sensitive to the value of A_θ. The value shown here is one example of A_θ.

Ranges of motion for the joints are determined as Table D.1. The values are not determined strictly for two reasons. One reason is that there is a large

Joint	Value
Shoulder	0.15
Elbow	0.34
Waist	0.021
Hip	0.016
Knee	0.023
Ankle	0.0020

Joint	Min(°)	Max(°)
Shoulder(x)	-180	180
Shoulder(z)	0	180
Elbow	-150	0
Waist(x)	-45	30
Waist(y)	-45	45
Waist(z)	-45	45
Hip(x)	-90	45
Hip(y)	-15	30
Hip(z)	0	45
Knee	0	150
Ankle(x)	-60	60
Ankle(z)	-30	45

Table D.1: Value of A_θ (left) and Range of motion for the joints (right): The joints that are not written in these tables are fixed in our method. In the right table, x and z-axes are horizontal axes. x-axis goes from the right to the left, and z-axis goes from the back to the front. y-axis is a vertical axis and goes from the bottom to the top. For the joints except "waist, " the value is about the joint in the left side.

individual difference. In this study, we try to extract characteristics of motion beyond such a difference. Therefore, it is sufficient that approximate values are determined. The other reason is that a strict model of joints is required to determine the range of motion precisely. The joint model in our method is not sufficiently strict for this purpose. However, an objective of the study is to represent whole-body motion using a simple model as much as possible. Determining strict values under strict joint models does not fit this objective. For the above reasons, we used the range of motion as Table D.1

References

[1] J. H. Allum, A. L. Adkin, M. G. Carpenter, M. Heldziolkowska, F. Honegger, and K. Pierchala. Trunk sway measures of postural stability during clinical balance tests: effects of a unilateral vestibular deficit. *Gait Posture*, Vol. 14, pp. 227–237, 2001.

[2] Okan Arikan and D. A. Forsyth. Interactive motion generation from examples. *ACM Transactions on Graphics (SIGGRAPH 2002)*, Vol. 21, No. 3, pp. 483–490, 2002.

[3] Okan Arikan, David A. Forsyth, and James F. O'Brien. Motion synthesis from annotations. *ACM Transactions on Graphics (SIGGRAPH 2003)*, Vol. 22, No. 3, pp. 402–408, 2003.

[4] Fumihiko Asano and Masaki Yamakita. Virtual gravity and coupling control for robotic gait. *IEEE Transactions on Systems, Man, and Cybernetics*, Vol. 31, No. 6, pp. 737–745, 2001.

[5] Fumihiko Asano, Masaki Yamakita, Norihiro Kamamichi, and Zhi-Wei Luo. A novel gait generation for biped walking robots based on mechanical energy constraint. In *Proceedings of the IEEE/RSJ International Conference on Intelligent Robots and Systems (IROS)*, pp. 2637–2644, 2002.

[6] Catherine E. Bauby and Arthur D. Kuo. Active control of lateral balance in human walking. *Journal of Biomechanics*, Vol. 33, pp. 1433–1440, 2000.

[7] Matthew Brand and Aaron Hertzmann. Style machines. In *Computer Graphics (SIGGRAPH 2000 Proceedings)*, pp. 183–192, 2000.

[8] Arimin Bruderlin and Lance Williams. Motion signal processing. In *Computer Graphics (SIGGRAPH 95 Proceedings)*, pp. 97–104, 1995.

[9] K. Le Clair and C. Riach. Postural stability measures: what to measure and for how long. *Clinical Biomechanics*, Vol. 11, No. 3, pp. 176–178, 1996.

[10] Steven H. Collins, Martijn Wisse, and Andy Ruina. A three-dimensional passive-dynamic walking robot with two legs and knees. *The International Journal of Robotics Research*, Vol. 20, No. 7, pp. 607–615, 2001.

[11] M. C. Do, C. Schneider, and R. K. Y. Chong. Factors influencing the quick onset of stepping following postural perturbation. *Journal of Biomechanics*, Vol. 32, No. 8, pp. 795–802, 1999.

[12] J. Maxwell Donelan, Rodger Kram, and Arthur D. Kuo. Simultaneous positive and negative external mechanical work in human walking. *Journal of Biomechanics*, Vol. 35, pp. 117–124, 2002.

[13] M. Duarte and V. M. Zatsiorsky. Effect of body lean and visual information on the equilibrium maintenance during stance. *Experimental Brain Research*, Vol. 146, pp. 60–69, 2002.

[14] Petros Faloutsos, Michiel van de Panne, and Demetri Terzopoulos. Composable controllers for physics-based character animation. In *Computer Graphics (SIGGRAPH 2001 Proceedings)*, pp. 251–260, 2001.

[15] Petros Faloutsos, Michiel van de Panne, and Demetri Terzopoulos. Autonomous reactive control for simulated humanoids. In *Proceedings of the 2003 IEEE International Conference on Robotics and Automation (ICRA)*, pp. 917–924, 2003.

[16] Anthony C. Fang and Nancy S. Pollard. Efficient synthesis of valid human motion. *ACM Transactions on Graphics (SIGGRAPH 2003)*, Vol. 22, No. 3, pp. 417–426, 2003.

[17] Kiyoshi Fujiwara, Fumio Kanehiro, Shuji Kajita, Kenji Kaneko, Kazuhito Yokoi, and Hirohisa Hirukawa. Ukemi: Falling motion control to minimize damage to biped humanoid robot. In *Proceedings of the IEEE/RSJ International Conference on Intelligent Robots and Systems (IROS)*, pp. 2521–2526, 2002.

[18] Kiyoshi Fujiwara, Fumio Kanehiro, Shuji Kajita, Kazuhito Yokoi, Hajime Saito, Kensuke Harada nad Kenji Kaneko, and Hiroshisa Hirukawa. The first human-size humanoid that can fall over safely and stand-up again. In *Proceedings of the IEEE/RSJ International Conference on Intelligent Robots and Systems (IROS)*, pp. 1920–1926, 2003.

[19] Kiyoshi Fujiwara, Fumio Kanehiro, Kajime Saito, Shuji Kajita, Kensuke harada, and Hirohisa Hirukawa. Falling motion control of a humanoid

robot trained by virtual supplementary tests. In *Proceedings of the 2003 IEEE International Conference on Robotics and Automation (ICRA)*, pp. 1077–1082, 2004.

[20] Kiyoshi Fujiwara, Jumio Kanehiro, Shinji Kajita, and Hirohisa Hirukawa. Safe knee landing of a human-size humanoid robot while falling forward. In *Proceedings of the 2004 IEEE/RSJ International Conference on Intelligent Robots and Systems (IROS)*, pp. 503–508, 2004.

[21] Michael Gleicher. Retargetting motion to new characters. In *Computer Graphics (SIGGRAPH 98 Proceedings)*, pp. 33–42, 1998.

[22] Ambarish Goswami. Postural stability of biped robots and the foot rotation indicator (fri) point. *The International Journal of Robotics Research*, Vol. 18, No. 6, pp. 523–533, 1999.

[23] Ambarish Goswami and Vinutha Kallem. Rate of change of angular momentum and balance maintenance of biped robots. In *Proceedings of the 2004 IEEE International Conference on Robotics and Automation (ICRA)*, pp. 3785–3790, 2004.

[24] Keith Grochow, Steven L. Martin, Aarno Hertzmann, and Zoran Popvić. Style-based inverse kinematics. *ACM Transactions on Graphics (SIGGRAPH 2004)*, Vol. 23, No. 3, pp. 522–531, 2004.

[25] Mian-Ju Gu, Alvert B. Schults, Neil T. Shepard, and Neil B. Alexander. Postural control in young and elderly adults when stance is perturbed: Dynamics. *Journal of Biomechanics*, Vol. 29, No. 3, pp. 319–329, 1996.

[26] Hitoshi Hasunuma, Masami Kobayashi, Hisashi Moriyama, Yoshiyuki Itoko, Yoshitaka Yanagihara, Takao Ueno, Kazuhisa Ohya, and Kazuhito Yokoi. A tele-operated humanoid robot drives a lift truck. In *Proceedings of the 2002 IEEE International Conference on Robotics and Automation (ICRA)*, pp. 2246–2252, 2002.

[27] Hitoshi Hasunuma, Katsumi Nakashima, Masami Kobayashi, Fumisato Mifune, Yoshitaka Yanagihara, Takao Ueno, Kazuhisa Ohya, and Kazuhito Yokoi. A tele-operated humanoid robot drives a backhoe. In *Proceedings of the 2003 IEEE International Conference on Robotics and Automation (ICRA)*, pp. 2998–3004, 2003.

[28] K. Hirai. Current and future perspective of honda humanoid robot. In *Proceedings of the IEEE/RSJ International Conference on Intelligent Robots and Systems (IROS)*, pp. 500–508, 1997.

[29] K. Hirai, M. Hirose, Y. Haikawa, and T. Takenaka. The development of honda humanoid robot. In *Proceedings of the 1998 IEEE International Conference on Robotics and Automation (ICRA)*, pp. 1321–1326, 1998.

[30] M. Hirose, H. Haikawa, T. Takenaka, and K. Hirai. Development of humanoid robot asimo. In *Proceedings of the IEEE/RSJ International Conference on Intelligent Robots and Systems (IROS), Workshop on Explorations towards Humanoid Robot Applications*, 2001.

[31] Jessica K. Hodgins and Nancy S. Pollard. Adapting simulated behaviors for new characters. In *Computer Graphics (SIGGRAPH 97 Proceedings)*, pp. 153–162, 1997.

[32] Jessica K. Hodgins, Wayne L. Wooten, David C. Brogan, and James F. O'Brien. Animating human athletics. In *Computer Graphics (SIGGRAPH 95 Proceedings)*, pp. 71–78, 1995.

[33] Elizabeth T. Hsiao and Stephen N. Robinovitch. Biomechanical influences on balance recovery by stepping. *Journal of Biomechanics*, Vol. 32, No. 10, pp. 1099–1106, 1999.

[34] Tatsuzo Ishida, Yoshihiro Kuroki, and Taro Takahashi. Analysis of motions of a small biped entertainment robot. In *Proceedings of the IEEE/RSJ International Conference on Intelligent Robots and Systems (IROS)*, pp. 142–147, 2004.

[35] Tatsuzo Ishida, Yoshihiro Kuroki, and Jin'ichi Yamaguchi. Mechanical system of a small biped entertainment robot. In *Proceedings of the IEEE/RSJ International Conference on Intelligent Robots and Systems (IROS)*, pp. 1129–1134, 2003.

[36] Tatsuzo Ishida, Yoshihiro Kuroki, Jin'ichi Yamaguchi, Masahiro Fujita, and TOshi T. Doi. Motion entertainment by a small humanoid robot based on open-r. In *Proceedings of the IEEE/RSJ International Conference on Intelligent Robots and Systems (IROS)*, pp. 1079–1086, 2001.

[37] Robert K. Jensen. Changes in segment inertia proportion between 4 and 20 years. *Journal of Biomechanics*, Vol. 22, No. 6/7, pp. 529–536, 1989.

[38] Satoshi Kagami, Fumio Kanehiro, Yukiharu Tamiya, Masayuki Inaba, and Hirochika Inoue. Autobalancer: An online dynamic balance compensation scheme for humanoid robots. In *Proceedings of the Fourth International Workshop on Algorithmic Foundation of Robotics (WAFR 2000)*, 2000.

[39] Satoshi Kagami, Tomonobu Kitagawa, Koichi Nishiwaki, Masayuki Inaba, and Hirochika Inoue. A fast dynamically equilibrated walking trajectory generation method of humanoid robot. *Autonomous Robots*, Vol. 12, No. 1, pp. 71–82, 2002.

[40] Satoshi Kagami, masaki Mochimaru, Yoshihiro Ehara, Natsuki Miyata, Koichi Nishiwaki, Takeo Kanade, and Hirochika Inoue. Measurement and comparison of human and humanoid walking. In *Proceedings 2003 IEEE International Symposium on Computational Intelligence in Robotics and Automation*, pp. 918–922, 2003.

[41] Shuji Kajita, Fumio Kanehiro, Kenji Kaneko, Kiyoshi Jujiwara, Kensuke Harada, Kazuhito Yokoi, and Hirohisa Hirukawa. Resolved momentum control: Humanoid motion planning based on the linear and angular momentum. In *Proceedings of the 2004 IEEE/RSJ International Conference on Intelligent Robots and Systems (IROS)*, pp. 1644–1650, 2004.

[42] Shuji Kajita, Fumio Kanehiro, Kenji Kaneko, Kazuhito Yokoi, and Hirohisa Hirukawa. The 3d linear inverted pendulum model: A simple modeling for a biped walking pattern generation. In *Proceedings of the IEEE/RSJ International Conference on Intelligent Robots and Systems (IROS)*, pp. 239–246, 2001.

[43] Shuji Kajita, Humio Kanehiro, Kenji Kaneko, Kiyoshi Hujiwara, Kazuhito Yokoi, and Hirohisa Hirukawa. A realtime pattern generator for biped walking. In *Proceedings of the 2002 IEEE International Conference on Robotics and Automation (ICRA)*, pp. 31–37, 2002.

[44] Shuji Kajita, Osamu Matsumoto, and Muneharu Saigo. Real-time 3d walking pattern generation for a biped robot with telescopic legs. In *Proceedings of the 2001 IEEE International Conference on Robotics and Automation (ICRA)*, pp. 2292–2036, 2001.

[45] Shuji Kajita, Takashi Nagasaki, Kenji Kaneko, Kazuhito Yokoi, and Kazuo Tanie. A hop towards running humanoid biped. In *Proceedings of the 2004 IEEE International Conference on Robotics and Automation (ICRA)*, pp. 629–635, 2004.

[46] Fmio Kanehiro, Kenji Kaneko, Kiyoshi Fujiwara, Kensuke Harada, Shuji Kajita, Kazuhito Yokoi, Hirohisa Hirukawa, Kazuhiko Akachi, and Takakatsu Isozumi. The first humanoid robot that has the same size as a human and that can lie down and get up. In *Proceedings of the 2003 IEEE International Conference on Robotics and Automation (ICRA)*, pp. 1633–1639, 2003.

[47] Thomas M. Kepple, Karen Lohmann Siegel, and Steven J. Stanhope. Relative contributions of the lower extremity joint moments to forward progression and support during gate. *Gate and Posture*, Vol. 6, pp. 1–8, 1997.

[48] Tae-Hoon Kim, Sang Il Park, and Sung Yong Shin. Rhythmic-motion synthesis based on motion-beat analysis. *ACM Transactions on Graphics (SIGGRAPH 2003)*, Vol. 22, No. 3, pp. 392–401, 2003.

[49] Hyeongseok Ko and Noramn I. Badler. Animating human locomotion with inverse dynamics. *IEEE Computer Graphics and Application*, Vol. 16, No. 2, pp. 50–59, 1996.

[50] Taku Komura and Yoshihisa Shinagawa. A muscle-based feed-forward controller of the human body. *Computer Graphics Forum*, Vol. 16, No. 3, pp. 165–176, 1997.

[51] Taku Komura, Yoshihisa Shinagawa, and Toshiyasu L. Kunii. Creating and retargetting motion by the muscloskeletal human body model. *The Visual Computer*, Vol. 16, No. 5, pp. 254–270, 2000.

[52] Lucas Kovar and Michael Gleicher. Flexible automatic motion blending with registration curves. In *Proceedings of the 2003 ACM SIGGRAPH/Eurographics Symposium on Computer animation*, pp. 214–224, 2003.

[53] Lucas Kovar, Michael Gleicher, and Frédéric Pighin. Motion graphs. *ACM Transactions on Graphics (SIGGRAPH 2002)*, Vol. 21, No. 3, pp. 473–482, 2002.

[54] Arthur D. Kuo. Stabilization of lateral motion in passive dynamic walking. *The International Journal of Robotics Research*, Vol. 18, No. 9, pp. 917–930, 1999.

[55] Arthur D. Kuo. Energetics of actively powered locomotion using the simplest walking model. *Journal of Biomechanics Engineering*, Vol. 124, pp. 113–120, 2002.

[56] Ryo Kurazume, Tsutomu Hasegawa, and Kan Yoneda. The sway compensation trajectory for a biped robot. In *Proceedings of the 2003 IEEE International Conference on Robotics and Automation (ICRA)*, pp. 925–931, 2003.

[57] Yoshihiro Kuroki, Bill Blank, Tatsuo Mikami, Patrick Mayeux, Atsushi Miyamoto, Robert Playter, Ken'ichiro Nagasaka, Marc Raibert, Masakuni Nagano, and Jin'ichi Yamaguchi. Motion creating system for a small biped entertainment robot. In *Proceedings of the IEEE/RSJ International Conference on Intelligent Robots and Systems (IROS)*, pp. 1394–1399, 2003.

[58] Jehee Lee, Jinxiang Chai, Paul S. A. Reitsma, Jessica K. Hodgins, and Nancy S. Pollard. Interactive control of avatars animated with human motion data. *ACM Transactions on Graphics (SIGGRAPH 2002)*, Vol. 21, No. 3, pp. 492–500, 2002.

[59] Jehee Lee and Sung Yong Shin. A hierarchical approach to interactive motion editing for human-like figures. In *Computer Graphics (SIGGRAPH 99 Proceedings)*, pp. 39–48, 1999.

[60] Yan Li, Tianshu Wang, and Heung-Yeung Shum. Motion texture: A two-level statistical model for character motion synthesis. *ACM Transactions on Graphics (SIGGRAPH 2002)*, Vol. 21, No. 3, pp. 465–472, 2002.

[61] C. Karen Liu and Zordan Popvić. Synthesis of complex dynamic character motion from simple animations. *ACM Transactions on Graphics (SIGGRAPH 2002)*, Vol. 21, No. 3, pp. 408–416, 2002.

[62] Zicheng Liu, Steven J. Gortler, and Michael F. Cohen. Hierarchical spacetime control. In *Computer Graphics (SIGGRAPH 94 Proceedings)*, pp. 35–42, 1994.

[63] Z. Matjačić, M. Voigt, D. Popvić, and T. Sinkjær. Functional postural responses after perturbations in multiple directions in a standing man: a principle of decoupled control. *Journal of Biomechanics*, Vol. 34, No. 2, pp. 187–196, 2001.

[64] Tad McGeer. Passive dynamic walking. *The International Journal of Robotics Research*, Vol. 9, No. 2, pp. 62–82, 1990.

[65] Tad McGeer. Passive walking with knees. In *Proceedings of the 1990 IEEE International Conference on Robotics and Automation (ICRA)*, pp. 1640–1645, 1990.

[66] Ken'ichiro Nagasaka, Yoshihiro Kuroki, Shin'ya Suzuki, Yoshihiro Itoh, and Jin'ichi Yamaguchi. Integrated motion control for walking, jumping and running on a small biped entertainment robot. In *Proceedings of the 2004 IEEE International Conference on Robotics and Automation (ICRA)*, pp. 3189–3194, 2004.

[67] Takashi Nagasaki, Shuji Kajita, Kenji Kaneko, Kazuhito Yokoi, and Kazuo Tanie. A running experiment of humanoid biped. In *Proceedings of the 2004 IEEE/RSJ International Conference on Intelligent Robots and Systems (IROS)*, pp. 136–141, 2004.

[68] Takashi Nagasaki, Shuji Kajita, Kazuhito Yokoi, Kenji Kaneko, and Kazuo Tanie. Running pattern generation and its evaluation using a realistic humanoid model. In *Proceedings of the IEEE/RSJ International Conference on Intelligent Robots and Systems (IROS)*, pp. 1336–1342, 2003.

[69] Y. Nakamura, K. Yamane, I. Suzuki, and Y. Fujita. Dynamic computation of musculo-skeletal human model based on efficient algorithm for closed kinematic chains. In *Proceedings of the 2nd International Symposium on Adaptive Motion of Animals and Machines*, 2003.

[70] Yoshihiko Nakamura, Hirohisa Hirukawa, and Katsu Yamane. Humanoid robot simulator for the meti hrp project. *Robotics and Autonomous Systems*, Vol. 37, pp. 101–114, 2001.

[71] Yoshihiko Nakamura and Katsu Yamane. Dynamics computation of structure-varying kinematic chains and its application to human figures. *IEEE Transactions on Robotics and Automation*, Vol. 16, No. 2, pp. 124–134, 2000.

[72] Shinichiro Nakaoka, Atsushi Nakazawa, Kazuhito Yokoi, Hirohisa Hirukawa, and Katsushi Ikeuchi. Generating whole body motions for a biped humanoid robot from captured human dances. In *Proceedings of the 2003 IEEE International Conference on Robotics and Automation (ICRA)*, pp. 3905–3910, 2003.

[73] Michael Neff and Eugene Fiume. Aesthetic edits for character animation. In *Proceedings of the 2003 ACM SIGGRAPH/Eurographics Symposium on Computer animation*, pp. 239–224, 2003.

[74] P. E. Nikravesh and G. Gim. Systematic construction of the equations of motion for multibody systems containing closed kinematic loops. *Journal of Mechanical Design*, Vol. 115, No. 1, pp. 143–149, 1993.

[75] Parviz E. Nikravesh. Systematic reduction of multibody equations of motion to a minimal set. *International Journal on Non-Linear Mechanics*, Vol. 25, No. 2/3, pp. 143–151, 1990.

[76] Parviz E. Nikravesh and Jorge A. C. Ambrosio. Systematic construction of equations of motion for rigid-flexible multibody systems containing open and closed kinematic loops. *International Journal for Numerical Methods in Engineering*, Vol. 32, pp. 1749–1766, 1991.

[77] Koichi Nishiwaki, Satoshi Kagami, Yasuo Kuniyoshi, Masayuki Inaba, and Hirochika Inoue. Online generation of humanoid walking motion based on a fast generation method of motion pattern that follows desired zmp. In *Proceedings of the IEEE/RSJ International Conference on Intelligent Robots and Systems (IROS)*, pp. 2684–2689, 2002.

[78] Masaki Oshita and Akifumi Makinouchi. A dynamic motion control technique for human-like articulated figures. *Computer Graphics Forum*, Vol. 20, No. 3, pp. 192–202, 2001.

[79] Yi-Chung Pai and Kamran Iqbal. Simulated movement termination for balance recovery: can movement strategies be sought to maintain stability in the presence of slipping or forced sliding? *Journal of Biomechanics*, Vol. 32, No. 779-786, 1999.

[80] Yi-Chung Pai and James Patton. Center of mass velocity-position predictions for balance control. *Journal of Biomechanics*, Vol. 30, No. 4, pp. 347–354, 1997.

[81] Elizabetta Papa and Aurelio Cappozzo. A telescopic inverted-pendulum model of the mulculo-skeletal system and its use for the analysis of the sit-to-stand motor task. *Journal of Biomechanics*, Vol. 32, pp. 1205–1212, 1999.

[82] Robert J. Peterka. Postural control model interpretation of stabilogram diffusion analysis. *Biological Cybernetics*, Vol. 82, No. 4, pp. 335–343, 2000.

[83] Zordan Popvić and Andrew Witkin. Physically based motion transformation. In *Computer Graphics (SIGGRAPH 99 Proceedings)*, pp. 11–20, 1999.

[84] Katherine Pullen and Christoph Bregler. Motion capture assisted animation: Texturing and synthesis. *ACM Transactions on Graphics (SIGGRAPH 2002)*, Vol. 21, No. 3, pp. 501–508, 2002.

[85] S. Rietdyk, A. E. Patla, D. A. Winter, M. G. Ishac, and C. E. Little. Balance recovery from medio-lateral perturbations of the upper body during standing. *Journal of Biomechanics*, Vol. 32, No. 11, pp. 1149–1158, 1999.

[86] Charles Rose, Brian Guenter, Bobby Bodenheimer, and Michael F. Cohen. Efficient generation of motion transitions using spacetime constraints. In *Computer Graphics (SIGGRAPH 96 Proceedings)*, pp. 147–154, 1996.

[87] Alla Safonova, Jessica K. Hodgins, and Nancy S. Plooard. Synthesizing physically realistic human motion in low-dimensional, behavior-specific spaces. *ACM Transactions on Graphics (SIGGRAPH 2004)*, Vol. 23, No. 3, pp. 514–521, 2004.

[88] Akihito Sano, Yoshito Ikemata, and Hideo Fujimoto. Analysis of dynamics of passive walking from storage energy and supply rate. In *Proceedings of the 2003 IEEE International Conference on Robotics and Automation (ICRA)*, pp. 2478–2483, 2003.

[89] Tomomichi Sugihara, Yoshihiko Nakamura, and Hirochika Inoue. Realtime humanoid motion generation through zmp manipulation based on inverted pendulum control. In *Proceedings of the 2002 IEEE International Conference on Robotics and Automation (ICRA)*, pp. 1404–1409, 2002.

[90] Yoshihiko Tagawa and Tadashi yamashita. Analysis of human abnormal walking using zero moment joint: required compensatory actions. *Journal of Biomechanics*, Vol. 34, pp. 783–790, 2001.

[91] Seyoon Tak, Oh-Young Song, and Hyeong-Seok Ko. Motion balance filtering. *Computer Graphics Forum*, Vol. 19, No. 3, pp. 435–446, 2000.

[92] Koji Terada, Yoshiyuki Ohmura, and Yasuo Kuniyoshi. Analysis and control of whole body dynamic humanoid motion – towards experiments on a roll-and-rise motion. In *Proceedings of the IEEE/RSJ International Conference on Intelligent Robots and Systems (IROS)*, pp. 1382–1387, 2003.

[93] M. Vukobratović and D. Juricic. Contribution to the synthesis of biped gait. *IEEE Transaction on Biomedical Engineering*, Vol. 16, No. 1, pp. 1–6, 1969.

[94] M. Vukobratović and J. Stepanenko. On the stability of anthropomorphic systems. *Mathematical Biosciences*, Vol. 15, pp. 1–37, 1972.

[95] David A. Winter, Aftab E. Patla, Francois Prince, Milad Ishac, and Krystyna Gielo-Perczak. Stiffness control of balance in quiet standing. *The Journal of Neurophysiology*, Vol. 80, No. 3, pp. 1211–1221, 1998.

[96] Andrew Witkin and Michael Kass. Spacetime constraints. In *Computer Graphics (SIGGRAPH 88 Proceedings)*, pp. 159–168, 1988.

[97] Andrew Witkin and Zoran Popvić. Motion warping. In *Computer Graphics (SIGGRAPH 95 Proceedings)*, pp. 105–108, 1995.

[98] W. L. Wooten and J. K. Hodgins. Simulating leaping, tumbling, landing and balancing humans. In *Proceedings of the 2000 IEEE International Conference on Robotics and Automation (ICRA)*, pp. 656–662, 2000.

[99] Jin-ichi Yamaguchi, Atsuo Tkanishi, and Ichiro Kato. Development of a biped walking robot compensating for three-axis moment by trunk motion. *Journal of the Robotics Society of Japan*, Vol. 11, No. 4, pp. 581–586, 1993. (in Japanese).

[100] Jin-ichi Yamaguchi, Atsuo Tkanishi, and Ichiro Kato. Development of a biped walking robot compensating for three-axis moment by trunk motion. In *Proceedings of the 1993 IEEE/RSJ International Conference on Intelligent Robots and Systems (IROS)*, pp. 561–566, 1993.

[101] Katsu Yamane, James J. Kuffner, and Jessica K. Hodgens. Synthesizing animations of human manipulation tasks. *ACM Transactions on Graphics (SIGGRAPH 2004)*, Vol. 23, No. 3, pp. 532–539, 2004.

[102] Katsu Yamane and Yoshihiko Nakamura. Dynamics computation of structure-varying kinematic chains for motion synthesis of humanoid. In *Proceedings of the 1999 IEEE International Conference on Robotics and Automation (ICRA)*, pp. 714–721, 1999.

[103] Katsu Yamane and Yoshihiko Nakamura. Dynamics filter — concept and implementation of on-line motion generator for human figures. In *Proceedings of the 2000 IEEE International Conference on Robotics and Automation (ICRA)*, pp. 688–695, 2000.

[104] Katsu Yamane and Yoshihiko Nakamura. Synergetic cg choreography through constraining and deconstraining at will. In *Proceedings of the 2002 IEEE International Conference on Robotics and Automation (ICRA)*, pp. 855–862, 2002.

[105] Katsu Yamane and Yoshihiko Nakamura. Dynamics filter - concept and implementation of on-line motion generator for human figures. *IEEE Transactions on Robotics and Automation*, Vol. 19, No. 3, pp. 421–432, 2003.

[106] Katsu Yamane and Yoshihiko Nakamura. Efficient parallel dynamics computation of human figures. In *Proceedings of the 2003 IEEE International Conference on Robotics and Automation (ICRA)*, pp. 530–537, 2003.

[107] Katsu Yamane and Yoshihiko Nakamura. Natural motion animation through constraining and deconstraining at will. *IEEE Transactions on Visualization and Computer Graphics*, Vol. 9, No. 3, pp. 352–360, 2003.

[108] Kazuhito Yokoi, Fumio Kanehiro, Kenji Kaneko, Kiyoshi Fujiwara, Shuji Kajita, and Hirohisa Hirukawa. A honda humanoid robot controlled by aist software. In *Proceedings of the IEEE-RAS International Conference on Humanoid Robots*, pp. 259–264, 2001.

[109] Kazuhiko Yokoyama, Hiroyuki Handa, Takakatsu Isozumi, Yutaro Fukase, Kenji Kaneko, Fumio Kanehiro, Yoshihiro Kawai, Fumiaki Tomita, and Hirohisa Hirukawa. Cooperative works by a human and a humanoid robot. In *Proceedings of the 2003 IEEE International Conference on Robotics and Automation (ICRA)*, pp. 2985–2991, 2003.

[110] Victor B. Zordan and Jessica K. Hodgins. Motion capture-driven simulations that hit and react. In *ACM SIGGRAPH Symposium on Computer Animation*, 2002.